

# Full One-loop Electroweak Corrections to the Decays $H^+ \rightarrow W^+ h/H$ in the Two-Higgs-Doublet Model

Masterarbeit  
von

Robin Lorenz

An der Fakultät für Physik  
Institut für Theoretische Physik

Referent: Prof. Dr. M. Mühlleitner  
Korreferent: Prof. Dr. U. Nierste

Juni 2015



Ich versichere, dass ich diese Arbeit selbstständig verfasst und ausschließlich die angegebenen Hilfsmittel verwendet habe.

---

Robin Lorenz  
Karlsruhe, den 20. Juni 2015

Als Masterarbeit anerkannt.

---

Prof. Dr. M. Mühlleitner  
Karlsruhe, den 20. Juni 2015



# Contents

<b>1. Introduction</b>	<b>1</b>
<b>2. The THDM - A Brief Introduction</b>	<b>5</b>
2.1. Why a Two-Higgs-Doublet-Model? . . . . .	5
2.2. The Scalar Potential . . . . .	7
2.3. THDMs and FCNCs . . . . .	11
2.4. Sets of Independent Parameters . . . . .	12
2.5. General Notation . . . . .	13
<b>3. The Decays <math>H^+ \rightarrow W^+ h/H</math> at LO</b>	<b>15</b>
<b>4. Renormalization of THDMs</b>	<b>17</b>
4.1. A General Note on Renormalization . . . . .	17
4.2. On-shell Conditions . . . . .	18
4.3. A Matter of the Order of Doing Things? . . . . .	20
4.4. Renormalization of the Scalar Sector . . . . .	22
4.4.1. Mass Renormalization . . . . .	22
4.4.2. On-shell Renormalized Fields . . . . .	24
4.4.3. Renormalization of the Angles . . . . .	25
4.4.4. Process-dependent Schemes . . . . .	25
4.4.5. The Kanemura Approach . . . . .	27
4.4.6. A Minimal Scheme . . . . .	30
4.4.7. A Word on the Last Parameter . . . . .	34
4.5. Renormalization of the Gauge Sector . . . . .	35
<b>5. The Decays <math>H^+ \rightarrow W^+ h/H</math> at NLO</b>	<b>37</b>
5.1. Virtual Corrections . . . . .	37
5.2. Real Corrections . . . . .	40
5.2.1. Soft Bremsstrahlung . . . . .	42
5.2.2. Additional Soft Corrections . . . . .	43
5.2.3. Cancellation of Infra-red Divergences . . . . .	45
5.2.4. Process-dependent Schemes Revisited . . . . .	46
<b>6. Numerical Results</b>	<b>49</b>
6.1. Used Software . . . . .	49
6.2. Input Parameters . . . . .	50
6.3. The NLO Results . . . . .	53
6.4. The <i>HybMS</i> Scheme . . . . .	56
6.5. Dependence on the Detector Sensitivity $\Delta E$ . . . . .	57
<b>7. Summary and Conclusion</b>	<b>59</b>

<b>A. Vertex Corrections</b>	<b>63</b>
<b>B. Tadpole Parameters</b>	<b>64</b>
<b>C. Alternative Parametrization of the Scalar Potential</b>	<b>65</b>
<b>Acknowledgement</b>	<b>67</b>
<b>References</b>	<b>69</b>

# CHAPTER 1

---

## Introduction

---

The idea that nothing comes from nothing and that there must exist indivisible parts in the universe dates back to ancient times. Modern particle physics is concerned with understanding what the fundamental constituents of matter are and how the interaction between them can be described. During the last half century this endeavour has seen several breakthroughs. In the sixties a theoretical framework emerged, that is now known as the Standard Model (SM) [1–5]. At its heart is the concept of gauge symmetry. Together with the mechanism of spontaneous symmetry breaking (SSB), these guiding principles have proved to be extraordinarily successful. The SM has predicted new particles and related observables with unprecedented precision.

This theoretical progress has gone hand in hand with great experimental achievements, above all the ability to build colliders with ever increasing energies and detectors that provide sufficient precision. The discovery of the  $W$ - and  $Z$ -bosons in 1983 at the Super Proton Synchrotron at CERN, the discovery of the top quark at Tevatron in 1995 and the high precision measurements at the Large Electron-Positron Collider (LEP), that was in operation at CERN between 1989 and 2000, mark milestones of particle physics of the last decades. In 2008 the Large Hadron Collider (LHC) at CERN started operation and with a center-of-mass energy of 7 TeV the LHC began a new era of collider experiments. After shutting down for the upgrade to the new center-of-mass energy of 13 TeV, run II has just started taking data and exciting times are ahead of us.

Until very recently, the last missing ingredient of the SM was the Higgs boson. On the one hand, a scalar particle was predicted as the consequence of the Higgs mechanism [6–10], through which the gauge bosons of the weak interaction acquire mass without violating the gauge invariance of the Lagrangian. On the other hand, the Higgs boson simultaneously solves the problem of unitarity violation in the scattering of longitudinal vector bosons. One of the main goals of the LHC thus was to discover the Higgs boson. On July the 4th 2012 a particle was discovered [11,12] with a mass of about 125 GeV, that looks like the SM Higgs boson.

Despite the enormous success of the SM, we are aware of phenomena and issues that the SM cannot explain. Among these are the questions of where the prevalence of matter over

antimatter in the universe comes from, what dark matter is or even how one could describe gravity and the electroweak and strong interactions within one common framework. Beyond the Standard Model (BSM) physics therefore aims at developing models that are able to address some of these issues while still reproducing the SM predictions that match so well with the experimental data. The Two-Higgs-Doublet Model (THDM) [13–15], which is treated in this thesis, is such a model. As the name suggests, it extends the scalar sector of the SM by a second complex scalar isospin doublet. This extension leads to a Higgs sector that features three neutral and two charged Higgs bosons. The THDM is one of the simplest extensions of the SM which is still compatible with the Higgs data from the LHC.

The cleanest THDM specific signature is provided by charged Higgs bosons [16]. In particular in the light of run II of the LHC, predictions for the production and decay of charged Higgs bosons in the context of THDMs are needed. This thesis will study the full electroweak (EW) next-to-leading order (NLO) corrections to the partial decay width of a charged Higgs boson decaying into an on-shell  $W$ -boson and a neutral CP-even scalar. Since the dominant decay channel into a top and anti bottom quark is a challenging search channel due to the large background from quantum chromodynamics (QCD), the decay mode considered in this thesis could prove relevant for BSM searches.

The study of EW processes in THDMs beyond leading order (LO) involves the renormalization of the mixing angles that rotate between the basis defined by the gauge interactions, and the basis of the mass eigenstates. While these angles appear in most THDM specific couplings and play a crucial phenomenological role, there is no obvious relation to observables which would tell us how to renormalize the angles in a physically meaningful way. There are different possibilities, each with their own advantages and disadvantages. It thus seems natural to ask whether there is an ideal scheme which is universally applicable. This thesis therefore compares different renormalization schemes with the purpose of illuminating what the intuitions behind each of them are and what subtleties may arise with regard to renormalizing mixing angles.

The thesis is structured as follows. Chapter 2 gives a brief introduction into THDMs. After motivating the extension of the scalar sector with a second doublet in Sec. 2.1, the scalar potential of a CP-conserving THDM is discussed in Sec. 2.2 in order to identify the physical degrees of freedom. The discussion of the Yukawa Lagrangian in Sec. 2.3 will show how to avoid flavour-changing neutral currents (FCNCs) at tree level. Section 2.4 presents the set of independent parameters used in this thesis and Sec. 2.5 introduces useful notation for dealing with pairs of mixing scalars in different bases.

In the subsequent Chapter 3 the tree-level partial decay width of the decays  $H^+ \rightarrow W^+ h/H$  is derived and further notation is introduced.

Chapter 4 is devoted to the renormalization of THDMs, with the main focus on its scalar sector. The introductory remarks in Sec. 4.1 on renormalization in general are followed by the presentation of on-shell renormalization conditions in Sec. 4.2. In particular, the case of mixing between scalars is considered. In Sec. 4.3 it is argued that for CP-conserving THDMs it is reasonable to choose all scalar masses as input parameters and to perform the renormalization in the mass basis. Once this is clarified, Sec. 4.4 treats the renormalization of the whole scalar sector. After having renormalized the masses and the scalar fields on-shell in Sec. 4.4.1 and Sec. 4.4.2, various schemes to renormalize the mixing angles are presented in Secs. 4.4.3–4.4.6. As a first approach, the idea of process-dependent renormalization conditions is explained. Secondly a scheme which employs a minimal subtraction condition is



---

defined. The third scheme is an approach suggested by Kanemura *et al.* [17, 18] and the fourth scheme features a minimum number of independent field renormalization constants. Section 4.5 finally covers the gauge sector by employing the standard way of renormalizing the masses of the  $W$ -boson and  $Z$ -boson as well as the electric charge in the SM.

Chapter 5 discusses the decays  $H^+ \rightarrow W^+ h/H$  at NLO, namely the virtual and the real corrections. The former are treated in Sec. 5.1, which comprises an overview of the contributing vertex corrections, as well as the counterterms of the  $H^+W^-h/H$ -vertices. The real corrections from additional soft photons that are needed to obtain an infra-red (IR) finite partial decay width, are treated in Sec. 5.2. The Secs. 5.2.1–5.2.3 successively deal with the contributions from ordinary bremsstrahlung, the contributions from a four-vertex and how IR finiteness was checked. Finally, Sec. 5.2.4 addresses the issue of process-dependent schemes and IR divergent virtual photon corrections.

Chapter 6 covers the discussion of the numerical results. The software tools used in the numerical analysis are listed in Sec. 6.1 and the input parameters are defined in Sec. 6.2. The two subsequent Secs. 6.3 and 6.4 show and discuss the plots with the results for the partial decay widths. In Sec. 6.5 it is checked that the dependence on the photon phase space cut is small and hence the soft photon approximation is justified.

Chapter 7 summarizes the findings of the preceding chapters and draws a comparison between the renormalization schemes considered. Finally it is suggested which further investigations are necessary to finally answer the question of whether an ideal renormalization scheme for THDMs exists.



---

The THDM - A Brief Introduction

---

### 2.1. Why a Two-Higgs-Doublet-Model?

As pointed out in the introduction, the Standard Model of particle physics has been very successful over the last decades in predicting new particles and related observables at high precision. At the same time we are well aware of its insufficiencies, that are the motivation for studying BSM physics. While the gauge boson and fermion sector of the SM have been extremely well probed, the predicted Higgs boson was the missing ingredient until very recently. Although the scalar particle, that was discovered at the LHC in 2012 [11, 12], so far seems to be compatible with the SM, the experimental data still leave space for the interpretation of the signals within BSM models.

Now that run II of the LHC has just started taking data at a center-of-mass energy of 13 TeV, predictions in the framework of BSM models are needed even more. When building models with an extended scalar sector, one has to respect the current experimental and the theoretical constraints. Among the most restrictive constraints from the experimental side is the measurement of the parameter  $\rho$ , that is defined as

$$\rho = \frac{M_W^2}{M_Z^2 \cos^2(\theta_W)}, \quad (2.1)$$

where  $M_W$  and  $M_Z$  are the masses of the  $W$ -boson and the  $Z$ -boson, respectively, and  $\theta_W$  is the Weinberg angle. Experimentally  $\rho$  is determined to be very close to one [19]. Since in the SM and in extensions of its scalar sector the masses of the gauge bosons are generated through EWSB, the prediction for the above defined  $\rho$  depends on the scalar structure of the model. While the SM with one complex scalar isospin doublet, predicts  $\rho$  to be exactly one, in an  $SU(2)_L \otimes U(1)_Y$  gauge theory with  $n$  scalar multiplets  $\Phi_i$  of isospin  $I_i$ , hypercharge  $Y_i$  and a vacuum expectation value (vev)  $v_i$ ,  $\rho$  is determined to be

$$\rho = \frac{\sum_{i=1}^n (I_i(I_i + 1) - \frac{1}{4}Y_i^2) v_i}{\sum_{i=1}^n \frac{1}{2}Y_i^2 v_i}. \quad (2.2)$$

As one can easily see, any number of singlets ( $I = 0$ ) with hypercharge  $Y = 0$  and doublets ( $I = 1/2$ ) with hypercharge  $Y = \pm 1$  will likewise lead to  $\rho = 1$ . Although compatibility with

this experimental value can in principle be possible in models with higher  $SU(2)$  multiplets, this is not guaranteed anymore. From this point of view  $SU(2)$  singlets and doublets are the simplest allowed scalar extensions.

Another severe constraint is the fact that the existence of flavour-changing neutral currents (FCNCs) is experimentally very restricted. In contrast to the SM, the coupling matrices between scalars and fermions and the fermionic mass matrices are in general not diagonal at the same time (see Sec. 2.3) and hence FCNCs may arise already at tree level. Any realistic scalar extension has to either prevent tree-level FCNCs in the first place or explain why they are sufficiently small to still be compatible with experimental data.

From the theoretical side unitarity imposes constraints on scattering amplitudes and consequently on coupling constants. In the SM it was the prediction of the Higgs boson that cured the violation of unitarity bounds in the scattering of longitudinal gauge bosons  $V_L V_L \rightarrow V_L V_L$ . Without the scalar particle the cross section diverges with the square of the center of mass energy of the process. Due to the mechanism of EWSB the structure of the interaction between the Higgs boson and the gauge bosons is such that this divergence is exactly cancelled.

In any model that has an extended scalar sector and that relies on the mechanism of EWSB, the same cancellation has to hold. This translates into sum rules for the scalar-gauge-boson couplings. For general multiplets these rules can be rather complicated. If there are however  $n$  physical scalars  $h_i$  that sit only in singlets and doublets, the sum rule imposed by longitudinal vector boson scattering on the coupling constants  $g_{h_i VV}$ , reads

$$\sum_i g_{h_i VV}^2 = (g_{h VV}^{\text{SM}})^2, \quad (2.3)$$

where  $g_{h VV}^{\text{SM}}$  denotes the SM coupling between gauge bosons and the Higgs boson.

Besides adding a singlet to the SM, the Two-Higgs-Doublet Model with two instead of only one complex scalar doublet is the simplest scalar extension of the SM. Additionally, it is capable of fulfilling the afore-mentioned selection of constraints. That THDMs have not yet been ruled out by experimental data, may in itself be seen as reason enough to study them. Apart from this fact and its simplicity, there are however various other sources of motivation for THDMs.

Supersymmetry is often adduced as one of the most prominent motivations for THDMs [20–24]. Due to the structure of the superpotential, one doublet is not sufficient to give mass to both, up-type and down-type quarks. In addition, a second doublet is required to ensure supersymmetric models to be anomaly-free. The scalar sector of the Minimal Supersymmetric Standard Model (MSSM) is indeed a special case of a type II THDM (see Sec. 2.3).

One of the insufficiencies of the SM is that it is not able to explain the prevalence of matter over antimatter in our universe. THDMs provide features and mechanisms that could help to explain baryogenesis [25–29]. On the one hand a larger parameter space compared to the SM and thus more flexibility in the scalar mass spectrum and on the other hand sources of both explicit and spontaneous CP-violation may be able to generate a sufficient asymmetry between matter and antimatter.

On a last note, THDMs are the low energy effective field theory of other BSM models, such as axion models [30], and are therefore an important tool when searching for new physics that may appear indirectly through loops.

In order to point out what the changes compared to the SM with one complex doublet are, when introducing two complex scalar  $SU(2)$  doublets  $\Phi_1$  and  $\Phi_2$  with hypercharge  $+1$ , we may cast the Lagrangian schematically into

$$\begin{aligned}
\mathcal{L}_{\text{EW}} = & \sum_{\psi} \bar{\psi} i \not{D} \psi - \frac{1}{4} W_{\mu\nu}^a W_a^{\mu\nu} - \frac{1}{4} F_{\mu\nu} F^{\mu\nu} + \mathcal{L}_{\text{Ghost}} \\
& + \sum_{i=1,2} (D_{\mu} \Phi_i)^{\dagger} (D^{\mu} \Phi_i) \\
& + \mathcal{L}_{\text{GF}}(\Phi_1, \Phi_2, A_{\mu}^a, B_{\mu}) \\
& - V(\Phi_1, \Phi_2) \\
& + \mathcal{L}_{\text{Yuk}}(\Phi_1, \Phi_2, \{\psi\}) .
\end{aligned} \tag{2.4}$$

Because the scalar doublets transform trivially under the  $SU(3)_C$  gauge group and do not couple strongly, the QCD structure is suppressed in the Lagrangian and only the EW gauge group is considered. The covariant derivative then reads

$$D_{\mu} = \partial_{\mu} + ig A_{\mu}^a \tau_a + ig' B_{\mu} , \tag{2.5}$$

where  $g$  and  $g'$  are the EW gauge couplings,  $\tau_a$  the Pauli matrices,  $B_{\mu}$  the  $U(1)_Y$  gauge field and  $A_{\mu}^a$  the  $SU(2)_L$  gauge fields ( $a = 1, 2, 3$ ). The first line of Eq. (2.4) is unchanged compared to the SM. The first term is the kinetic term of all fermions (the sum runs over all fermion doublets). The second and the third term are the kinetic terms of the  $SU(2)_L$  gauge fields, constructed from their field strength tensor  $W_{\mu\nu}^a$  and the  $U(1)_Y$  gauge field with the field strength tensor  $F_{\mu\nu}$ . The last term is the ghost Lagrangian from quantizing the former non-abelian  $SU(2)_L$  gauge fields.

The second and third line of Eq. (2.4) contain the kinetic terms of the scalars and the gauge fixing Lagrangian, that are the straight forward generalizations of their analogue terms in the SM. For the most general THDM the scalar potential  $V$  and the Yukawa-Lagrangian  $\mathcal{L}_{\text{Yuk}}$  finally will contain all operators up to dimension four, that are compatible with the gauge symmetry and Lorentz invariance. These requirements still allow for a wide range of models with different phenomenology and physics as will be explained in the following two sections.

## 2.2. The Scalar Potential

The most general scalar potential, that can be constructed from two complex scalar isospin doublets such that it respects the  $SU(2)_L \otimes U(1)_Y$  gauge symmetry and the requirement of renormalizability has 14 real-valued independent parameters [15]. After unphysical phases have been rotated away, one is left with 11 physical parameters and a potential, in which in general CP symmetry is broken explicitly and which has a very rich vacuum structure. If the potential is bounded from below, a global minimum has to exist, however in contrast to the SM, it is in general not unique. Strongly depending on the 11 parameters, the global minimum can be charge breaking, (spontaneously) CP-breaking or a ‘normal’ minimum where the latter refers to the analogue of the SM with a real-valued vev in the lower component of each doublet.

Although before the background of baryogenesis, THDMs with explicit and spontaneous CP-breaking have their own strong motivation, the focus in this thesis lies on a phenomenological study of the decays  $H^+ \rightarrow W^+ h/H$  in a CP-conserving THDM as well as the comparison of renormalization schemes for the scalar sector thereof. Requiring a CP-conserving potential and additionally imposing a  $Z_2$  symmetry, allows to restrict the most general scalar potential to the following form

$$\begin{aligned} V(\Phi_1, \Phi_2) = & m_{11}^2 \Phi_1^\dagger \Phi_1 + m_{22}^2 \Phi_2^\dagger \Phi_2 - m_{12}^2 (\Phi_1^\dagger \Phi_2 + \Phi_2^\dagger \Phi_1) \\ & + \frac{\lambda_1}{2} (\Phi_1^\dagger \Phi_1)^2 + \frac{\lambda_2}{2} (\Phi_2^\dagger \Phi_2)^2 + \lambda_3 \Phi_1^\dagger \Phi_1 \Phi_2^\dagger \Phi_2 + \lambda_4 \Phi_1^\dagger \Phi_2 \Phi_2^\dagger \Phi_1 \\ & + \frac{\lambda_5}{2} \left( (\Phi_1^\dagger \Phi_2)^2 + (\Phi_2^\dagger \Phi_1)^2 \right), \end{aligned} \quad (2.6)$$

that has 8 independent real-valued parameters. The parameters  $m_{11}, m_{22}$  and  $m_{12}$  have mass dimension, while the  $\lambda_i$  ( $i = 1, \dots, 5$ ) are dimensionless. The reason behind imposing a  $Z_2$  symmetry is to avoid FCNCs and will be explained in Sec. 2.3. Note that the bilinear term proportional to  $m_{12}$ , that mixes the two doublets, is in general kept in this potential, although it softly breaks the latter symmetry. The parametrization of the potential in Eq. (2.6) is very common in the literature [15, 17, 31]. Nonetheless an alternative parametrization of the CP-conserving potential is presented in App. C. This parametrization is used in the Higgs Hunter's Guide [14] as well as in the `FeynArts` model file (see Sec. 6.1).

Assuming normal vacua

$$\langle \Phi_i \rangle_0 = \begin{pmatrix} 0 \\ \frac{v_i}{\sqrt{2}} \end{pmatrix} \quad \text{with } i = 1, 2, \quad (2.7)$$

each doublet may be expanded around its vev and split into the charged complex field  $\omega_i^+$ , the neutral CP-even real field  $\rho_i$  and the neutral CP-odd real field  $\eta_i$

$$\Phi_i = \begin{pmatrix} \omega_i^+ \\ \frac{v_i + \rho_i + i\eta_i}{\sqrt{2}} \end{pmatrix} \quad \text{with } i = 1, 2. \quad (2.8)$$

For the vevs to be minima of the potential, the two stationary conditions

$$\frac{\partial V(\langle \Phi_1 \rangle_0, \langle \Phi_2 \rangle_0)}{\partial v_i} = 0 \quad \text{with } i = 1, 2 \quad (2.9)$$

have to be fulfilled, which translate into the following conditions for the parameters of the potential

$$T_1 \equiv m_{12}^2 v_2 - m_{11}^2 v_1 - \frac{1}{2} \lambda_1 v_1^2 - \frac{1}{2} \underbrace{(\lambda_3 + \lambda_4 + \lambda_5)}_{\equiv \lambda_{345}} v_1 v_2^2 = 0, \quad (2.10)$$

$$T_2 \equiv m_{12}^2 v_1 - m_{22}^2 v_2 - \frac{1}{2} \lambda_2 v_2^2 - \frac{1}{2} (\lambda_3 + \lambda_4 + \lambda_5) v_1^2 v_2 = 0. \quad (2.11)$$

For later convenience the abbreviation  $\lambda_{345}$  and the tadpole parameters  $T_1$  and  $T_2$  are defined in Eq. (2.10) and Eq. (2.11). Although at leading order the tadpole parameters vanish, they allow to preserve the minimum conditions in a convenient way when going beyond LO (see Sec. 4.4.1).

In order to identify the physical degrees of freedom, the mass matrices have to be diagonalized. Due to gauge and CP invariance of the considered model, only fields with the same quantum numbers for the electric charge and the CP behaviour can mix. The bilinear terms of the scalar potential may therefore be rearranged in the following way

$$V|_{\text{bilinear}} = \frac{1}{2} (\rho_1, \rho_2) \mathcal{M}_\rho \begin{pmatrix} \rho_1 \\ \rho_2 \end{pmatrix} + \frac{1}{2} (\eta_1, \eta_2) \mathcal{M}_\eta \begin{pmatrix} \eta_1 \\ \eta_2 \end{pmatrix} + \frac{1}{2} (\omega_1^-, \omega_2^-) \mathcal{M}_\omega \begin{pmatrix} \omega_1^+ \\ \omega_2^+ \end{pmatrix}, \quad (2.12)$$

where by comparison the entries of the mass matrices  $\mathcal{M}_\rho$ ,  $\mathcal{M}_\eta$  and  $\mathcal{M}_\omega$  can be read off the potential [15] as

$$\mathcal{M}_\rho = \begin{pmatrix} -m_{12}^2 \frac{v_2}{v_1} - \lambda_1 v_1^2 & m_{12}^2 - \lambda_{345} v_1 v_2 \\ m_{12}^2 - \lambda_{345} v_1 v_2 & -m_{12}^2 \frac{v_2}{v_1} - \lambda_1 v_1^2 \end{pmatrix}, \quad (2.13)$$

$$\mathcal{M}_\eta = \left[ \frac{m_{12}^2}{v_1 v_2} - \lambda_5 \right] \begin{pmatrix} v_2^2 & -v_2 v_1 \\ -v_2 v_1 & v_1^2 \end{pmatrix}, \quad (2.14)$$

$$\mathcal{M}_\omega = \left[ \frac{m_{12}^2}{v_1 v_2} - \lambda_4 - \lambda_5 \right] \begin{pmatrix} v_2^2 & -v_2 v_1 \\ -v_2 v_1 & v_1^2 \end{pmatrix}. \quad (2.15)$$

As a real symmetric matrix, each of the three mass matrices can be diagonalized by an orthogonal matrix. In 2 dimensions this rotation matrix can be parametrized by one single angle  $\theta$  and reads in the chosen sign convention

$$R(\theta) \equiv \begin{pmatrix} \cos(\theta) & -\sin(\theta) \\ \sin(\theta) & \cos(\theta) \end{pmatrix}. \quad (2.16)$$

For the trigonometric functions the short-hand notations  $c_\theta = \cos(\theta)$ ,  $s_\theta = \sin(\theta)$  and  $t_\theta = \tan(\theta)$  will be used from here on. From observing that  $\mathcal{M}_\eta$  and  $\mathcal{M}_\omega$  are proportional to each other, it is clear that two angles are sufficient to describe the change of basis for the whole scalar sector. Conventionally these angles are called  $\alpha$  and  $\beta$  and are defined through

$$\begin{pmatrix} \rho_1 \\ \rho_2 \end{pmatrix} = R(\alpha) \begin{pmatrix} H \\ h \end{pmatrix}, \quad (2.17)$$

$$\begin{pmatrix} \eta_1 \\ \eta_2 \end{pmatrix} = R(\beta) \begin{pmatrix} G^0 \\ A^0 \end{pmatrix}, \quad (2.18)$$

$$\begin{pmatrix} \omega_1^+ \\ \omega_2^+ \end{pmatrix} = R(\beta) \begin{pmatrix} G^+ \\ H^+ \end{pmatrix}, \quad (2.19)$$

where the pairs of scalars on the left-hand side are referred to as the gauge basis, as it is those fields, in terms of which the kinetic term in the Lagrangian is formulated. The pairs of scalars on the right-hand side of the Eqs. (2.17–2.19) are accordingly referred to as the mass

basis, as in this basis the mass matrices become diagonal

$$R(\alpha)^T M_\rho R(\alpha) = \begin{pmatrix} m_H^2 & 0 \\ 0 & m_h^2 \end{pmatrix}, \quad (2.20)$$

$$R(\beta)^T M_\eta R(\beta) = \begin{pmatrix} 0 & 0 \\ 0 & m_{A^0}^2 \end{pmatrix}, \quad (2.21)$$

$$R(\beta)^T M_\omega R(\beta) = \begin{pmatrix} 0 & 0 \\ 0 & m_{H^\pm}^2 \end{pmatrix}. \quad (2.22)$$

Like in the SM there are three massless would-be Goldstone bosons  $G^0$ ,  $G^+$  and  $G^-$  that correspond to the three broken symmetries and provide the longitudinal polarizations of the three massive gauge bosons. Given that two complex scalar doublets contain 8 real fields, one is thus left with 5 physical degrees of freedom corresponding to the massive eigenstates of the Eqs. (2.20–2.22). These are the two neutral CP-even scalars denoted by  $H$  and  $h$ , where it is convention to assume  $m_H \geq m_h$  for their masses, the neutral CP-odd field  $A^0$  with the mass  $m_{A^0}$  and finally the two charged complex fields  $H^+$  and  $H^-$  with the mass  $m_{H^\pm}$ .

The mixing angles  $\alpha$  and  $\beta$  play a crucial role for the phenomenology of the THDM as they appear in most couplings in which physical scalar fields are involved. The diagonalization yields the following relations between these angles and the parameters of the potential

$$\tan(\beta) = \frac{v_2}{v_1}, \quad (2.23)$$

$$\tan(2\alpha) = \frac{s_{2\beta} (M^2 - \lambda_{345} v^2)}{c_\beta^2 (M^2 - \lambda_1 v^2) - s_\beta^2 (M^2 - \lambda_2 v^2)}, \quad (2.24)$$

where the following definitions have been used

$$M^2 \equiv \frac{m_{12}^2}{c_\beta s_\beta}, \quad (2.25)$$

$$v \equiv \sqrt{v_1^2 + v_2^2}. \quad (2.26)$$

$v$  represents the scale of electro-weak symmetry breaking and is experimentally fixed to be  $v \approx 246$  GeV [32]. Since needed later, the relations between the masses and the five coupling constants  $\lambda_1 - \lambda_5$  from the potential are given explicitly

$$\lambda_1 = \frac{1}{v^2 c_\beta^2} (s_\alpha^2 m_h^2 + c_\alpha^2 m_H^2 - s_\beta^2 M^2), \quad (2.27)$$

$$\lambda_2 = \frac{1}{v^2 s_\beta^2} (c_\alpha^2 m_h^2 + s_\alpha^2 m_H^2 - c_\beta^2 M^2), \quad (2.28)$$

$$\lambda_3 = 2 \frac{m_{H^\pm}^2}{v^2} + \frac{1}{v^2} \frac{s_{2\alpha}}{s_{2\beta}} (m_H^2 - m_h^2) - \frac{M^2}{v^2}, \quad (2.29)$$

$$\lambda_4 = \frac{1}{v^2} (M^2 + m_{A^0}^2 - 2m_{H^\pm}^2), \quad (2.30)$$

$$\lambda_5 = \frac{1}{v^2} (M^2 - m_{A^0}^2). \quad (2.31)$$



## 2.3. THDMs and FCNCs

Flavor-changing neutral currents are severely restricted by experiment. Any model that allows for tree-level FCNCs is therefore either already excluded or has to explain why these FCNCs have not yet appeared at energies probed so far. The phenomenon of tree-level FCNCs arises from the structure of the interaction between fermions and scalars in the Yukawa Lagrangian  $\mathcal{L}_{\text{Yuk}}$ . In general there exist only the following two independent  $SU(2)_L$  invariant and Lorentz invariant combinations of a fermion doublet  $\Psi = (\psi_1, \psi_2)^T$  and a scalar doublet  $\Phi = (\phi_1, \phi_2)^T$

$$\bar{\Psi}_L \Phi \psi_{2,R} \quad \text{and} \quad (2.32)$$

$$\bar{\Psi}_L \tilde{\Phi} \psi_{1,R} \quad \text{with} \quad \tilde{\Phi}_i \equiv \epsilon_{ji} \Phi_j^* \quad (i, j = 1, 2), \quad (2.33)$$

where  $\epsilon$  is the totally antisymmetric tensor in 2 dimensions with  $\epsilon_{12} = 1$ . The subscripts  $R$  and  $L$  indicate the right-handed (RH) and left-handed (LH) projections  $\psi_{R,L} = P_{R,L} \psi = \frac{1}{2}(1 \pm \gamma_5) \psi$ . The most general  $\mathcal{L}_{\text{Yuk}}$  for two scalar doublets  $\Phi_1$  and  $\Phi_2$  can thus be written as

$$\begin{aligned} \mathcal{L}_{\text{Yuk}} = & - \left( \bar{Q}_L [\Gamma_1^D \Phi_1 + \Gamma_2^D \Phi_2] D_R + \bar{Q}_L [\Gamma_1^U \tilde{\Phi}_1 + \Gamma_2^U \tilde{\Phi}_2] U_R \right. \\ & \left. + \bar{L}_L [\Gamma_1^E \Phi_1 + \Gamma_2^E \Phi_2] E_R \right) + h.c. \quad . \end{aligned} \quad (2.34)$$

The scalar doublets only have  $SU(2)$  structure, while the fermions  $Q \equiv (U, D)^T$  and  $L \equiv (\nu, E)^T$  are  $SU(2)$  doublets and at the same time triplets in flavour space in the sense that  $U \equiv (u, c, t)^T$ ,  $D \equiv (d, s, b)^T$ ,  $\nu \equiv (\nu_e, \nu_\mu, \nu_\tau)^T$  and  $E \equiv (e, \mu, \tau)^T$ . The RH projections are singlets with respect to  $SU(2)$  transformations and the Yukawa coupling matrices  $\Gamma_i^F$  ( $i = 1, 2$  and  $F = U, D, L$ ) are  $3 \times 3$  complex matrices in flavour space.

In the SM without a second doublet  $\Phi_2$ , the mass matrix of the fermions is given by  $v_1/\sqrt{2}$  times  $\Gamma_1^F$ . Hence this mass matrix and the coupling matrix  $\Gamma_1^F$  between scalars and fermions can be simultaneously diagonalized in flavor space, which means that there are no tree-level FCNCs. However in the presence of two scalar doublets like in Eq. (2.34),  $\Gamma_1^F$  and  $\Gamma_2^F$  do not necessarily diagonalize at the same time. In general there will therefore be non-vanishing couplings between a neutral scalar  $\phi$  and two fermions of different flavours. This would for instance allow for  $\bar{d}s\phi$  terms that induce  $K-\bar{K}$ -mixing at tree level.

General THDMs thus suffer from FCNCs, but the structure of  $\mathcal{L}_{\text{Yuk}}$  makes it evident how this issue can be circumvented. If each type of right-handed fermions of the same electric charge coupled to only one scalar doublet, a situation analogous to the SM case is restored and the existence of tree-level FCNCs is prevented. To this end either  $\Gamma_1^F$  or  $\Gamma_2^F$  has to vanish for each group of fermions  $F$ , which in the following will be formulated more elegantly in terms of symmetry requirements [15]. As far as the quarks are concerned, there are only two possibilities. Either both types of RH quarks couple to one and the same doublet or they couple to different ones. Conventionally these two cases are denoted and defined as follows, where it is assumed that the charged leptons couple to the same doublet as the RH down-type quarks:

- **Type I:** All RH quarks and RH charged leptons couple to the same doublet  $\Phi_2$ . This is achieved by a  $Z_2$ -symmetry under  $\Phi_1 \mapsto -\Phi_1$ .
- **Type II:** All RH up-type quarks couple only to  $\Phi_2$ , while all RH down-type quarks and RH charged leptons couple only to  $\Phi_1$ . This is achieved by the symmetry under the simultaneous  $Z_2$ -transformations  $\Phi_1 \mapsto -\Phi_1$ ,  $(D_R)_i \mapsto -(D_R)_i$  and  $(E_R)_i \mapsto -(E_R)_i$  ( $i$  being the flavour index).

Of course it is not a necessity to require the same transformations for the charged leptons as for the down-type quarks. Consequently there are two more models:

- **Lepton-specific model:** All RH down-type quarks couple to  $\Phi_2$  but all RH charged leptons couple to  $\Phi_1$ . This is achieved by the symmetry under the simultaneous  $Z_2$ -transformations  $\Phi_1 \mapsto -\Phi_1$ , and  $(E_R)_i \mapsto -(E_R)_i$ .
- **Flipped model:** The RH up-type quarks and the RH charged leptons couple to  $\Phi_2$ , while the RH down-type quarks couple to  $\Phi_1$ . This is achieved by the symmetry under the simultaneous  $Z_2$ -transformations  $\Phi_1 \mapsto -\Phi_1$  and  $(D_R)_i \mapsto -(D_R)_i$ .

The scalar sector of the MSSM is a type II THDM. Due to relations that are imposed by supersymmetry, it has however a smaller number of independent parameters than a general THDM (see e.g. [15]). See Djouadi's review [33] for details on the Higgs sector of the MSSM.

## 2.4. Sets of Independent Parameters

The question of complete sets of independent parameters is naturally a crucial one, not only as it gives a lower bound to the number of measurements needed to fix the parameters of a THDM, but it is also important in order to develop consistent renormalization schemes. At LO the mixing angle  $\tan(\beta)$  is given by the ratio of the vevs, which in turn feed into masses of the gauge bosons. Since also the EW gauge couplings  $g$  and  $g'$  or the masses  $M_W$  and  $M_Z$ , respectively, will have to be renormalized, it is sensible to examine the set of parameters from the scalar potential together with the electroweak parameters  $g$  and  $g'$  or  $M_W$  and  $M_Z$ , respectively.

In the gauge basis one counts 8 parameters from the scalar potential, two vevs and the two gauge couplings. Most conveniently the tadpole parameters  $T_1$  and  $T_2$  are used to replace  $m_{11}$  and  $m_{22}$ . One is hence left with the following set of 12 independent parameters in the gauge basis

$$\boxed{\{ T_1, T_2, m_{12}, \lambda_1 - \lambda_5, v_1, v_2, g, g' \} \equiv SG .} \quad (2.35)$$

In the mass basis a set of independent parameters will certainly contain all the scalar masses, the masses of the gauge bosons, the electron charge as well as  $\tan(\beta)$ . In order to avoid complication when renormalizing the scalar sector, it is feasible to also choose the tadpole parameters  $T_h$  and  $T_H$ , though now rotated into the mass basis. This gives a set of 10 independent parameters that is not yet a complete one. Due to the structure of the equations (2.27) to (2.31) there are restrictions to which other two parameters can be chosen. Despite the phenomenological relevance, e.g.  $m_{12}$  and  $\lambda_5$  cannot be chosen at the same time. Below possible choices are given names for later reference

$$\boxed{\{m_h, m_H, m_{H^\pm}, m_{A^0}, M_W, M_Z, e, \tan(\beta), T_h, T_H\} \cup \begin{cases} \{\alpha, M\} \\ \{\alpha, \lambda_5\} \\ \{\lambda_3, \lambda_5\} \end{cases} \equiv \begin{cases} SP1 \\ SP2 \\ SP3 \end{cases}} \quad (2.36)$$

## 2.5. General Notation

For later convenience the following general notation shall be introduced in order to refer to any pair of scalar fields of the same quantum numbers in the gauge and the mass basis respectively

$$\begin{pmatrix} \gamma_1 \\ \gamma_2 \end{pmatrix} \in \left\{ \begin{pmatrix} \rho_1 \\ \rho_2 \end{pmatrix}, \begin{pmatrix} \eta_1 \\ \eta_2 \end{pmatrix}, \begin{pmatrix} \omega_1^+ \\ \omega_2^+ \end{pmatrix} \right\}, \quad (2.37)$$

$$\begin{pmatrix} f_1 \\ f_2 \end{pmatrix} \in \left\{ \begin{pmatrix} H \\ h \end{pmatrix}, \begin{pmatrix} G^0 \\ A \end{pmatrix}, \begin{pmatrix} G^+ \\ H^+ \end{pmatrix} \right\}, \quad (2.38)$$

where the transformation between the two basis may be formulated with a general rotation angle  $\theta$

$$\begin{pmatrix} \gamma_1 \\ \gamma_2 \end{pmatrix} = R(\theta) \begin{pmatrix} f_1 \\ f_2 \end{pmatrix}, \quad \theta \in \{\alpha, \beta\}. \quad (2.39)$$

Accordingly a subscript ' $\gamma$ ' or ' $f$ ' indicates a pair of scalars in the gauge or mass basis. With the mass matrices in the gauge basis  $\mathcal{M}_\gamma$  and the diagonal mass matrices  $\mathcal{D}_f$ , the bilinear terms of the potential read in this notation

$$\sum_{\text{all pairs } \gamma} \frac{1}{2} \begin{pmatrix} \gamma_1^\dagger & \gamma_2^\dagger \end{pmatrix} \mathcal{M}_\gamma \begin{pmatrix} \gamma_1 \\ \gamma_2 \end{pmatrix} = \sum_{\text{all pairs } f} \frac{1}{2} \begin{pmatrix} f_1^\dagger & f_2^\dagger \end{pmatrix} \mathcal{D}_f \begin{pmatrix} f_1 \\ f_2 \end{pmatrix}. \quad (2.40)$$



---

 The Decays  $H^+ \rightarrow W^+ h/H$  at LO
 

---

As motivated in Chapter 1 the process that is explicitly studied in this thesis is the decay of a charged Higgs boson into an on-shell  $W$ -Boson and an on-shell neutral CP-even scalar in a general CP-conserving THDM,

$$H^+ \rightarrow W^+ h/H \quad (3.1)$$

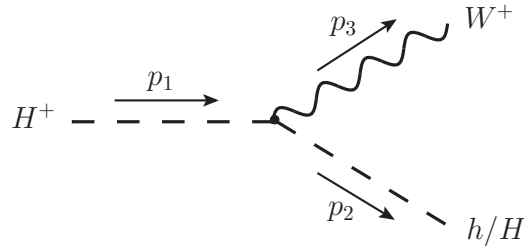


**Figure 3.1.:** Tree-level Feynman diagram for the decays  $H^+ \rightarrow W^+ h/H$  including the definition of momenta.

The Feynman diagram contributing at LO is shown in Fig. 3.1, where additionally the definition for the momenta is introduced that will be used in the following. Despite its triviality and the fact that one can find the tree-level decay width e.g. in [16], it shall be presented in order to introduce the necessary notation. The amplitude  $A_\phi^{\text{LO}}$  corresponding to Fig. 3.1 with  $\phi$  standing for  $h$  or  $H$  respectively, reads

$$A_\phi^{\text{LO}} = \frac{ig}{2} \rho_\phi (p_1 + p_2)_\mu \epsilon_3^{*\mu} = \frac{ie}{2s_W} \rho_\phi 2 (p_1 \epsilon_3^*) , \quad (3.2)$$

where conservation of momentum and the Ward-identity for the on-shell  $W$ -boson have been used.  $g$  is the gauge coupling,  $s_W$  the sine of the Weinberg angle. The vertices for the two different scalars differ only in their dependence on the mixing angles

$$\rho_\phi = \begin{cases} -c_{\beta-\alpha} & \text{for } \phi = h \\ s_{\beta-\alpha} & \text{for } \phi = H . \end{cases} \quad (3.3)$$

The partial decay width is given by (see e.g. [34])

$$\Gamma_\phi \equiv \Gamma(H^+ \rightarrow W^+ s) = \frac{1}{2m_{H^\pm}} \int d\Pi_2 \sum_{\lambda_3} |A_\phi|^2 . \quad (3.4)$$

$\lambda_3$  denotes the polarization of the  $W$ -boson and, given an isotropic squared amplitude, the two-body phase space after integration in the rest frame of the charged Higgs boson is

$$\begin{aligned} \int d\Pi_2 &= \left( \prod_{i=2,3} \int \frac{d^3 p_i}{(2\pi)^3} \frac{1}{2E_i} \right) (4\pi) \delta^{(4)}(p_1 - p_2 - p_3) \\ &= \int d\Omega \frac{|\vec{p}_2|}{(4\pi)^2 m_{H^\pm}} \\ &= \underbrace{\frac{1}{8\pi m_{H^\pm}^2} \lambda(m_{H^\pm}^2, M_W^2, m_\phi^2)}_{\equiv \mathcal{F}_\phi^{\text{Kin}}} , \end{aligned} \quad (3.5)$$

where  $d\Omega$  is the differential solid angle in three dimensions and the phase space function

$$\lambda(a, b, c) \equiv (a^2 + b^2 + c^2 - 2ab - 2bc - 2ca)^{\frac{1}{2}} \quad (3.6)$$

has been used to express the final state momenta in the  $H^+$  rest frame as

$$|\vec{p}_2| = |\vec{p}_3| = \frac{2}{m_{H^\pm}} \lambda(m_{H^\pm}^2, M_W^2, m_\phi^2) . \quad (3.7)$$

Since at any loop order the dependence of the corresponding amplitude on the polarization vector  $\epsilon_3$  of the on-shell  $W$ -boson can be written in terms of only one contraction  $p_1 \epsilon_3$ , it is helpful to define the following factor

$$\begin{aligned} \mathcal{F}_\phi^{\text{Pol}} &\equiv \sum_{\lambda_3} (p_1 \epsilon_3^*) (p_1 \epsilon_3) \\ &= p_1^\mu p_1^\nu \left( -g_{\mu\nu} + \frac{p_{3\mu} p_{3\nu}}{M_W^2} \right) \\ &= \frac{1}{4M_W^2} \lambda^2(m_{H^\pm}^2, M_W^2, m_\phi^2) , \end{aligned} \quad (3.8)$$

where in the second line the polarization sum of a massive vector boson (see e.g. [34]) has been used. The leading order (i.e.  $\propto \alpha_{\text{EM}}$ ) partial decay width is thus given by

$$\Gamma_\phi^{\text{LO}} = \frac{1}{2m_{H^\pm}} \mathcal{F}_\phi^{\text{Kin}} \mathcal{F}_\phi^{\text{Pol}} \left| 2 \frac{ie}{2s_W} \rho_\phi \right|^2 \quad (3.9)$$

$$= \frac{\alpha_{\text{EM}}}{16M_W^2 s_W^2 m_{H^\pm}^3} \rho_\phi^2 \lambda^3(m_{H^\pm}^2, M_W^2, m_\phi^2) . \quad (3.10)$$

### 4.1. A General Note on Renormalization

In a quantum field theory, one will in general encounter correlation functions that are divergent. These divergences manifest themselves in a perturbative framework as ultra-violet (UV) and infra-red (IR) divergences due to arbitrarily large and small loop momenta. However, since the seventies it has been known that the standard model with the  $SU(3)_C \otimes SU(2)_L \otimes U(1)_Y$  gauge group is renormalizable [35]. This means that in relations between only observable quantities all divergent parts drop out at any order of perturbation theory. The same holds for a THDM as it obeys the same gauge symmetries and no operators with dimension higher than four are considered.

In order to investigate the cancellation of divergences, they first have to be regularized so that divergent integrals can be subtracted from one another in a mathematically sensible way - in other words, the divergences have to be under control. In the literature, a variety of different regularization methods can be found. To regularize the UV divergences, we will use dimensional regularization, which preserves both Lorentz invariance and gauge invariance. The treatment of the IR divergences will be postponed to Sec. 5.2. Dimensional regularization [35, 36] means to calculate the loop integrals in  $D$  dimensions, where the real number  $D$  is the dimension of both the spacetime or respectively the momentum space as well as the fields. Defining  $\epsilon \equiv (D - 4)/2$ , the physically relevant case of four dimensions is retained in the limit of sending  $\epsilon$  to zero. The cancellation of UV divergent terms then translates into the cancellation of singular poles in  $\epsilon$  such that after renormalization the limit of  $\epsilon \rightarrow 0$  can safely be taken.

Instead of speaking about relations between only observables, as used above to define the concept of renormalizability, the so-called counterterm formalism shall be used. Renormalizability in this formalism means that redefining a finite set of parameters is enough to render all correlation functions UV finite at any order of perturbation theory. If the bare Lagrangian before renormalization has  $n$  independent bare parameters  $\{p_{1,0}, \dots, p_{n,0}\}$ , each of them is split into the corresponding renormalized parameter  $p_i$  and its counterterm (CT)  $\delta p_i$  by defining

$$p_{i,0} = p_i + \delta p_i \quad \text{for } i = 1, \dots, n . \quad (4.1)$$

These  $n$  CTs  $\delta p_i$  must be fixed by a set of  $n$  renormalization conditions. This is sufficient to render all  $S$ -Matrix elements finite [37]. However, in order to also obtain finite Green functions, in particular finite self energies, additional field renormalization parameters  $Z_\phi$  have to be introduced, which mediate between bare fields  $\phi_0$  and renormalized fields  $\phi$ :

$$\phi_0 = \sqrt{Z_\phi} \phi. \quad (4.2)$$

What is called a renormalization scheme therefore is a specific choice of a set of  $n$  independent parameters that get independent CTs, a set of  $m$  field renormalization parameters and finally a set of  $n + m$  renormalization conditions that fix the introduced parameters.

Essentially, the counterterm formalism is a convenient way of bookkeeping the regularized poles so that in contrast to the bare parameters, the renormalized ones are UV finite. A physical meaning can therefore be assigned to those renormalized parameters, although this need not be the case depending on what particular finite value they are defined to acquire. Also note that the number of field renormalization parameters  $m$  is not necessarily equal to the number of degrees of freedom of the model. It can be larger as well as smaller and examples for both will be discussed in the following sections.

The renormalization of the SM at one-loop level is well studied and can be found in an abundance of literature (see e.g. [37]). The renormalization of fermionic and gauge bosonic fields as well as electroweak and strong coupling constants is the same in the THDM, except for the fact that corresponding self energies and vertex functions have contributions from a larger scalar sector. The focus shall therefore lie on the scalar sector and in the following sections different renormalization schemes for the THDM shall be discussed in detail and compared with each other.

## 4.2. On-shell Conditions

At the heart of on-shell renormalization conditions lies the idea of using observables to formulate renormalization conditions. These conditions fix counterterms in such a way that, by absorbing particular finite parts, the renormalized parameters of the theory correspond to observables. To only meet the necessary requirement of rendering  $S$ -Matrix elements finite, parameters do not have to be renormalized on-shell. Doing so is rather exploiting the freedom of choice in a way that appeals to physical intuition.

Apart from this intuition, there is however another reason to use on-shell conditions. As long as observable quantities like cross sections and decay widths are calculated, no matter which renormalization scheme is used, eventually all fields of the external particles of this process, have to fulfil on-shell relations. It may therefore seem natural to work with renormalization schemes in which the renormalization conditions preserve the on-shell relations for any physical field at any order of perturbation theory. Through such conditions the scheme becomes generically applicable to any process. Otherwise higher order corrections may lead to a violation of the on-shell relations of the fields which thus have to be restored after the renormalization procedure (see discussion in Sec. 4.4.6).

Since we are mainly concerned with the scalar sector of a THDM, on-shell renormalization conditions will be discussed in this context. The basic procedure is however the same for fermions and gauge bosons. Recalling that the notion of a particle in a quantum field theory can be identified with a single pole of a correlation function in the Källén-Lehmann spectral representation (see e.g. [34]), it can be readily understood why the term ‘on-shell conditions’ refers to a set of three conditions, namely:



- |  |       |
|--|-------|
| <ol style="list-style-type: none"> <li>1. The real part of the pole of the propagator is given by the physical mass <math>m</math>.</li> <li>2. The mixing with other fields of the same quantum numbers vanishes on the mass shell, which is defined by <math>p^2 = m^2</math>.</li> <li>3. The field is properly normalized, i.e. the residue of the propagator at the pole is equal to <math>i</math>.</li> </ol> | (4.3) |
|--|-------|

The central object for the discussion therefore is the propagator  $G(p^2)$  in momentum space. For a single scalar field  $\phi$ , i.e. in the absence of further scalar fields with equal quantum numbers, we can write schematically

$$\begin{aligned}
G(p^2) &= \sqrt{Z_\phi^*} \sqrt{Z_\phi} \int d^4x e^{ipx} \langle \Omega | T \phi(x) \phi(0) | \Omega \rangle \\
&= \int d^4x e^{ipx} \langle \Omega | T \phi_0(x) \phi_0(0) | \Omega \rangle
\end{aligned} \tag{4.4}$$

$$= \text{---} + \text{---} \textcircled{1PI} \text{---} + \text{---} \textcircled{1PI} \textcircled{1PI} \text{---} + \dots \tag{4.5}$$

$$= \frac{i}{p^2 - m_0^2 + \Sigma + i\epsilon} , \tag{4.6}$$

where in the first two lines the definition of the field renormalization constant of Eq. (4.2) was used to transform between the bare scalar field  $\phi_0$  and the corresponding renormalized field  $\phi$ . The symbol  $T$  stands for the time ordered product,  $|\Omega\rangle$  is the vacuum state of the interacting theory and  $i\Sigma$  represents the one-particle-irreducible (1PI) two-point-function that is shown pictorially in Eq. (4.5) and which will from here on be called self energy. Defining  $\hat{\Gamma}(p^2)$  as the inverse of the renormalized propagator  $\hat{G}(p^2)$  with a relative factor  $i$  as

$$\hat{G}(p^2) = i\hat{\Gamma}^{-1}(p^2) , \tag{4.7}$$

and introducing a mass CT through  $m_0^2 = m^2 + \delta m^2$ , one can easily identify that

$$\hat{\Gamma}(p^2) = \sqrt{Z^*} \sqrt{Z} [ p^2 - (m^2 + \delta m^2) + \Sigma ] . \tag{4.8}$$

In a CP-conserving THDM however, there are three pairs of scalars as defined in Eq. (2.38), within each of which mixing is allowed. Most conveniently the inverse propagator is then cast into a  $(2 \times 2)$ -matrix structure. Making use of the general notation, introduced in Sec. 2.5, the field renormalization, which is to be specified later, may in general be denoted by a  $(2 \times 2)$ -matrix  $\sqrt{Z_f}$

$$\begin{pmatrix} f_1 \\ f_2 \end{pmatrix}_0 = \sqrt{Z_f} \begin{pmatrix} f_1 \\ f_2 \end{pmatrix} \equiv \left( \mathbf{1}_{2 \times 2} + \frac{1}{2} \delta Z_f \right) \begin{pmatrix} f_1 \\ f_2 \end{pmatrix} . \tag{4.9}$$

With  $D_f$  being the corresponding diagonal mass matrix and  $\Sigma_f$  the matrix with the self energies  $\Sigma_{f_i f_j}$  of the scalars  $f_i$  and  $f_j$  as entries, the generalized version of Eq. (4.8) is given by

$ \hat{\Gamma}_f(p^2) = \sqrt{Z_f^\dagger} [ p^2 \mathbf{1}_{2 \times 2} - (D_f + \delta D_f) + \Sigma_f ] \sqrt{Z_f} . $	(4.10)
---	--------

To translate the general on-shell conditions into conditions in terms of this  $\hat{\Gamma}_f(p^2)$ , we first observe that

$$\begin{aligned}\hat{G}_f &= i \hat{\Gamma}_f^{-1} \\ &= \frac{i}{\underbrace{\hat{\Gamma}_{f_1 f_1} \hat{\Gamma}_{f_2 f_2} - \hat{\Gamma}_{f_1 f_2}^2}_{=\det(\hat{\Gamma}_f)}} \begin{pmatrix} \hat{\Gamma}_{f_2 f_2} & -\hat{\Gamma}_{f_1 f_2} \\ -\hat{\Gamma}_{f_1 f_2} & \hat{\Gamma}_{f_1 f_1} \end{pmatrix},\end{aligned}\quad (4.11)$$

where the momentum dependence has been suppressed and it has been made explicit that  $\hat{\Gamma}_f$  is always symmetric. The pole condition defines the physical masses as the real parts of the solutions to the equation

$$\det(\hat{\Gamma}_f(p^2)) = 0. \quad (4.12)$$

This simplifies, if first imposing that the mixing has to vanish on the mass shell<sup>1</sup>

$$\boxed{\operatorname{Re}(\hat{\Gamma}_{f_1 f_2}(m_{f_1}^2)) \stackrel{!}{=} 0, \quad \operatorname{Re}(\hat{\Gamma}_{f_1 f_2}(m_{f_2}^2)) \stackrel{!}{=} 0.} \quad (4.13)$$

From Eq. (4.12) it then follows that for the masses  $m_{f_1}$  and  $m_{f_2}$ , it must hold that

$$\boxed{\operatorname{Re}(\hat{\Gamma}_{f_1 f_1}(m_{f_1}^2)) \stackrel{!}{=} 0, \quad \operatorname{Re}(\hat{\Gamma}_{f_2 f_2}(m_{f_2}^2)) \stackrel{!}{=} 0.} \quad (4.14)$$

The third condition that the residue at the pole of the propagator is equal to  $i$ , eventually translates into

$$\boxed{\operatorname{Re}\left(\frac{\partial \hat{\Gamma}_{f_1 f_1}(p^2)}{\partial p^2}\right)\bigg|_{p^2=m_{f_1}^2} \stackrel{!}{=} 1, \quad \operatorname{Re}\left(\frac{\partial \hat{\Gamma}_{f_2 f_2}(p^2)}{\partial p^2}\right)\bigg|_{p^2=m_{f_2}^2} \stackrel{!}{=} 1.} \quad (4.15)$$

Note that beyond one-loop level one has to replace the ‘Re’ in the Eqs. (4.13–4.15) by ‘ $\widetilde{\operatorname{Re}}$ ’ [37] which takes only the real parts of the loop integrals while taking into account the imaginary parts from coupling constants.

The term ”on-shell conditions” will only be used in the strict sense as defined above, which is literally ensuring that a field satisfies the three on-shell relations of Eq. (4.3) beyond LO. In a broader sense, it is sometimes used to refer to a renormalization condition, through which a counterterm absorbs particular finite parts, such as defining the electric charge  $e$  to be the coupling constant for the  $ee\gamma$  interaction in the Thomson-limit. It will not be used in this sense here.

### 4.3. A Matter of the Order of Doing Things?

In the context of the MSSM, whose scalar sector is a type II THDM (see Sec. 2.3), an often drawn distinction is the order of renormalizing and rotating from the gauge to the mass basis.

<sup>1</sup>As at NLO only the interference term of the LO amplitude and the NLO amplitude contributes to the correction of the decay widths, the imaginary parts in the counterterms drop out. In the following sections of this thesis the ‘Re’ in the on-shell conditions that require the vanishing mixing of physical scalars on their mass shell will therefore be omitted in order to have the same notation as used in the formulae given in [17].

Because this appears to be a potentially confusing issue, I shall briefly outline it and discuss the connection to the situation in a general THDM.

Given two relevant bases, the mass basis and the gauge basis, one may wonder in which basis to renormalize. A priori, both options must be possible and this distinction is often framed as a choice between first renormalizing and then rotating or vice versa. The latter is what has been introduced in Sec. 4.2, but what are the implications of the former?

The mixing angles appear only when going from one basis to another. Taking seriously that the renormalization is carried out in the gauge basis, where  $\alpha$  and  $\beta$  do not yet exist, suggests not to renormalize these mixing angles. This is to say that the very definition of the angles is that they diagonalize the already renormalized mass matrices. A consequence of this is that beyond leading order, one has to distinguish between  $\beta$  as defined by the ratio of vevs ( $\Phi_{i,2}$  refers to the lower component of the  $i$ th doublet) on the one hand,

$$\tan(\beta) \equiv \frac{\langle \Phi_{2,2} \rangle_0}{\langle \Phi_{1,2} \rangle_0} \mapsto \tan(\beta) + \delta \tan(\beta) \quad (4.16)$$

and the two distinct angles  $\beta_c$  and  $\beta_n$  on the other hand, which diagonalize the renormalized mass matrix of the charged scalars and the neutral CP-odd scalars, respectively,

$$\begin{pmatrix} \omega_1^+ \\ \omega_2^+ \end{pmatrix} = R(\beta_c) \begin{pmatrix} G^+ \\ H^+ \end{pmatrix}, \quad (4.17)$$

$$\begin{pmatrix} \eta_1 \\ \eta_2 \end{pmatrix} = R(\beta_n) \begin{pmatrix} G^0 \\ A^0 \end{pmatrix}. \quad (4.18)$$

This is important, because in the mass matrices and vertices the vevs  $v_1$  and  $v_2$  are typically replaced by  $M_W$ ,  $M_Z$ ,  $e$  and  $\tan(\beta)$ . As a result ‘ $\tan(\beta)$ ’ appears in the sense of the definition in Eq. (4.16) as well as in the role of a mixing angle. Once the replacement rule of taking  $\tan(\beta)$  to  $\tan(\beta) + \delta \tan(\beta)$  has been applied consistently to only  $\tan(\beta)$  but not  $\tan(\beta_c)$  and  $\tan(\beta_n)$ , the indices can be dropped again, since at LO all three are identical.

If one still chose scalar masses as input parameters, which implies that they preserve their meaning as physical masses beyond LO, the on-shell pole conditions would have to be imposed on the inverse propagator for physical fields, which in analogy to Eq. (4.10), now reads

$$\Gamma_f(p^2) = R^\dagger(\theta) \left[ \sqrt{Z}_\gamma^\dagger \left[ p^2 \mathbb{1}_{2 \times 2} - (M_\gamma + \delta M_\gamma) + \Sigma_\gamma \right] \sqrt{Z}_\gamma \right] R(\theta), \quad (4.19)$$

where  $\gamma$  indicates the gauge basis and  $\theta$  is the corresponding mixing angle  $\alpha$ ,  $\beta_c$  or  $\beta_n$ . This step is technically inconvenient considering the mass matrices  $M_\gamma$  of the Eqs. (2.13–2.15) and the relations between masses and the parameters of the potential in Eqs. (2.27–2.31). This observation is admittedly no surprise as saying to ‘first renormalize and then rotate’ already suggests that this approach is at odds with choosing the physical masses  $m_{f_i}$  as input parameters.

The reason why this approach of renormalizing in the gauge basis is applied in certain models is that the analytical diagonalization of the mass matrices can be difficult or even impossible if these are complicated matrices in more than two dimensions. This is indeed the case in CP-violating THDMs or in the next-to-minimal supersymmetric model. One therefore chooses only those scalar masses as input parameters for which the analytical diagonalization

is accessible, while the other input parameters are chosen from the gauge basis.

In a CP-conserving THDM however, the analytical relations between all scalar masses and the parameters of the scalar potential are easy to derive and are known. It is therefore natural to choose all scalar masses as input parameters, i.e. to choose one of the physical parameter sets described in Eq. (2.36) and to perform the renormalization in the mass basis. This is reflected in the fact that typical parametrizations of the Feynman rules use all scalar masses [17, 38]. On a last note, it may in general seem clearer and more instructive to talk about which set of independent parameters is chosen, instead of talking about whether to first renormalize and then rotate or vice versa.

## 4.4. Renormalization of the Scalar Sector

### 4.4.1. Mass Renormalization

As pointed out in the last section, for a CP-conserving THDM it is both natural and convenient to choose the masses as independent parameters and to renormalize the scalar sector in the mass basis. The inverse propagator is thus given by Eq. (4.10) and as a complete set of independent parameters *SP1* defined in Eq. (2.36) shall be chosen. The latter choice is also convenient because this is the set in terms of which the THDM model file of the mathematica package *FeynArts* [38] is formulated (except for the necessary transformation between  $M$  and  $\Lambda_5$  given in Eq. (C.7)).

For better readability, the index "0" for bare quantities will from here on be dropped and the relation between bare and renormalized parameters will instead be expressed by replacement rules. The inverse propagator, expanded to NLO, reads

$$\hat{\Gamma}_f(p^2) = p^2 \mathbb{1} - D_f + \underbrace{\Sigma_f - \delta D_f + \frac{1}{2} \delta Z_f^\dagger (p^2 \mathbb{1} - D_f) + \frac{1}{2} (p^2 \mathbb{1} - D_f) \delta Z_f}_{\equiv \hat{\Sigma}_f(p^2)}. \quad (4.20)$$

As introduced in the equation above,  $\hat{\Sigma}_f$  denotes the matrix of renormalized self energies. The mass counterterms, defined through

$$\begin{aligned} m_H^2 &\mapsto m_H^2 + \delta m_H^2, \\ m_h^2 &\mapsto m_h^2 + \delta m_h^2, \\ m_{A^0}^2 &\mapsto m_{A^0}^2 + \delta m_{A^0}^2, \\ m_{H^\pm}^2 &\mapsto m_{H^\pm}^2 + \delta m_{H^\pm}^2, \end{aligned} \quad (4.21)$$

are fixed by the corresponding on-shell pole conditions of Eq. (4.14). To this end, it is first necessary to derive the explicit expressions in the matrix  $\delta D_f$ , in which the tadpole counterterms

$$\begin{aligned} T_1 &\mapsto 0 + \delta T_1, \\ T_2 &\mapsto 0 + \delta T_2 \end{aligned} \quad (4.22)$$

show up. Recalling that in the gauge basis the parameters  $m_{11}$  and  $m_{22}$  have been replaced by the tadpole parameters, we observe that before setting the latter to zero they appear in  $M_\gamma$  in the same way for all three pairs of scalars

$$M_\gamma = M_\gamma |_{\{T_i=0\}} + \begin{pmatrix} \frac{T_1}{v_1} & 0 \\ 0 & \frac{T_2}{v_2} \end{pmatrix}. \quad (4.23)$$

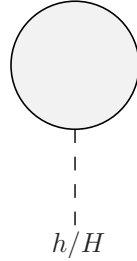
For the diagonal mass matrix this translates into

$$D_f = R^\dagger(\theta) M_\gamma R(\theta) = \begin{pmatrix} m_{f_1}^2 & 0 \\ 0 & m_{f_2}^2 \end{pmatrix} + R^T(\theta) \begin{pmatrix} \frac{T_1}{v_1} & 0 \\ 0 & \frac{T_2}{v_2} \end{pmatrix} R(\theta), \quad (4.24)$$

which allows to identify  $\delta D_f$  as

$$\delta D_f = \begin{pmatrix} \delta m_{f_1}^2 & 0 \\ 0 & \delta m_{f_2}^2 \end{pmatrix} + \underbrace{R(\theta)^T \begin{pmatrix} \frac{\delta T_1}{v_1} & 0 \\ 0 & \frac{\delta T_2}{v_2} \end{pmatrix} R(\theta)}_{\equiv \delta T}, \quad (4.25)$$

where the counterterms for the angles  $\delta\alpha$  and  $\delta\beta$ , which in principle enter through  $R(\theta)$ , do not appear at NLO. Only beyond NLO, terms of the order  $\delta\theta\delta T$  would have to be considered. The explicit forms of the matrices  $\delta T$  are given in App. B. The counterterms  $\delta T_1$  and  $\delta T_2$  therein are fixed by the following renormalization conditions that ensure that the vevs are minima of the Higgs potential also beyond LO



$$+ \delta T_{h/H} \stackrel{!}{=} 0. \quad (4.26)$$

The circle in the above pictorial equation represents the sum of all tadpole diagrams contributing at the corresponding order. Having in mind that the scalar potential appears with a relative minus sign in the Lagrangian,  $T_{h/H}$  can be identified in the following manner

$$\begin{aligned} -V(\Phi_1, \Phi_2)|_{\text{lin. terms}} &= -T_1\rho_1 - T_2\rho_2 \\ &= \underbrace{(-c_\alpha T_1 - s_\alpha T_2)}_{=:T_H} H + \underbrace{(-c_\alpha T_2 + s_\alpha T_1)}_{=:T_h} h. \end{aligned} \quad (4.27)$$

The pole condition of Eq. (4.14) hence in general notation leads to

$$\delta m_{f_i}^2 = \text{Re} \left( \Sigma_{f_i f_i}(m_{f_i}^2) - \delta T_{f_i f_i} \right) \quad \text{for } i = 1, 2, \quad (4.28)$$

where  $\delta T_{f_i f_i}$  stand for the corresponding entry of the matrix  $\delta T$  defined in Eq. (4.25). The four scalar mass CTs of a THDM read explicitly

$$\begin{aligned} \delta m_H^2 &= \text{Re} \left( \Sigma_{HH}(m_H^2) - \delta T_{HH} \right), \\ \delta m_h^2 &= \text{Re} \left( \Sigma_{hh}(m_h^2) - \delta T_{hh} \right), \\ \delta m_{A^0}^2 &= \text{Re} \left( \Sigma_{A^0 A^0}(m_{A^0}^2) - \delta T_{A^0 A^0} \right), \\ \delta m_{H^\pm}^2 &= \text{Re} \left( \Sigma_{H^+ H^+}(m_{H^\pm}^2) - \delta T_{H^+ H^+} \right). \end{aligned} \quad (4.29)$$

What has yet to be specified is what the field renormalization matrix  $\delta Z_f$  is, how its entries are fixed and how the mixing angles are renormalized. Before turning to the renormalization of the angles the so far followed on-shell approach shall first be extended to the scalar fields.

#### 4.4.2. On-shell Renormalized Fields

The most general field renormalization matrix  $\delta Z_f$  is a non-symmetric real matrix

$$\sqrt{Z_f} = \mathbf{1}_{2 \times 2} + \frac{1}{2} \delta Z_f = \mathbf{1}_{2 \times 2} + \frac{1}{2} \begin{pmatrix} \delta Z_{f_1 f_1} & \delta Z_{f_1 f_2} \\ \delta Z_{f_2 f_1} & \delta Z_{f_2 f_2} \end{pmatrix}. \quad (4.30)$$

The pole conditions of Eq. (4.14) have been used to fix the mass counterterms. The four  $\delta Z_{f_i f_j}$  above can be used to allow for all four conditions in Eq. (4.13) and Eq. (4.15) to hold, that ensure correct normalization of the fields and vanishing mixing on the mass shell. Plugging the inverse propagator, expanded to NLO as given in Eq. (4.20) into those conditions, yields

$$\delta Z_{f_i f_i}^{os} = \operatorname{Re} \left( \frac{\partial \Sigma_{f_i f_i}}{\partial p^2} \right) \Big|_{p^2=m_{f_i}^2} \quad \text{for } i = 1, 2, \quad (4.31)$$

$$\delta Z_{f_i f_j}^{os} = \frac{2}{m_{f_i}^2 - m_{f_j}^2} \left[ \Sigma_{f_i f_j}(m_{f_j}^2) - \delta T_{f_i f_j} \right] \quad \begin{array}{l} \text{for } i, j = 1, 2 \\ \text{and } i \neq j. \end{array} \quad (4.32)$$

In this approach for the field renormalization, which is for later distinction indicated by the superscript "os", the scalar sector of the THDM thus has  $3 \cdot 4 = 12$  independent field renormalization constants that are fixed by exactly the same number of  $3 \cdot 4$  conditions. Since needed for later reference the formulas for all three pairs of scalars will be given explicitly

$$\delta Z_{G^+ G^+}^{os} = -\operatorname{Re} \left( \Sigma'_{G^+ G^+}(0) \right), \quad \delta Z_{H^+ H^+}^{os} = -\operatorname{Re} \left( \Sigma'_{H^+ H^+}(m_{H^\pm}^2) \right), \quad (4.33)$$

$$\delta Z_{G^+ H^+}^{os} = -\frac{2}{m_{H^\pm}^2} \left[ \Sigma_{G^+ H^+}(m_{H^\pm}^2) - \delta T_{G^+ H^+} \right], \quad (4.34)$$

$$\delta Z_{H^+ G^+}^{os} = \frac{2}{m_{H^\pm}^2} \left[ \Sigma_{G^+ H^+}(0) - \delta T_{H^+ G^+} \right], \quad (4.35)$$

$$\delta Z_{G^0 G^0}^{os} = -\operatorname{Re} \left( \Sigma'_{G^0 G^0}(0) \right), \quad \delta Z_{A^0 A^0}^{os} = -\operatorname{Re} \left( \Sigma'_{A^0 A^0}(m_{A^0}^2) \right), \quad (4.36)$$

$$\delta Z_{G^0 A^0}^{os} = -\frac{2}{m_{A^0}^2} \left[ \Sigma_{G^0 A^0}(m_{A^0}^2) - \delta T_{G^0 A^0} \right], \quad (4.37)$$

$$\delta Z_{A^0 G^0}^{os} = \frac{2}{m_{A^0}^2} \left[ \Sigma_{G^0 A^0}(0) - \delta T_{A^0 G^0} \right], \quad (4.38)$$

$$\delta Z_{HH}^{os} = -\operatorname{Re} \left( \Sigma'_{HH}(m_H^2) \right), \quad \delta Z_{hh}^{os} = -\operatorname{Re} \left( \Sigma'_{hh}(m_h^2) \right), \quad (4.39)$$

$$\delta Z_{Hh}^{os} = \frac{2}{m_H^2 - m_h^2} \left[ \Sigma_{Hh}(m_h^2) - \delta T_{Hh} \right], \quad (4.40)$$

$$\delta Z_{hH}^{os} = -\frac{2}{m_H^2 - m_h^2} \left[ \Sigma_{hH}(m_H^2) - \delta T_{hH} \right], \quad (4.41)$$

where the shorthand notation  $\Sigma'_{f_i f_i}(p^2) \equiv \frac{\partial \Sigma_{f_i f_i}(p^2)}{\partial p^2}$  has been used.

### 4.4.3. Renormalization of the Angles

So far, all presented renormalization conditions were on-shell conditions that shared the same physical intuition laid out in Sec. 4.2. The mixing angles  $\alpha$  and  $\beta$  are neither observables themselves, nor is there any physically obvious way of fixing their counterterms by relating them to observables.

In any consistent renormalization scheme, the counterterms  $\delta\alpha$  and  $\delta\beta$  will always contain the same UV divergent part. However, the finite terms which are defined to be contained these counterterms, lead to differences such as the extent to which the angles can be given a physical interpretation, whether their value becomes gauge dependent and how numerically stable the calculations are [39].

It turns out that the questions of what the field renormalization matrix  $\delta Z_f$  is, how its entries are fixed and how the mixing angles are renormalized, are inseparably linked. In the following, different schemes are presented to reveal how these questions are linked and what subtleties may arise with respect to the consequences of different finite parts. A final comparison and discussion of the different schemes will be postponed to Chapter 7.

### 4.4.4. Process-dependent Schemes

The idea of a process-dependent scheme to renormalize the mixing angles is similar to the standard way of renormalizing the electric charge in the SM (see Sec. 4.5). Knowing that the theory is renormalizable, the requirement that the amplitude of a physical process has to be UV finite can be used to fix counterterms. It is a consistency check for the scheme that the same such defined CT renders other amplitudes finite, too.

In their paper [16] from 1997 Santos *et al.* calculated the dominant one-loop corrections from top and bottom quarks to the decay  $H^+ \rightarrow W^+ h$  in a CP-conserving THDM. To this end, it is necessary to fix  $\delta(\beta - \alpha)$ . Since the only difference between the  $H^+W^-h$  and  $H^+W^-H$ -vertices is the proportionality to either  $c_{\beta-\alpha}$  or  $s_{\beta-\alpha}$ , both their counterterms share the same  $\delta(\beta - \alpha)$ . It therefore may seem at hand to use the decay  $H^+ \rightarrow W^+ H$  with a heavy Higgs boson to fix  $\delta(\beta - \alpha)$ . This is what has been done in [16] and may serve as an example to illustrate the idea of a process-dependent scheme.

The complete CT of the  $H^+W^-H$ -vertex (see Chapter 5 for further details) can be written schematically as

$$\begin{aligned}
 \text{Diagram: } H^+ \text{ (dashed line, } p_1 \text{)} \text{ --- } \bigotimes \text{ --- } W^+ \text{ (wavy line, } p_3 \text{)} \text{ and } H \text{ (dashed line, } p_2 \text{)} \\
 = 2(p_1 \epsilon_3^*) \frac{ig}{2} s_{\beta-\alpha} \left[ \frac{\delta g}{g} + \frac{\delta s_{\beta-\alpha}}{s_{\beta-\alpha}} \right. \\
 \left. + \frac{1}{2} \delta Z_{WW} + \frac{1}{2} \delta Z_{H^+H^+} + \frac{1}{2} \delta Z_{HH} \right. \\
 \left. - \frac{c_{\beta-\alpha}}{s_{\beta-\alpha}} \left( \frac{1}{2} \delta Z_{G^+H^+} + \frac{1}{2} \delta Z_{hH} \right) \right] \quad (4.42)
 \end{aligned}$$

where, as defined in Chapter 3,  $\epsilon_3$  denotes the polarization vector of the on-shell  $W$ -boson.

The UV finiteness of the amplitude of the decay  $H^+ \rightarrow W^+ H$  implies

$$\left[ \begin{array}{c} \text{Diagram 1: } H^+ \text{ (dashed) enters a circle vertex, } W^+ \text{ (wavy) exits, } h/H \text{ (dashed) exits.} \\ \text{Diagram 2: } H^+ \text{ (dashed) enters a crossed-circle vertex, } W^+ \text{ (wavy) exits, } h/H \text{ (dashed) exits.} \\ \text{Sum of all virtual vertex corrections} \\ \equiv A_H^{\text{VC}} \end{array} \right] \stackrel{!}{=} \text{finite} . \quad (4.43)$$

Using the NLO expansion

$$s_{\beta-\alpha} = c_{\beta-\alpha} \delta(\beta - \alpha) , \quad (4.44)$$

this translates in general into the following expression for  $\delta(\beta - \alpha)$

$$\begin{aligned} \delta(\beta - \alpha) &\stackrel{!}{=} \frac{i}{g c_{\beta-\alpha} (p_1 \epsilon_3^*)} A_H^{\text{VC}} \\ &\quad - \frac{s_{\beta-\alpha}}{c_{\beta-\alpha}} \left( \frac{\delta g}{g} + \frac{1}{2} \delta Z_{WW} + \frac{1}{2} \delta Z_{H^+H^+} + \frac{1}{2} \delta Z_{HH} \right) \\ &\quad + \frac{1}{2} \delta Z_{G^+H^+} + \frac{1}{2} \delta Z_{hH} \\ &\quad + C^{\text{finite}} , \end{aligned} \quad (4.45)$$

where  $C^{\text{finite}}$  is some UV finite constant through which the following three possible choices can be differentiated:

1. The last section opened by saying that the mixing angles themselves are not observables. Nonetheless, the afore-noted analogy to the electric charge renormalization appealed to allow for a, though process-dependent, more physical interpretation of the angles. Applying the same kind of condition for  $\beta - \alpha$  would mean to choose  $C^{\text{finite}}$  such that the predicted NLO partial decay width is equal to the actually measured one. The difference between the present situation and the renormalization of the electric charge is that even before the advent of the SM, measuring electron scattering in the Thomson limit was in principle possible, while we have not yet observed any BSM scalars.
2. What has instead been done by Santos *et al.* in [16], is to set  $C^{\text{finite}}$  to zero, which means that the virtual one-loop corrections to the amplitude of  $H^+ \rightarrow W^+ H$  vanishes and hence the NLO decay width is supposed to be set equal to the LO decay width. In [16], where only top and bottom quarks have been taken into account, this works perfectly fine. Aiming for the full electroweak corrections, this, however, leads to conceptual problems which make it impossible to use the decay  $H^+ \rightarrow W^+ H$  to fix  $\delta(\beta - \alpha)$  in this way. This is due to the issue of IR divergences, which accompany charged external particles. This will be explained in detail in Sec. 5.2.4.
3. If the equal sign in Eq. (4.45) is to be taken in terms of only the UV-divergent parts of the r.h.s. of the equation, then this condition is a minimal subtraction (MS) condition that defines the angle counterterm  $\delta(\beta - \alpha)$  to contain only the term proportional to



the  $1/\epsilon$  pole. The hybrid scheme consisting of on-shell renormalization conditions for the masses and all scalar fields (Eq. (4.29) and Eqs. (4.33–4.41)) together with this  $\overline{\text{MS}}$  condition for  $\delta(\beta - \alpha)$  shall be called *HybMS* for later reference. As far as the UV finiteness is concerned, this scheme works fine, but it turns out not to be a good scheme in terms of the numerical stability of the results. This will be discussed further in Sec. 6.4.

Using the decay  $H^+ \rightarrow W^+ H$  to renormalize mixing angles proved to be unsatisfactory. Once the treatment of real corrections has been introduced, more promising suggestions for a process-dependent scheme, which circumvent the issue of IR divergences, will be discussed in Sec. 5.2.4. As far as the concept of a process-dependent renormalization condition is concerned, using another process will still be along the lines of the example discussed above. Also note that a process-dependent scheme for the mixing angles, which could be applied in any calculation, would have to consist of two different processes to fix both independent counterterms  $\delta\alpha$  and  $\delta\beta$  separately.

#### 4.4.5. The Kanemura Approach

Another way to renormalize the angles is based on work by Kanemura *et al.* [17, 18]. The essential idea is to make the counterterms of the angles,  $\delta\alpha$  and  $\delta\beta$ , show up in the inverse propagator matrix  $\hat{\Gamma}_f(p^2)$  in a way that is consistent with the internal relations of the THDM. Once this is achieved, the angle counterterms can be fixed by imposing the on-shell conditions from Sec. 4.2.

While actually renormalizing in the mass basis, temporarily switching to the gauge basis and back again, reveals the following ansatz for the field renormalization

$$\begin{pmatrix} f_1 \\ f_2 \end{pmatrix} = R(\theta)^T \begin{pmatrix} \gamma_1 \\ \gamma_2 \end{pmatrix} \quad \mapsto \quad R(\theta + \delta\theta)^T \sqrt{Z_\gamma} \begin{pmatrix} \gamma_1 \\ \gamma_2 \end{pmatrix} \quad (4.46)$$

$$\stackrel{\text{NLO}}{=} \underbrace{R(\delta\theta)^T R(\theta)^T \sqrt{Z_\gamma} R(\theta)}_{=: \sqrt{Z_f}} R(\theta)^T \begin{pmatrix} \gamma_1 \\ \gamma_2 \end{pmatrix} \quad (4.47)$$

$$= \sqrt{Z_f} \begin{pmatrix} f_1 \\ f_2 \end{pmatrix}. \quad (4.48)$$

The ‘NLO’ over the equal sign in Eq. (4.47) indicates that in the expansion of the sine and cosine, any term beyond linear order in  $\delta\theta$  has been neglected and that only terms linear in  $\delta\theta$  and  $\delta Z_\gamma$  are taken into account. Apart from this approximation, in which  $R(\theta + \delta\theta)^T = R(\delta\theta)^T R(\theta)^T$  holds, only a unit matrix has been inserted. Identifying the matrix in front of the physical scalars  $f_i$  as the field renormalization matrix leads to the definition of  $\sqrt{Z_f}$  as a product of  $R(\delta\theta)^T$  and  $\sqrt{Z_\gamma}$  that is embraced by rotation matrices. This  $\sqrt{Z_\gamma}$  is some field renormalization matrix in the gauge basis and the naturally arising question is how many free parameters it has.

In their paper [17] from 2008, in which Kanemura *et al.* suggested this approach,  $\sqrt{Z_\gamma}$  is said to be any real but symmetric matrix. It thus has three free parameters and leads to the

following parametrization of the field renormalization matrices in the mass basis

$$\begin{aligned}\sqrt{Z_f^{Kan}} &= R(\delta\theta)^T \begin{pmatrix} 1 + \frac{1}{2}\delta Z_{f_1 f_1} & \delta C_{f_2} \\ \delta C_{f_2} & 1 + \frac{1}{2}\delta Z_{f_2 f_2} \end{pmatrix} \\ &= \begin{pmatrix} 1 + \frac{1}{2}\delta Z_{f_1 f_1} & \delta C_{f_2} + \delta\theta \\ \delta C_{f_2} - \delta\theta & 1 + \frac{1}{2}\delta Z_{f_2 f_2} \end{pmatrix},\end{aligned}\quad (4.49)$$

that are labelled with the superscript "Kan" for later distinction. These matrices read explicitly for the three pairs of scalars

$$\begin{pmatrix} H \\ h \end{pmatrix} \mapsto \begin{pmatrix} 1 + \frac{1}{2}\delta Z_{HH} & \delta C_h + \delta\alpha \\ \delta C_h - \delta\alpha & 1 + \frac{1}{2}\delta Z_{hh} \end{pmatrix} \begin{pmatrix} H \\ h \end{pmatrix}, \quad (4.50)$$

$$\begin{pmatrix} G^0 \\ A^0 \end{pmatrix} \mapsto \begin{pmatrix} 1 + \frac{1}{2}\delta Z_{G^0 G^0} & \delta C_{A^0} + \delta\beta \\ \delta C_{A^0} - \delta\beta & 1 + \frac{1}{2}\delta Z_{A^0 A^0} \end{pmatrix} \begin{pmatrix} G^0 \\ A^0 \end{pmatrix}, \quad (4.51)$$

$$\begin{pmatrix} G^+ \\ H^+ \end{pmatrix} \mapsto \begin{pmatrix} 1 + \frac{1}{2}\delta Z_{G^+ G^+} & \delta C_{H^+} + \delta\beta \\ \delta C_{H^+} - \delta\beta & 1 + \frac{1}{2}\delta Z_{H^+ H^+} \end{pmatrix} \begin{pmatrix} G^+ \\ H^+ \end{pmatrix}. \quad (4.52)$$

The off-diagonal elements for the neutral CP-even scalars contain two free renormalization parameters, which is exactly the amount needed to require both corresponding on-shell conditions of Eq. (4.13),

$$\hat{\Gamma}_{Hh}(m_H^2) \stackrel{!}{=} 0, \quad \hat{\Gamma}_{Hh}(m_h^2) \stackrel{!}{=} 0. \quad (4.53)$$

This is equivalent to simply identifying the off-diagonal elements here with the ones from Eq. (4.30)

$$\frac{1}{2}\delta Z_{Hh}^{os} \stackrel{!}{=} \delta C_h + \delta\alpha, \quad (4.54)$$

$$\frac{1}{2}\delta Z_{hH}^{os} \stackrel{!}{=} \delta C_h - \delta\alpha. \quad (4.55)$$

Using Eq. (4.40) and Eq. (4.41) this yields

$$\delta\alpha = \frac{1}{4}(\delta Z_{Hh}^{os} - \delta Z_{hH}^{os}) = \frac{1}{m_H^2 - m_h^2} \left[ \frac{1}{2}\Sigma_{Hh}(m_h^2) + \frac{1}{2}\Sigma_{Hh}(m_H^2) - \delta T_{Hh} \right], \quad (4.56)$$

$$\delta C_h = \frac{1}{4}(\delta Z_{Hh}^{os} + \delta Z_{hH}^{os}) = \frac{1}{m_H^2 - m_h^2} \left[ \frac{1}{2}\Sigma_{Hh}(m_h^2) - \frac{1}{2}\Sigma_{Hh}(m_H^2) \right]. \quad (4.57)$$

Note that  $\delta C_h$  alone will not be used anywhere, as for physical fields only  $\delta Z_{Hh}^{os}$  and  $\delta Z_{hH}^{os}$  appear in counterterms of vertices.

As far as the off-diagonal elements for the charged and neutral CP-odd scalars are concerned, there are only three free parameters to be fixed by renormalization conditions because the same angle  $\beta$  diagonalizes both the charged and CP-odd mass matrix. This is one parameter fewer than in the general case of Eq. (4.30), which is also to say that it

is one parameter fewer than needed to require all on-shell conditions. As a consequence, one has to choose three out of four possible conditions and not all scalar fields can be on-shell at the same time. Kanemura *et al.* present two out of the four possible choices:

$$\begin{aligned} \text{Set 1:} \quad \delta\beta^{(1)} &= -\frac{1}{2m_{A^0}^2} [\Sigma_{G^0 A^0}(m_{A^0}^2) - \delta T_{G^0 A^0}] \\ &\quad + \Sigma_{G^0 A^0}(0) - \delta T_{G^0 A^0} \quad (4.58) \\ \left\{ \begin{array}{l} \hat{\Gamma}_{G^0 A^0}(0) \stackrel{!}{=} 0 \\ \hat{\Gamma}_{G^0 A^0}(m_{A^0}^2) \stackrel{!}{=} 0 \\ \hat{\Gamma}_{G^+ H^+}(0) \stackrel{!}{=} 0 \end{array} \right\} \Rightarrow \delta C_{H^+}^{(1)} &= \frac{1}{2} \delta Z_{H^+ G^+}^{os} + \delta\beta^{(1)} \quad (4.59) \\ \delta C_{A^0}^{(1)} &= \frac{1}{4} [\delta Z_{A^0 G^0}^{os} + \delta Z_{G^0 A^0}^{os}] \quad (4.60) \end{aligned}$$

and

$$\begin{aligned} \text{Set 2:} \quad \delta\beta^{(2)} &= -\frac{1}{2m_{H^\pm}^2} [\Sigma_{G^+ H^+}(m_{H^\pm}^2) - \delta T_{G^+ H^+}] \\ &\quad + \Sigma_{G^+ H^+}(0) - \delta T_{G^+ H^+} \quad (4.61) \\ \left\{ \begin{array}{l} \hat{\Gamma}_{G^0 A^0}(0) \stackrel{!}{=} 0 \\ \hat{\Gamma}_{G^+ H^+}(m_{H^\pm}^2) \stackrel{!}{=} 0 \\ \hat{\Gamma}_{G^+ H^+}(0) \stackrel{!}{=} 0 \end{array} \right\} \Rightarrow \delta C_{H^+}^{(2)} &= \frac{1}{4} [\delta Z_{H^+ G^+}^{os} + \delta Z_{G^+ H^+}^{os}] \quad (4.62) \\ \delta C_{A^0}^{(2)} &= \frac{1}{2} \delta Z_{A^0 G^0}^{os} + \delta\beta^{(2)}. \quad (4.63) \end{aligned}$$

Concerning the different definitions of  $\delta\beta$ , clearly, different choices for renormalization conditions can only differ in what finite part  $\delta\beta$  contains, but the UV-divergent parts must not differ. This is already remarked in [17] and has been checked again, both numerically and analytically for the Feynman gauge that is being used in this thesis.

Note that in [17] the sum of the two terms in the second line of Eq. (4.58) and Eq. (4.61), respectively, vanish and the equations therefore simplify further. This however only holds in the Landau gauge. In a general gauge, particularly the Feynman gauge,  $\Sigma_{G^0 A^0}(0) - \delta T_{G^0 A^0}$  and  $\Sigma_{G^+ H^+}(0) - \delta T_{G^+ H^+}$  do not vanish and have to be included.

Aiming at on-shell renormalized fields, this scheme can be used as long as not both, a charged Higgs  $H^+$  and a neutral CP-odd scalar  $A^0$ , are external particles of the physical process. Given that this is not the case for the decays  $H^+ \rightarrow W^+ h/H$ , this approach with the choice of Set2 to ensure  $H^+$  to be on-shell, will be referred to as the *Kan* scheme.

In their later paper [18] from 2015, Kanemura *et al.* react to the issue of gauge dependence of  $\tan(\beta)$  in certain renormalization schemes. For the scalar sector of the MSSM this has been discussed in general and exhaustively by Freitas *et al.* [39]. In any renormalization scheme a relation between only observables is necessarily gauge independent. Having to choose a gauge is a consequence of the quantization of gauge fields but is itself an unphysical choice and must not affect physical statements in the afore-mentioned sense. Through the choice of renormalization conditions the gauge independence of parameters such as  $\tan(\beta)$ , that are not observable themselves, may well be affected. This is to say that the relation between observables and  $\tan(\beta)$  can become gauge dependent and therefore in different gauges one would infer a different numerical value for  $\tan(\beta)$  from experimental measurements. Although this is no conceptual or physical problem, it is not desirable if one wishes to assign a physical

intuition to  $\tan(\beta)$ .

The suggestion by Kanemura *et al.* to get rid of such a gauge dependence of  $\tan(\beta)$  goes back to Eq. (4.49). The earlier assumption that  $\sqrt{Z_\gamma}$  is a symmetric matrix is dropped, which of course is nothing else but to introduce more free renormalization parameters that can be used to impose further conditions. The matrices  $\sqrt{Z^{Kan}}$  may now be parametrized as

$$\sqrt{Z_f^{Kan}} = \begin{pmatrix} 1 + \frac{1}{2}\delta Z_{f_1 f_1} & \delta C_{f_1 f_2} + \delta\theta \\ \delta C_{f_2 f_1} - \delta\theta & 1 + \frac{1}{2}\delta Z_{f_2 f_2} \end{pmatrix}. \quad (4.64)$$

Only the off-diagonal elements are affected compared to the former definition in Eq. (4.49). With 8 free parameters for the off-diagonals, there are two more than on-shell conditions ( $3 \cdot 2 = 6$ ), whereas in the first version there was one fewer than possible on-shell conditions. In the neutral CP-even sector the additional freedom is not needed and in [18], it is simply eliminated again by setting

$$\delta C_{Hh} \stackrel{!}{=} \delta C_{hH} \stackrel{!}{=} \delta C_h \quad (4.65)$$

and therefore restoring the situation as in Eq. (4.50). With 5 free parameters on the off-diagonals of the charged and neutral CP-odd sectors, first of all, it is now possible to enforce all scalar fields to be renormalized on-shell by requiring

$$\left\{ \begin{array}{l} \hat{\Gamma}_{G^0 A^0}(m_{A^0}^2) \stackrel{!}{=} 0, \quad \hat{\Gamma}_{G^0 A^0}(0) \stackrel{!}{=} 0, \\ \hat{\Gamma}_{G^+ H^+}(m_{H^\pm}^2) \stackrel{!}{=} 0, \quad \hat{\Gamma}_{G^+ H^+}(0) \stackrel{!}{=} 0 \end{array} \right\}. \quad (4.66)$$

The first two of those conditions imply the following underconstrained system of equations

$$\delta\beta - \delta C_{A^0 G^0} = -\frac{1}{m_{A^0}^2} [\Sigma_{G^0 A^0}(0) - \delta T_{A^0 G^0}], \quad (4.67)$$

$$\delta\beta + \delta C_{G^0 A^0} = -\frac{1}{m_{A^0}^2} [\Sigma_{G^0 A^0}(m_{A^0}^2) - \delta T_{G^0 A^0}]. \quad (4.68)$$

In [18], it is stated that it is the right-hand side of Eq. (4.68), that introduces the gauge dependence. The additional freedom to fix  $\delta C_{A^0 G^0}$  and  $\delta C_{G^0 A^0}$  is then used such that, by definition,  $\delta\beta$  contains only the gauge independent (G.I.) part of the right-hand side of Eq. (4.68)

$$\delta\beta \equiv -\frac{1}{m_{A^0}^2} [\Sigma_{G^0 A^0}(m_{A^0}^2) - \delta T_{G^0 A^0}] \Big|_{\text{G.I.}}. \quad (4.69)$$

As a result the gauge dependence is moved to  $\delta C_{G^0 A^0}$ , which is indeed acceptable as there is no physical meaning to it. Formally this looks like an appealing step, however it remains unclear what Eq. (4.69) means practically speaking. It seems that, unless one does the calculation for the tadpoles and the  $\Sigma_{G^0 A^0}$  self energy with the full dependence on a general  $R_\xi$  gauge parameter, it is hard to know how  $\delta\beta$  would read explicitly.

#### 4.4.6. A Minimal Scheme

As demonstrated in the last sections, for each pair of scalars four independent field renormalization parameters are necessary to fulfil all of the on-shell conditions in Eq. (4.13) and Eq. (4.15). However this is not necessary to only render all S-Matrix elements and self energies UV finite. One may wonder, what the minimum number of field renormalization parameters

in the scalar sector is to meet this requirement.

Due to SU(2)-invariance [40] the minimum number is two, one for each scalar doublet

$$\Phi_i \mapsto \sqrt{Z_i} \Phi_i = \left( 1 + \frac{1}{2} \delta Z_i \right) \Phi_i \quad \text{for } i = 1, 2, \quad (4.70)$$

where  $Z_i, \delta Z_i \in \mathbb{R}$ . Hence in the gauge basis the field renormalization matrix is identical for each of the three pairs of scalars

$$\sqrt{Z_\gamma^{Min}} = \begin{pmatrix} 1 + \frac{1}{2} \delta Z_1 & 0 \\ 0 & 1 + \frac{1}{2} \delta Z_2 \end{pmatrix}. \quad (4.71)$$

Defining the corresponding field renormalization matrices in the mass basis by mere basis transformation of  $\sqrt{Z_\gamma^{Min}}$

$$\sqrt{Z_f^{Min'}} \equiv R(\theta)^T \sqrt{Z_\gamma^{Min}} R(\theta), \quad (4.72)$$

while  $\delta D_f$  is however still the same as defined in Eq. (4.25), turns out not to be sufficient to ensure all renormalized self energies to be UV finite [40]. While this  $\sqrt{Z_f^{Min'}}$  is sufficient to render the amplitude of  $H^+ \rightarrow W^+ h/H$  UV finite, it does not have the needed divergence structure to cancel all divergent parts of the self energies. Where  $\sqrt{Z_f^{Min'}}$  is used in the literature (e.g. [41, 42]),  $\delta D_f$  always contains other off-diagonal contributions that, after all, are linked to the angle counterterms  $\delta\alpha$  and  $\delta\beta$ .

The Kanemura approach does essentially the same, only by defining the angle counterterms to be contained in  $\delta Z_f$  instead of in  $\delta D_f$ . Given how simple and instructive the manipulations of Eq. (4.47) are, it seems natural to just replace  $\sqrt{Z_\gamma}$  by  $\sqrt{Z_\gamma^{Min}}$  and to define

$$\sqrt{Z_f^{Min}} \equiv R(\delta\theta)^T R(\theta)^T \sqrt{Z_\gamma^{Min}} R(\theta) \quad (4.73)$$

$$= \mathbf{1} + \frac{1}{2} \underbrace{\begin{pmatrix} c_\theta^2 \delta Z_1 + s_\theta^2 \delta Z_2 & c_\theta s_\theta (\delta Z_2 - \delta Z_1) + 2\delta\theta \\ c_\theta s_\theta (\delta Z_2 - \delta Z_1) - 2\delta\theta & s_\theta^2 \delta Z_1 + c_\theta^2 \delta Z_2 \end{pmatrix}}_{= \delta Z_f^{Min}}. \quad (4.74)$$

Formally we can then identify

$$\delta Z_{G^+G^+}^{Min} = c_\beta^2 \delta Z_1 + s_\beta^2 \delta Z_2 = \delta Z_{G^0G^0}^{Min}, \quad (4.75)$$

$$\delta Z_{H^+H^+}^{Min} = s_\beta^2 \delta Z_1 + c_\beta^2 \delta Z_2 = \delta Z_{A^0A^0}^{Min}, \quad (4.76)$$

$$\delta Z_{G^+H^+}^{Min} = c_\beta s_\beta (\delta Z_2 - \delta Z_1) + 2 \delta\beta^{Min} = \delta Z_{G^0A^0}^{Min}, \quad (4.77)$$

$$\delta Z_{H^+G^+}^{Min} = c_\beta s_\beta (\delta Z_2 - \delta Z_1) - 2 \delta\beta^{Min} = \delta Z_{A^0G^0}^{Min}, \quad (4.78)$$

$$\delta Z_{HH}^{Min} = c_\alpha^2 \delta Z_1 + s_\alpha^2 \delta Z_2, \quad (4.79)$$

$$\delta Z_{hh}^{Min} = s_\alpha^2 \delta Z_1 + c_\alpha^2 \delta Z_2, \quad (4.80)$$

$$\delta Z_{Hh}^{Min} = c_\alpha s_\alpha (\delta Z_2 - \delta Z_1) + 2 \delta\alpha^{Min}, \quad (4.81)$$

$$\delta Z_{hH}^{Min} = c_\alpha s_\alpha (\delta Z_2 - \delta Z_1) - 2 \delta\alpha^{Min}, \quad (4.82)$$

where the superscript ‘*Min*’ has also been added to the angle CTs to prevent confusion with the ones from other schemes. Given only four free renormalization parameters to be fixed by some set of four renormalization conditions, there is a large variety of possible choices and certainly not all scalars can fulfil on-shell relations at the same time. First a possible choice of four conditions will be presented, then the correct normalization of those fields that are not renormalized on-shell, will be treated.

In order to reduce the complexity of the renormalization procedure for the decay  $H^+ \rightarrow W^+ h/H$ , at least the decaying charged scalar can be forced to fulfil on-shell relations by requiring

$$\left\{ \hat{\Gamma}_{G^+H^+}(m_{H^\pm}^2) \stackrel{!}{=} 0, \quad \text{Re} \left( \frac{\partial \hat{\Gamma}_{H^+H^+}(p^2)}{\partial p^2} \right) \Big|_{p^2=m_{H^\pm}^2} \stackrel{!}{=} 1 \right\}. \quad (4.83)$$

This is equivalent to

$$\left\{ \delta Z_{G^+H^+}^{Min} \stackrel{!}{=} \delta Z_{G^+H^+}^{os}, \quad \delta Z_{H^+H^+}^{Min} \stackrel{!}{=} \delta Z_{H^+H^+}^{os} \right\}, \quad (4.84)$$

where the on-shell  $Z$ -factors are given in Eq. (4.33) and Eq. (4.34). It follows that

$$\delta Z_1 = \delta Z_{H^+H^+}^{os} - \frac{1}{t_\beta} \delta Z_{G^+H^+}^{os} + \frac{2}{t_\beta} \delta \beta^{Min}, \quad (4.85)$$

$$\delta Z_2 = \delta Z_{H^+H^+}^{os} + t_\beta \delta Z_{G^+H^+}^{os} - 2t_\beta \delta \beta^{Min}. \quad (4.86)$$

By requiring <sup>1</sup>

$$\frac{\delta v_1}{v_1} \stackrel{!}{=} \frac{\delta v_2}{v_2}, \quad (4.87)$$

$\delta \beta$  is automatically fixed, too,

$$(1 + t_\beta^2) \delta \beta = \delta t_\beta = \frac{t_\beta}{2} \left( \frac{\delta v_2}{v_2} - \frac{\delta v_1}{v_1} + \delta Z_2 - \delta Z_1 \right) = \frac{t_\beta}{2} (\delta Z_2 - \delta Z_1), \quad (4.88)$$

where the relation between  $\delta \beta$  and  $\delta t_\beta$  only holds at NLO. Inserting Eq. (4.85) and Eq. (4.86) into this result, yields the simple relation

$$\delta \beta^{Min} = \frac{1}{4} \delta Z_{G^+H^+}^{os}, \quad (4.89)$$

which in turn allows to reformulate  $\delta Z_1$  and  $\delta Z_2$  independently of  $\delta \beta^{Min}$

$$\delta Z_1 = \delta Z_{H^+H^+}^{os} - \frac{1}{2t_\beta} \delta Z_{G^+H^+}^{os}, \quad (4.90)$$

$$\delta Z_2 = \delta Z_{H^+H^+}^{os} + \frac{t_\beta}{2} \delta Z_{G^+H^+}^{os}. \quad (4.91)$$

The only renormalization parameter yet to be fixed is  $\delta \alpha^{Min}$ . This can be done by one more on-shell condition, e.g.

$$\hat{\Gamma}_{Hh}(m_H^2) = \hat{\Sigma}_{Hh}(m_H^2) \stackrel{!}{=} 0, \quad (4.92)$$

which determines  $\delta \alpha^{Min}$  to be

$$\delta \alpha^{Min} = \frac{1}{m_H^2 - m_h^2} \left[ \Sigma_{Hh}(m_H^2) - \delta T_{Hh} + \frac{c_\alpha s_\alpha}{2} (m_H^2 - m_h^2) (\delta Z_2 - \delta Z_1) \right]. \quad (4.93)$$

<sup>1</sup>See e.g. [43–45]. Although these papers treat the MSSM, the therein given argument for the legitimacy of this condition is independent of supersymmetry.

The scheme, given through the definition of  $\delta Z_f^{Min}$  and the conditions in the Eqs. (4.29, 4.83, 4.87 and 4.92) will be referred to as the *Min* scheme. I have checked that in this scheme both the renormalized self energies as well as the decay amplitudes of  $H^+ \rightarrow W^+ h/H$  are UV finite.

In order to calculate observables like decay widths and cross sections, it is not sufficient that the amplitude is UV finite. Additionally the fields that correspond to external particles have to fulfil on-shell relations. Apart from their propagators having the pole at the right position, these fields also have to be correctly normalized and to have vanishing mixing on the mass shell. As mentioned in Sec. 4.2, if higher order corrections violate these relations, then they have to be restored after the renormalization procedure. This is well known [41, 46] and can be achieved by a wave function normalization matrix  $Z_N$  that acts on the tuple of amplitudes that differ only by external fields that mix,

$$\begin{pmatrix} \tilde{A}_{\dots f_1 \dots} \\ \dots \\ \tilde{A}_{\dots f_n \dots} \end{pmatrix} = Z_N \begin{pmatrix} A_{\dots f_1 \dots} \\ \dots \\ A_{\dots f_n \dots} \end{pmatrix}. \quad (4.94)$$

The tilde denotes the new linear combinations of fields that satisfy on-shell relations. In Eq. (4.94) a general case with  $n$  mixing scalars has been assumed, while for a CP-conserving THDM there are only pairs of two scalars that mix. In general for any process, there will be as many  $(n \times n)$ -matrices  $Z_N$  acting on the corresponding tuple of amplitudes as there are fields  $f_1 \dots f_n$  in the initial and final state of the process. Parametrizing the wave function normalization matrix  $Z_N$  by [41]

$$Z_N = \begin{pmatrix} \sqrt{Z_{f_1}} & \sqrt{Z_{f_1}} Z_{f_1 f_2} \\ \sqrt{Z_{f_2}} Z_{f_2 f_1} & \sqrt{Z_{f_2}} \end{pmatrix}, \quad (4.95)$$

its entries are given in terms of renormalized self energies  $\hat{\Sigma}_{f_i f_j}$  ( $i, j = 1, 2; i \neq j$ )

$$Z_{f_i f_j} = -\frac{\hat{\Sigma}_{f_i f_j}(m_{f_i}^2)}{m_{f_i}^2 - m_{f_j}^2 + \hat{\Sigma}_{f_j f_j}(m_{f_i}^2)}, \quad (4.96)$$

$$\sqrt{Z_{f_i}} = \left[ 1 + \text{Re} \left( \hat{\Sigma}'_{f_i f_i}(p^2) \right) - \text{Re} \left( \frac{\left( \hat{\Sigma}_{f_i f_j}(p^2) \right)^2}{p^2 - m_{f_j}^2 + \hat{\Sigma}_{f_j f_j}(p^2)} \right) \right]^{-\frac{1}{2}} \Bigg|_{p^2=m_{f_i}^2}. \quad (4.97)$$

Hence it is manifest that  $Z_N$  is a UV finite matrix. It only reshuffles the amplitudes such that they correspond to a physical process. To be consistent in the order of perturbation theory,  $Z_N$  has to be expanded so that after acting on the amplitudes  $A_{\dots f_1 \dots}$ , the tilde amplitudes  $\tilde{A}_{\dots f_1 \dots}$  have only terms of the required order. At NLO only terms up to order  $\alpha$  have to be considered for  $Z_N$

$$Z_{f_i f_j} = \Delta Z_{f_i f_j}^\alpha + \mathcal{O}(\alpha^2), \quad (4.98)$$

$$\sqrt{Z_{f_i}} = 1 - \frac{1}{2} \Delta Z_{f_i}^\alpha + \mathcal{O}(\alpha^2). \quad (4.99)$$

Formally  $Z_N$  then has the form

$$Z_N = \mathbb{1} + \begin{pmatrix} -\frac{1}{2} \Delta Z_{f_1}^\alpha & \Delta Z_{f_1 f_2}^\alpha \\ \Delta Z_{f_2 f_1}^\alpha & -\frac{1}{2} \Delta Z_{f_2}^\alpha \end{pmatrix} + \mathcal{O}(\alpha^2). \quad (4.100)$$

Because of the square in the numerator of the last term in Eq. (4.97), expanding its denominator will not contribute at NLO and one is simply left with

$$\Delta Z_{f_i f_j}^\alpha = - \frac{\hat{\Sigma}_{f_i f_j}(m_{f_i}^2)}{m_{f_i}^2 - m_{f_j}^2}, \quad (4.101)$$

$$\Delta Z_{f_i}^\alpha = \text{Re} \left( \hat{\Sigma}'_{f_i f_i}(m_{f_i}^2) \right). \quad (4.102)$$

The calculation of the decay amplitudes of  $H^+ \rightarrow W^+ h/H$  in the *Min* scheme requires such a wave function normalization matrix  $Z_N$  for the neutral CP-even scalars, whereas the charged  $H^+$  is already on-shell due to the choice of renormalization conditions. By decomposing the amplitude with  $H$  and  $h$ , respectively, in the final state into its LO and NLO part,

$$A_H = A_H^{\text{LO}} + A_H^{\text{NLO}} + \mathcal{O}(\alpha^2), \quad (4.103)$$

$$A_h = A_h^{\text{LO}} + A_h^{\text{NLO}} + \mathcal{O}(\alpha^2) \quad (4.104)$$

and then acting with  $Z_N$  on  $\begin{pmatrix} A_H \\ A_h \end{pmatrix}$ , yields

$$\tilde{A}_H = A_H^{\text{LO}} - \underbrace{\frac{1}{2} \Delta Z_H^\alpha A_H^{\text{LO}} + \Delta Z_{Hh}^\alpha A_h^{\text{LO}}}_{=: \tilde{A}_H^{\text{NLO}}} + A_H^{\text{NLO}} + \mathcal{O}(\alpha^2), \quad (4.105)$$

$$\tilde{A}_h = A_h^{\text{LO}} - \underbrace{\frac{1}{2} \Delta Z_h^\alpha A_h^{\text{LO}} + \Delta Z_{hH}^\alpha A_H^{\text{LO}}}_{=: \tilde{A}_h^{\text{NLO}}} + A_h^{\text{NLO}} + \mathcal{O}(\alpha^2). \quad (4.106)$$

With the above choice of renormalization conditions (Eqs. (4.83), (4.87) and (4.92)) for the *Min* scheme,  $Z_N$  still contains IR divergent terms. It is therefore a good consistency check for this wave function normalization matrix to check whether the final decay width is IR finite after adding real soft photon corrections. I have checked that this is indeed the case. This will be discussed in more detail in Sec. 5.2.

#### 4.4.7. A Word on the Last Parameter

For the sake of completeness, a last remark on the parameter  $M$  may be appropriate. It is the only element of the chosen set of independent parameters *SPI*, whose renormalization has not been covered yet in the previous sections. However, because the  $H^+ W^- h/H$ -vertex is independent of  $M$ , there is no need to renormalize it for the decays  $H^+ \rightarrow W^+ h/H$  at NLO. Moreover, any renormalization condition for  $\delta M$ , that works in one scheme, could be added to any of the discussed renormalization schemes. In contrast to the renormalization of the mixing angles, there is no subtlety involved that would link it to the field renormalization.

Because the only vertices, where  $M$  appears, are the trilinear and quartic scalar couplings, a reasonable possibility to renormalize  $M$  is a  $\overline{\text{MS}}$  condition requiring the UV finiteness of a corresponding renormalized vertex function. Possible choices would be e.g. the following trilinear couplings [17]

$$\lambda_{HA^0 A^0} = -\frac{1}{4vs_2\beta} \left[ (s_{\alpha-3\beta} + 3s_{\alpha+\beta}) m_H^2 + 4s_2\beta c_{\alpha-\beta} m_{A^0}^2 - 4s_{\alpha+\beta} M^2 \right], \quad (4.107)$$

$$\lambda_{hhH} = -\frac{c_{\alpha-\beta}}{2vs_2\beta} \left[ 2s_2\alpha m_h^2 + s_2\alpha m_H^2 - (3s_2\alpha - s_2\beta) M^2 \right]. \quad (4.108)$$



## 4.5. Renormalization of the Gauge Sector

In order to study the decays  $H^+ \rightarrow W^+ h/H$  at NLO the only other ingredients apart from the scalar sector, that need to be renormalized, are the electroweak gauge bosons and their coupling constants. In the previously discussed spirit of the on-shell conditions this shall be briefly presented as it is given in [37]. The  $W$ - and  $Z$ -boson masses  $M_W$ ,  $M_Z$  and the electric charge  $e$  are shifted by the following counterterms

$$M_W^2 \mapsto M_W^2 + \delta M_W^2, \quad (4.109)$$

$$M_Z^2 \mapsto M_Z^2 + \delta M_Z^2, \quad (4.110)$$

$$e \mapsto (1 + \delta Z_e) e. \quad (4.111)$$

For the gauge fields in the mass basis the following field renormalization constants are introduced

$$W^\pm \mapsto \sqrt{Z_W} W^\pm = \left(1 + \frac{1}{2}\delta Z_W\right) W^\pm, \quad (4.112)$$

$$\begin{pmatrix} Z \\ A \end{pmatrix} \mapsto \begin{pmatrix} \sqrt{Z_{ZZ}} & \sqrt{Z_{ZA}} \\ \sqrt{Z_{AZ}} & \sqrt{Z_{AA}} \end{pmatrix} \begin{pmatrix} Z \\ A \end{pmatrix} \quad (4.113)$$

$$= \begin{pmatrix} 1 + \frac{1}{2}\delta Z_{ZZ} & \frac{1}{2}\delta Z_{ZA} \\ \frac{1}{2}\delta Z_{AZ} & 1 + \frac{1}{2}\delta Z_{AA} \end{pmatrix} \begin{pmatrix} Z \\ A \end{pmatrix}, \quad (4.114)$$

where the mixing of the  $Z$ -boson and the photon  $A$  calls for the matrix structure. These renormalization constants for masses and fields are then fixed by on-shell conditions along the lines of Sec. 4.2 for the scalar fields. This finally leads to

$$\begin{aligned} \delta M_W^2 &= \widetilde{\text{Re}}(\Sigma_{WW}^T(M_W^2)), & \delta M_Z^2 &= \widetilde{\text{Re}}(\Sigma_{ZZ}^T(M_Z^2)), \\ \delta Z_{WW} &= -\text{Re}\left(\left.\frac{\partial \Sigma_{WW}^T}{\partial p^2}\right|_{p^2=M_W^2}\right), & \delta Z_{ZZ} &= -\text{Re}\left(\left.\frac{\partial \Sigma_{ZZ}^T}{\partial p^2}\right|_{p^2=M_Z^2}\right), \\ \delta Z_{AZ} &= -2\text{Re}\left(\frac{\Sigma_{ZA}^T(M_Z^2)}{M_Z^2}\right), & \delta Z_{ZA} &= 2\frac{\Sigma_{ZA}^T(0)}{M_Z^2}, \\ \delta Z_{AA} &= -\left.\frac{\partial \Sigma_{AA}^T}{\partial p^2}\right|_{p^2=0}, \end{aligned} \quad (4.115)$$

where the superscript  $T$  indicates the transverse part of the self energy. As it was the case in Sec. 4.2 for the discussion of scalars, beyond one-loop level ‘Re’ has to be replaced everywhere by ‘ $\widetilde{\text{Re}}$ ’ in order to distinguish between imaginary parts that originate from loop integrals and the imaginary parts from the CKM matrix which, on the contrary, have to be included. For the  $W$ -boson the distinction between ‘ $\widetilde{\text{Re}}$ ’ and ‘Re’ is in general already relevant at one-loop level and therefore shown in Eq. (4.115), despite the fact that in this thesis the CKM matrix is set to be real (see Sec. 6.2).

Eventually the electric charge is defined to be the  $ee\gamma$ -coupling in the Thomson limit, which after some manipulation yields

$$\delta Z_e = \frac{1}{2} \left.\frac{\partial \Sigma_{AA}^T}{\partial p^2}\right|_{p^2=0} + \frac{s_W}{c_W} \frac{\Sigma_{AZ}^T(0)}{M_Z^2}. \quad (4.116)$$

Note that the second summand in Eq. (4.116) has a relative minus sign if for the covariant derivative the sign convention is chosen, in which the terms with the electroweak gauge fields carry inverse signs compared to Eq. (2.5).

The electroweak gauge coupling  $g$  appears in the vertex Eq. (3.2), and hence  $\delta g$  will be needed in terms of  $\delta M_W^2$ ,  $\delta M_Z^2$  and  $\delta Z_e$ . With the leading order relation

$$g = \frac{e}{s_W} = \frac{e M_Z}{\sqrt{M_Z^2 - M_W^2}}, \quad (4.117)$$

it can easily be verified that at NLO  $\delta g$  is given by

$$\frac{\delta g}{g} = \delta Z_e + \frac{1}{2} \frac{1}{M_Z^2 - M_W^2} \left( \delta M_W^2 - \frac{M_W^2}{M_Z^2} \delta M_Z^2 \right). \quad (4.118)$$

Compared to the SM, one difference in the treatment of the gauge sector of a THDM concerns the gauge fixing Lagrangian [47]. In the SM, the linear  $R_\xi$  gauge is chosen such that the mixing term  $-iM_W(\partial^\mu W_\mu^-)G^+$ , which is by this choice contained in the gauge fixing Lagrangian, cancels the same term with opposite sign from the kinetic term of the scalar doublet. When renormalizing the kinetic term as well as the gauge fixing Lagrangian the same cancellation automatically holds for the counterterms of the mixing at any order of perturbation theory.

In a THDM a  $W^-H^+$ -CT results from the mentioned  $iM_W(\partial^\mu W_\mu^-)G^+$  part of the kinetic term due to  $H^+G^+$ -mixing. If one followed the approach of the SM, analogous terms from the gauge fixing Lagrangian would cancel this CT, which is, however, necessary in a THDM to ensure the vanishing of the  $W^-H^+$  two-point function on the mass shell. As has been shown in [48, 49], it is legitimate not to renormalize the gauge fixing Lagrangian; that is, the latter is formulated in already renormalized fields when adding it to the rest of the bare THDM Lagrangian. Consequently the  $W^-H^+$ -CT from the kinetic term is indeed not cancelled.

---

The Decays  $H^+ \rightarrow W^+ h/H$  at NLO

---

### 5.1. Virtual Corrections

The generic virtual correction and counterterm diagrams that contribute to the EW corrections of the decays  $H^+ \rightarrow W^+ h/H$  at NLO are shown in Fig. 5.1 [16].

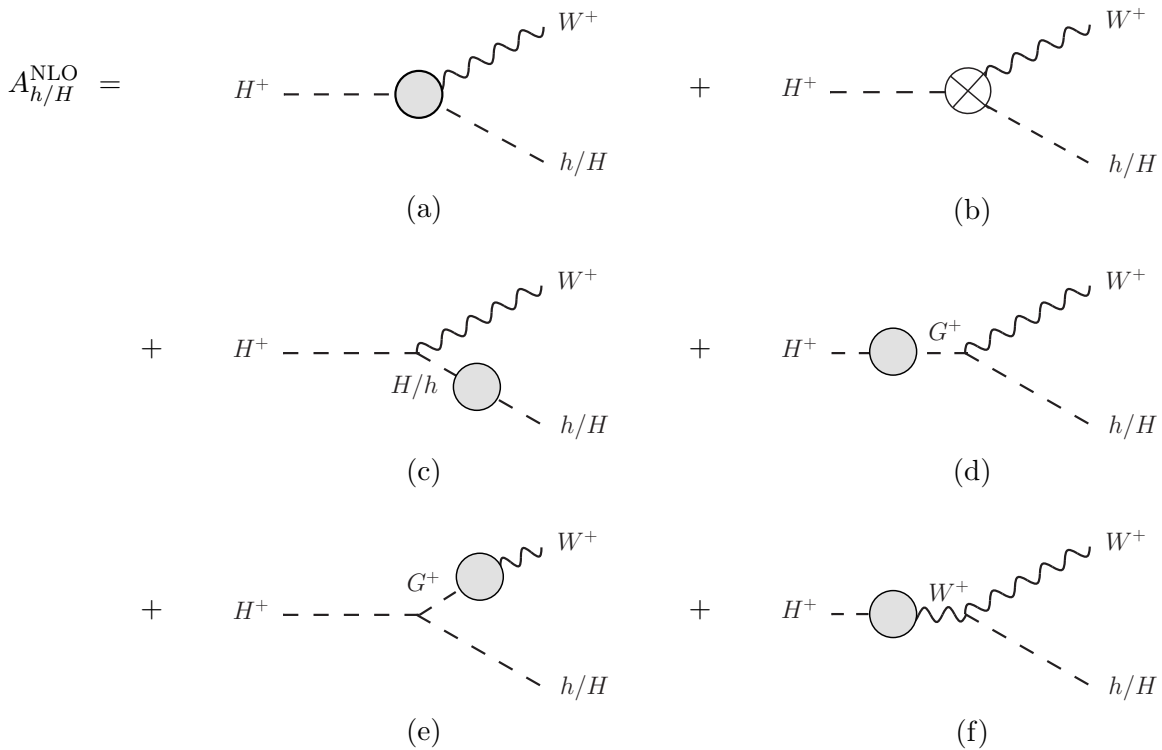


**Figure 5.1.:** Generic diagrams contributing to the decays  $H^+ \rightarrow W^+ h/H$ : Vertex corrections (a), vertex counterterm (b), corrections to the external legs (c-f).

The corrections to the external legs in (c) and (d) of Fig. 5.1 vanish by definition for on-shell renormalized scalars (see discussion in Sec. 4.2), while the mixing in (d) vanishes due to the

Ward-identity for an on-shell  $W$ -boson. The vanishing of the fourth and last correction to an external leg, shown in Fig. 5.1(g) is ensured by a Slavnov-Taylor-identity [46]. Note that for this to hold, the following counterterm

$$-\frac{M_W}{2} W_\mu^+ (\partial^\mu H^-) \delta Z_{G-H^-} \quad (5.1)$$

is needed, that is already fixed through the renormalization of the scalar fields and follows from the THDM specific treatment of the gauge fixing Lagrangian as discussed in Sec. 4.5. For the virtual radiative corrections at NLO one is thus left with the vertex corrections in (a) (that represents all possible one-loop diagrams) and the CT in (b) of Fig. 5.1.

At one-loop level there are four different topologies contributing to the three-point functions of the vertex corrections. Restricted by the vertices of a CP-conserving THDM, these four topologies result in eleven different Lorentz structures of Feynman diagrams that connect the three fields  $H^+ h W^-$  and  $H^+ H W^-$ , respectively. Generic diagrams of these structures can be found in Fig. A.1 of App. A. They are corrections from either purely electroweak vertices Figs. A.1(d), A.1(f)–A.1(j), a mixture of electroweak and trilinear or quartic scalar vertices Figs. A.1(b), A.1(c), A.1(e), A.1(k) or a mixture of electroweak and Yukawa couplings Fig. A.1(a). The latter with top and bottom quarks in the loop will give the largest contribution to the vertex correction [16]. QCD corrections will only contribute from next-to-next-to leading order on.

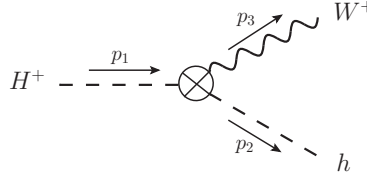
On particle level there are in total 73 Feynman diagrams contributing to the vertex corrections as represented by Fig. 5.1(a). The diagrams in the classes Figs. A.1(a), A.1(d), A.1(g)–A.1(k) contain UV divergences that are cancelled by adding the counterterm for the corresponding vertex. The decay amplitude may then be decomposed into the tree-level part and NLO part (order  $\alpha$ )

$$\begin{aligned} A_H &= A_H^{\text{LO}} + \underbrace{A_H^{\text{VC}} + A_H^{\text{CT}}}_{\equiv A_H^{\text{NLO}}} + \mathcal{O}(\alpha^2), \\ A_h &= A_h^{\text{LO}} + \underbrace{A_h^{\text{VC}} + A_h^{\text{CT}}}_{\equiv A_h^{\text{NLO}}} + \mathcal{O}(\alpha^2), \end{aligned} \quad (5.2)$$

where  $A_\phi^{\text{VC}}$  ( $\phi = h, H$ ) represents the sum of all vertex corrections and  $A_\phi^{\text{CT}}$  the corresponding total counterterm. Independent of the particular choice of the renormalization scheme, the CT can be cast into

$$\begin{aligned} \text{Diagram: } H^+ \text{ (dashed, } p_1) \text{ and } H \text{ (dashed, } p_2) \text{ meet at a vertex } \otimes \text{, from which } W^+ \text{ (wavy, } p_3) \text{ and } H \text{ (dashed, } p_2) \text{ emerge.} \\ = \underbrace{2(p_1 \epsilon_3^*) \frac{ig}{2} s_{\beta-\alpha}}_{= A_H^{\text{LO}}} \left[ \frac{\delta g}{g} + \frac{\delta s_{\beta-\alpha}}{s_{\beta-\alpha}} \right. \\ \left. + \frac{1}{2} \delta Z_{WW} + \frac{1}{2} \delta Z_{H^+ H^+} + \frac{1}{2} \delta Z_{HH} \right. \\ \left. - \frac{c_{\beta-\alpha}}{s_{\beta-\alpha}} \left( \frac{1}{2} \delta Z_{G^+ H^+} + \frac{1}{2} \delta Z_{hH} \right) \right] \end{aligned} \quad (5.3)$$

for the decay into  $W^+H$  and likewise for the decay into  $W^+h$



$$\begin{aligned}
 H^+ \xrightarrow{p_1} \text{---} \bigcirc \text{---} \begin{cases} \xrightarrow{p_3} W^+ \\ \xrightarrow{p_2} h \end{cases} &= \underbrace{2(p_1 \epsilon_3^*) (-) \frac{ig}{2} c_{\beta-\alpha}}_{= A_h^{\text{LO}}} \left[ \frac{\delta g}{g} + \frac{\delta c_{\beta-\alpha}}{c_{\beta-\alpha}} \right. \\
 &+ \frac{1}{2} \delta Z_{WW} + \frac{1}{2} \delta Z_{H^+H^+} + \frac{1}{2} \delta Z_{hh} \quad (5.4) \\
 &\left. + \frac{s_{\beta-\alpha}}{c_{\beta-\alpha}} \left( \frac{1}{2} \delta Z_{G^+H^+} - \frac{1}{2} \delta Z_{Hh} \right) \right].
 \end{aligned}$$

In both Eq. (5.3) and Eq. (5.4) the first line in the brackets contains the CTs from the parameters of the corresponding vertex, while the second line contains the field renormalization constants coming from the external fields. The third line finally contains the contributions of mixing effects from the  $G^+HW^-$  and  $H^+hW^-$  vertices (for Eq. (5.3)) and the  $G^+hW^-$  and  $H^+HW^-$  vertices, respectively (for Eq. (5.4)). The CTs  $\delta g$  and  $\delta Z_{WW}$  were defined in Sec. 4.5 and are independent of the renormalization scheme for the scalar sector. The scalar field renormalization parameters as well as the angle CTs depend on the chosen scheme. At one-loop level  $\delta s_{\beta-\alpha}$  and  $\delta c_{\beta-\alpha}$  are related to  $\delta\alpha$  and  $\delta\beta$  as follows

$$\begin{aligned}
 \delta s_{\beta-\alpha} &= c_{\beta-\alpha} \delta(\beta - \alpha) = c_{\beta-\alpha} (\delta\beta - \delta\alpha), \\
 \delta c_{\beta-\alpha} &= -s_{\beta-\alpha} \delta(\beta - \alpha) = -s_{\beta-\alpha} (\delta\beta - \delta\alpha).
 \end{aligned} \quad (5.5)$$

The UV finiteness of  $A_\phi^{\text{NLO}}$  has been checked numerically for all three renormalization schemes *HybMS*, *Kan* and *Min* (see Sec. 6.1 for more details). At NLO the only new contribution to the squared amplitude is the interference term of the LO amplitude and the order  $\mathcal{O}(\alpha)$  corrections

$$\begin{aligned}
 |A_\phi|^2 &= |A_\phi^{\text{LO}}|^2 + \left( A_\phi^{\text{LO}} (A_\phi^{\text{NLO}})^* + \text{c.c.} \right) \\
 &= |A_\phi^{\text{LO}}|^2 + 2 \text{Re} \left( A_\phi^{\text{LO}} (A_\phi^{\text{NLO}})^* \right),
 \end{aligned} \quad (5.6)$$

where  $\phi$  stands for either  $h$  or  $H$ . Recalling Eq. (3.4) the NLO partial decay width is accordingly given by

$$\Gamma_\phi = \frac{1}{2m_{H^\pm}} \int d\Pi_2 \sum_{\lambda_3} \left[ |A_\phi^{\text{LO}}|^2 + 2 \text{Re} \left( A_\phi^{\text{LO}} (A_\phi^{\text{NLO}})^* \right) \right]. \quad (5.7)$$

From the tensor structure it is clear that also in  $A_\phi^{\text{NLO}}$  the dependence on the polarization vector  $\epsilon_3$  can be reduced due to the Ward-identity to the contraction with the incoming momentum  $p_1$ . The LO correction factorizes from the vertex correction,

$$A_\phi^{\text{VC}} \equiv A_\phi^{\text{LO}} F_{H^+W^-\phi}^{\text{NLO}}, \quad (5.8)$$

and the partial decay width at NLO can hence be written as

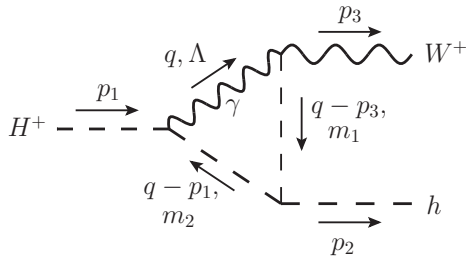
$$\begin{aligned}
 \Gamma_H^{\text{NLO}} &= \Gamma_H^{\text{LO}} \left[ 1 + 2 \text{Re} \left( F_{H^+W^-\phi}^{\text{NLO}} \right) + \delta Z_{WW} + \delta Z_{H^+H^+} + \delta Z_{HH} \right. \\
 &\quad \left. - \frac{c_{\beta-\alpha}}{s_{\beta-\alpha}} (\delta Z_{G^+H^+} + \delta Z_{hH}) + 2 \frac{\delta g}{g} + 2 \frac{\delta s_{\beta-\alpha}}{s_{\beta-\alpha}} \right] \quad (5.9)
 \end{aligned}$$

and

$$\begin{aligned} \Gamma_h^{\text{NLO}} = \Gamma_h^{\text{LO}} & \left[ 1 + 2 \operatorname{Re} (F_{H^+W^-h}^{\text{NLO}}) + \delta Z_{WW} + \delta Z_{H^+H^+} + \delta Z_{hh} \right. \\ & \left. + \frac{s_{\beta-\alpha}}{c_{\beta-\alpha}} (\delta Z_{G^+H^+} - \delta Z_{Hh}) + 2 \frac{\delta g}{g} + 2 \frac{\delta c_{\beta-\alpha}}{c_{\beta-\alpha}} \right]. \end{aligned} \quad (5.10)$$

## 5.2. Real Corrections

When dealing with electroweak radiative corrections for a process with charged particles in the initial or final state, one encounters infra-red (IR) divergences already at one-loop level. These divergent terms stem from virtual photon corrections such as the following example of a loop diagram that belongs to the class of triangles in Fig. A.1(e),



$$\propto \int \frac{d^4 q}{(2\pi)^4} \frac{(q - 2p_1)^\mu}{(q^2 - \Lambda^2) \left( (q - p_3)^2 - m_1^2 \right) \left( (q - p_1)^2 - m_2^2 \right)}. \quad (5.11)$$

Because the photon is massless, its propagator diverges for vanishing loop momentum  $q^2$ . This divergence has been regularized in Eq. (5.11) by artificially introducing a finite photon mass  $\Lambda$ .

Note that we will have to also include diagrams with additional photons. Due to its vanishing mass, the photon can have an arbitrarily small energy. If its energy is smaller than the detector sensitivity  $\Delta E$ , such a so-called soft photon will escape any detection. Processes with additional soft photons in the final state will thus add to the measurable signal. As a consequence one has to sum incoherently over processes with any number of additional soft photons that is consistent with the order in perturbation theory considered for the original process.

The emission of real soft photons off charged particles leads to IR divergences in the limit of vanishing photon momentum. This is because the propagator of the charged particle then becomes on-shell. It turns out that both IR divergences, the ones from virtual photon corrections and the ones from additional real soft photons, exactly cancel each other. That this holds generally for any process to any order of perturbation theory, has been shown by Bloch and Nordsieck [50].

At NLO only real corrections with one additional soft photon have to be considered. For the decay  $H^+ \rightarrow W^+ \phi$ , where  $\phi$  stands for either  $h$  or  $H$ , this leaves one with four diagrams contributing to the tree-level amplitude  $A_{\phi\gamma}$  of the decay  $H^+ \rightarrow W^+ \phi\gamma$ . They are shown in Fig. 5.2 and Fig. 5.3.

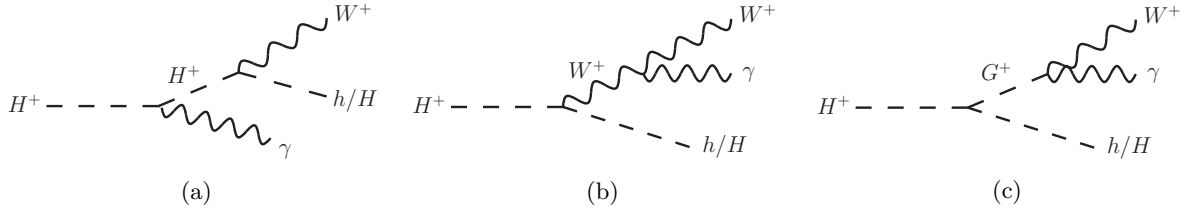


**Figure 5.2.:** Feynman diagrams for bremsstrahlung off the initial state  $H^+$  (a), bremsstrahlung off the final state  $W^+$  (b) and the contribution from the  $G^+W^-\gamma$ -vertex (c).

The three diagrams in Fig. 5.2 are proper bremsstrahlung contributions from the initial and final state charged particles, whereas the diagram in Fig. 5.3 comes from a single THDM specific 4-vertex that is proportional to  $\alpha$  as well.

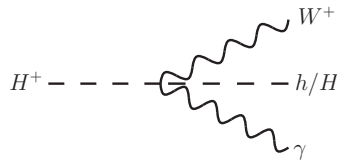


**Figure 5.3.:** Feynman diagram for the 4-vertex contribution.

The incoherent sum of both final states, with and without an additional soft photon, gives the measurable partial width for the decay  $H^+ \rightarrow W^+\phi$  as

$$\Gamma_{\phi\gamma}^{\text{obs}} \equiv \Gamma^{\text{obs}}(H^+ \rightarrow W^+\phi) = \underbrace{\Gamma(H^+ \rightarrow W^+\phi)}_{\equiv \Gamma_{\phi}} + \underbrace{\Gamma(H^+ \rightarrow W^+\phi\gamma)|_{E_4 \leq \Delta E}}_{\equiv \Gamma_{\phi\gamma}^{\text{soft}}}, \quad (5.12)$$

where  $E_4$  denotes the energy of the photon. Denoting by  $p_4$  its momentum and  $\lambda_4$  its polarization and adopting the nomenclature for the rest of the kinematics from Chapter 3, the soft real corrections are given by

$$\Gamma_{\phi\gamma}^{\text{soft}} = \frac{1}{2m_{H^\pm}} \left( \prod_{i=2,3,4} \int \frac{d^3 p_i}{(2\pi)^3} \frac{1}{2E_i} \right) \Big|_{E_4 \leq \Delta E} (4\pi)\delta^{(4)}(p_1 - p_2 - p_3 - p_4) \sum_{\lambda_3, \lambda_4} |A_{\phi\gamma}|^2. \quad (5.13)$$

As only photons with a small energy are to be taken into account, the so-called soft photon approximation neglects the dependence on  $p_4$  of the integrand in Eq. (5.13) anywhere but in the denominator of  $A_{\phi\gamma}$ , where it constitutes the pole. One can then separate the phase space integrals

$$\Gamma_{\phi\gamma}^{\text{soft}} = \frac{1}{2m_{H^\pm}} \int d\Pi_2 \sum_{\lambda_3} \left[ \int_{E_4 \leq \Delta E} \frac{d^3 p_4}{(2\pi)^3} \frac{1}{2E_4} \sum_{\lambda_4} |A_{\phi\gamma}|^2 \right]. \quad (5.14)$$

By calling the amplitude of the bremsstrahlung diagrams  $A_{\text{brems}}$  and the amplitude corresponding to the 4-vertex diagram  $A_{4V}$ , the squared amplitude at order  $\alpha^2$  reads

$$|A_{\phi\gamma}|^2 = |A_{\text{brems}} + A_{4V}|^2 \quad (5.15)$$

$$= |A_{\text{brems}}|^2 + |A_{4V}|^2 + 2\text{Re}(A_{\text{brems}}A_{4V}^*). \quad (5.16)$$

The contributions from only  $A_{\text{brems}}$  on the one hand and the contribution from  $A_{4V}$  including the interference term on the other hand will be treated separately in the following two sections.

### 5.2.1. Soft Bremsstrahlung

In the soft photon approximation the amplitude for photon emission from the initial state charged Higgs boson (Fig. 5.2(a)) is given by

$$A = A_\phi^{\text{LO}} e \frac{2p_1 \epsilon_4^*}{(p_1 - p_4)^2 - m_{H^\pm}^2}, \quad (5.17)$$

where  $A_\phi^{\text{LO}}$  denotes the LO amplitude as defined in Chapter 3. Using the same approximation, the radiation off the  $W$ -boson in the final state (Fig. 5.2(b)) yields

$$A = A_\phi^{\text{LO}} e \frac{2p_3 \epsilon_4^*}{(p_3 + p_4)^2 - M_W^2} - A_\phi^{\text{LO}} e \frac{m_{H^\pm}^2 - m_h^2}{(p_3 + p_4)^2 - M_W^2} \frac{\epsilon_3 \epsilon_4^*}{2p_1 \epsilon_3^*}. \quad (5.18)$$

The second term in Eq. (5.18) originates from the longitudinal part of the  $W$ -boson propagator. As expected, it is cancelled by the diagram Fig. 5.2(c) with the Goldstone boson propagator which leads to the same expression but with opposite sign. In summary the Bremsstrahlung amplitude in the soft photon approximation can be written as

$$A_{\text{brems}} = A_\phi^{\text{LO}} e \left[ \frac{2p_3 \epsilon_4^*}{(p_3 + p_4)^2 - M_W^2} + \frac{2p_1 \epsilon_4^*}{(p_1 - p_4)^2 - m_{H^\pm}^2} \right] \quad (5.19)$$

$$= A_\phi^{\text{LO}} e \sum_{i=1,3} \left( \pm \frac{p_i \epsilon_4^*}{p_i p_4} \right). \quad (5.20)$$

In the last line terms in the denominator proportional to  $p_4^2 = \Lambda^2$  have been neglected. The lower sign in "±" holds for radiation off the initial  $H^+$ , while the upper sign holds for the radiation off the final state  $W^+$ . Note that if replacing "±" by "± $Q_i$ " with  $Q_i$  being the electric charge of the corresponding initial or final state particle and with  $i$  running over all external charged particles, Eq. (5.20) directly generalizes to soft bremsstrahlung corrections at NLO for processes of arbitrary multiplicity [37]. The sum over the photon polarizations leads to

$$\sum_{\lambda_4} |A_{\text{brems}}|^2 = -e^2 |A_\phi^{\text{LO}}|^2 \sum_{i,j=1,3} \frac{\pm p_i p_j}{(p_i p_4)(p_j p_4)}, \quad (5.21)$$

where the '+' sign holds for  $i = j$  and the '-' sign for  $i \neq j$ . Due to the proportionality of  $A_{\text{brems}}$  to the Born amplitude, we can then write

$$\begin{aligned} \Gamma_{\phi\gamma}^{\text{soft}} \Big|_{\text{brems}} &= \frac{1}{2m_{H^\pm}} \int d\Pi_2 \sum_{\lambda_3} |A_\phi^{\text{LO}}|^2 (-e^2) \int_{E_4 \leq \Delta E} \frac{d^3 p_4}{(2\pi)^3} \frac{1}{2E_4} \sum_{i,j=1,3} \frac{\pm p_i p_j}{(p_i p_4)(p_j p_4)} \\ &= -\frac{e^2}{2(2\pi)^3} \Gamma_\phi^{\text{LO}} \sum_{i,j=1,3} \underbrace{\left( \int_{E_4 \leq \Delta E} \frac{d^3 p_4}{2E_4} \frac{2p_i p_j}{(p_i p_4)(p_j p_4)} \right)}_{\equiv I_{ij}}. \end{aligned} \quad (5.22)$$



The above defined standard integrals  $I_{ij}$  have first been calculated by 't Hooft and Veltman [51], while the following representation of the general result is taken from [37]

$$I_{ij} = 4\pi \frac{ap_i p_j}{a^2 p_i^2 - p_j^2} \left\{ \frac{1}{2} \ln \left( \frac{a^2 p_i^2}{p_j^2} \right) \ln \left( \frac{4\Delta E^2}{\Lambda^2} \right) + \left[ \frac{1}{4} \left( \ln \left( \frac{u_0 - |\vec{u}|}{u_0 + |\vec{u}|} \right) \right)^2 + \text{Li}_2 \left( 1 - \frac{u_0 + |\vec{u}|}{v} \right) + \text{Li}_2 \left( 1 - \frac{u_0 - |\vec{u}|}{v} \right) \right] \Big|_{u=p_j}^{u=ap_i} \right\}, \quad (5.23)$$

where  $v$  is defined as

$$v \equiv \frac{a^2 p_i^2 - p_j^2}{2(ap_{i0} - p_{j0})} \quad (5.24)$$

and  $a$  as the solution of

$$a^2 p_i^2 - 2a(p_i p_j) + p_j^2 = 0 \quad \wedge \quad \frac{ap_{i0} - p_{j0}}{p_{j0}} > 0. \quad (5.25)$$

Three different combinations of indices feed into Eq. (5.22)

$$\Gamma_{\phi\gamma}^{\text{soft}} \Big|_{\text{brems}} = -\frac{e^2}{2(2\pi)^3} \Gamma_{\phi}^{\text{LO}} (I_{11} + I_{33} - 2I_{13}). \quad (5.26)$$

For identical indices Eq. (5.23) simplifies significantly [37],

$$I_{33} = 2\pi \left[ \ln \left( \frac{4\Delta E^2}{\Lambda^2} \right) + \frac{E_3}{|\vec{p}_3|} \ln \left( \frac{E_3 - |\vec{p}_3|}{E_3 + |\vec{p}_3|} \right) \right]. \quad (5.27)$$

In the rest frame of the decaying  $H^+$  the momentum  $|\vec{p}_3|$  of the  $W$ -boson cannot be zero, however the incoming momentum  $|\vec{p}_1|$  vanishes in this frame. For  $I_{11}$  the term corresponding to the second logarithm in Eq. (5.27) therefore first has to be expanded so that one can take the limit  $\frac{|\vec{p}_1|}{E_1} \rightarrow 0$  in a well-defined way. This yields

$$I_{11} = 2\pi \left[ \ln \left( \frac{4\Delta E^2}{\Lambda^2} \right) - 2 \right]. \quad (5.28)$$

Finally for  $I_{13}$ , the needed solution of Eq. (5.25) is given by

$$a = \frac{E_3 + |\vec{p}_3|}{m_{H^\pm}} \quad \Rightarrow \quad v = \frac{(E_3 + |\vec{p}_3|)^2 - M_W^2}{2|\vec{p}_3|}. \quad (5.29)$$

### 5.2.2. Additional Soft Corrections

The Feynman diagram with the four-vertex in Fig. 5.3 contributes to the decay  $H^+ \rightarrow W^+ \phi \gamma$  at order  $\alpha$  as well. The corresponding amplitude is obviously IR finite and given by

$$A_{4V} = -\rho_\phi \frac{ie^2}{2s_W} \epsilon_3^* \epsilon_4^*, \quad (5.30)$$

with  $\rho_\phi$  referring to either a sine or cosine of the angle  $\beta - \alpha$  as defined in Eq. (3.3). The absolute square of the amplitude when summed over  $\lambda_4$ ,

$$\sum_{\lambda_4} |A_{4V}|^2 = - \left| \rho_\phi \frac{ie^2}{2s_W} \right|^2 \epsilon_3^* \epsilon_3, \quad (5.31)$$

is independent of the photon kinematics. The integration over the photon phase space thus gives a constant that only depends on  $\Delta E$

$$\int_{E_4 \leq \Delta E} \frac{d^3 p_4}{(2\pi)^3} \frac{1}{2E_4} = \frac{4\pi}{2(2\pi)^3} \int_0^{\sqrt{\Delta E^2 - \Lambda^2}} d|\vec{p}_4| \frac{|\vec{p}_4|^2}{\sqrt{\Lambda^2 + |\vec{p}_4|^2}} \quad (5.32)$$

$$= \frac{1}{(2\pi)^2} \left[ \frac{1}{2} (\Delta E^2 - \Lambda^2) - \Lambda^2 \ln \left( \frac{\Delta E}{\Lambda} \right) \right] \quad (5.33)$$

$$\Lambda \xrightarrow{\rightarrow} 0 \quad \frac{1}{(2\pi)^2} \frac{\Delta E^2}{2} . \quad (5.34)$$

The interference term  $A_{\text{brems}} A_{4V}^*$ , on the contrary, contains an IR divergent factor which originates from the  $H^+$ -propagator

$$\sum_{\lambda_4} [A_{\text{brems}} A_{4V}^* + c.c.] = \sum_{\lambda_4} \left[ e A_\phi^{\text{LO}} \left( \sum_{i=1,3} \pm \frac{p_i \epsilon_4^*}{p_i p_4} \right) \epsilon_3 \epsilon_4 \rho_\phi \frac{ie^2}{2s_W} + c.c. \right] \quad (5.35)$$

$$= - \sum_{i=1,3} \left[ \pm e A_\phi^{\text{LO}} \frac{p_i \epsilon_3}{p_i p_4} \rho_\phi \frac{ie^2}{2s_W} + c.c. \right] \quad (5.36)$$

$$\stackrel{\text{Ward-Id.}}{=} e^2 \left[ A_\phi^{\text{LO}} \rho_\phi \frac{ie}{2s_W} (p_1 \epsilon_3) + c.c. \right] \frac{1}{p_1 p_4} \quad (5.37)$$

$$= - e^2 |A_\phi^{\text{LO}}|^2 \frac{1}{p_1 p_4} . \quad (5.38)$$

After the integration over the photon phase space in the rest frame of the charged Higgs boson,

$$\int_{E_4 \leq \Delta E} \frac{d^3 p_4}{(2\pi)^3} \frac{1}{2E_4} \frac{1}{p_1 p_4} = \frac{1}{(2\pi)^3} \frac{4\pi}{2m_{H^\pm}} \int_0^{\sqrt{\Delta E^2 - \Lambda^2}} d|\vec{p}_4| \frac{|\vec{p}_4|^2}{E_4^2} \quad (5.39)$$

$$= \frac{1}{(2\pi)^2 m_{H^\pm}} \Lambda \int_0^\Lambda d\eta \frac{\eta^2}{1 + \eta^2} \quad (5.40)$$

$$= \frac{1}{(2\pi)^2 m_{H^\pm}} \left[ \sqrt{\Delta E^2 - \Lambda^2} - \Lambda \arctan \left( \sqrt{\frac{\Delta E^2}{\Lambda^2} - 1} \right) \right] \quad (5.41)$$

$$\Lambda \xrightarrow{\rightarrow} 0 \quad \frac{1}{(2\pi)^2} \frac{\Delta E}{m_{H^\pm}} , \quad (5.42)$$

the limit  $\Lambda \rightarrow 0$  turns out to exist. Consequently the interference term leads only to an IR finite contribution as well. Adding up these two finite contributions yields

$$\frac{1}{2m_{H^\pm}} \int d\Pi_2 \sum_{\lambda_3} \left[ \int_{E_4 \leq \Delta E} \frac{d^3 p_4}{(2\pi)^3} \frac{1}{2E_4} \sum_{\lambda_4} \left( 2\text{Re} ( A_{\text{brems}} A_{4V}^* ) + |A_{4V}|^2 \right) \right] \quad (5.43)$$

$$= \frac{1}{2m_{H^\pm}} \int d\Pi_2 \sum_{\lambda_3} \left[ -e^2 |A_\phi^{\text{LO}}|^2 \frac{1}{(2\pi)^2} \frac{\Delta E}{m_{H^\pm}} \right] \quad (5.44)$$

$$- \left| \rho_\phi \frac{ie^2}{2s_W} \right|^2 \epsilon_3^* \epsilon_3 \frac{1}{(2\pi)^2} \frac{\Delta E^2}{2} \right]$$

$$= -e^2 \Gamma_\phi^{\text{LO}} \frac{1}{(2\pi)^2} \frac{\Delta E}{m_{H^\pm}} \quad (5.45)$$

$$- e^2 \frac{1}{2m_{H^\pm}} \mathcal{F}_\phi^{\text{Kin}} (-3) \left( \frac{\rho_\phi e}{2s_W} \right)^2 \frac{1}{(2\pi)^2} \frac{\Delta E^2}{2},$$

where in the last line the kinematical factor  $\mathcal{F}_\phi^{\text{Kin}}$ , introduced in Eq. (3.5), has been used, as well as the normalization of the polarization vectors of the  $W$ -boson,

$$\sum_{\lambda_3} \epsilon_{3,\mu}^* \epsilon_3^\mu = \sum_{\lambda_3} -1 = -3. \quad (5.46)$$

### 5.2.3. Cancellation of Infra-red Divergences

In summary, the soft real corrections up to order  $\alpha^2$  for the decay width, are given by

$$\begin{aligned} \Gamma_{\phi\gamma}^{\text{soft}} &= -e^2 \Gamma_\phi^{\text{LO}} \frac{1}{2(2\pi)^3} ( I_{11} + I_{33} - 2I_{13} ) \\ &- e^2 \Gamma_\phi^{\text{LO}} \frac{1}{(2\pi)^2} \frac{\Delta E}{m_{H^\pm}} \\ &- e^2 \left( \frac{\rho_\phi e}{2s_W} \right)^2 \frac{1}{2m_{H^\pm}} \mathcal{F}_\phi^{\text{Kin}} (-3) \frac{1}{(2\pi)^2} \frac{\Delta E^2}{2}. \end{aligned} \quad (5.47)$$

The IR divergent terms coming from these real corrections have been regularized with a finite photon mass  $\Lambda$ . They are contained in the  $I_{ij}$  integrals of Eq. (5.23) and come in the form of terms proportional to  $\ln(\Delta E/\Lambda)$ . Within the virtual corrections the IR divergent terms come from the  $H^+$  and  $W^+$  self energies that enter the field renormalization factors  $\delta Z_{H^+H^+}$  and  $\delta Z_{WW}$ , as well as from the diagrams in Fig. A.1(d) and Fig. A.1(e), in case it is a photon that connects  $H^+$  and  $W^+$ .

An infra-red finite  $\Gamma_\phi^{\text{obs}}$ , as defined in Eq. (5.12), is obtained by the cancellation of the  $\ln(\Lambda)$  terms from the real corrections with the ones coming from the virtual corrections, where necessarily the same regularization method has been used. After any dependence on  $\Lambda$  has dropped out, the limit  $\Lambda \rightarrow 0$  can be taken to retain a massless photon again.

Note that this formalism introduces a dependence of the decay width on the detector sensitivity  $\Delta E$ , where the value of  $\Delta E$  says what "soft" in the context of a particular experimental setup means. If the soft photon approximation is a justified approximation, then the final

result for  $\Gamma_\phi^{\text{obs}}$  must not depend strongly on the choice of  $\Delta E$  [37] (see discussion in Sec. 6.5).

The cancellation of the  $\Lambda$ -dependence has been checked numerically by varying  $\Lambda$  over a wide range of ten orders of magnitude. If the resulting variation of  $\Gamma_\phi^{\text{obs}}$  is beyond the significant digits of a double precision type, the check is passed. This has been done for each renormalization scheme that was introduced in Chapter 4:

- ***Kan* scheme:** infra-red finite
- ***HybMS* scheme:** infra-red finite.

Given that the *Kan* scheme yields an IR finite result, it is obvious that the same holds for the *HybMS* scheme. The only part of the CT in which the two schemes differ is  $\delta(\beta - \alpha)$ . In the minimal subtraction condition  $\delta(\beta - \alpha)$  is defined to only contain UV divergent terms, while in the *Kan* scheme  $\delta(\beta - \alpha)$  is constructed from the  $\Sigma_{Hh}$  and  $\Sigma_{G^+H^+}$  self energies as well as the tadpoles, none of which can have IR divergent photon loops at one-loop level.

- ***Min* scheme:** infra-red finite.

As already mentioned in Sec. 4.4.6, it is only after acting with the wave function normalization matrix  $Z_N$  on the tuple of amplitudes,

$$\begin{pmatrix} \tilde{A}_H \\ \tilde{A}_h \end{pmatrix} = Z_N \begin{pmatrix} A_H \\ A_h \end{pmatrix}, \quad (5.48)$$

that  $\Gamma_\phi^{\text{obs}}$  is infra-red finite. This is to say that at NLO the expansions for  $\tilde{A}_\phi$ , that are given in Eqs. (4.105,4.106), have to enter  $\Gamma_\phi$  in Eq. (5.12) to yield an IR finite result.

One might be inclined to think that the choice of renormalization scheme is completely independent of the treatment of real corrections. Indeed in all three cases so far, exactly the same  $\Gamma_{\phi\gamma}^{\text{soft}}$  has been added to  $\Gamma_\phi$  to obtain a finite partial width. Note, however, that this is only strictly true in renormalization schemes where all fields of external particles are on-shell. In schemes like the *Min* scheme, in which this is not the case, the normalization matrices  $Z_N$  must in general also affect the amplitudes entering  $\Gamma_{\phi\gamma}^{\text{soft}}$ . It is only because the tree-level amplitude  $A_{\phi\gamma}$  of the real corrections is already of the order  $\mathcal{O}(\alpha)$ , that at NLO there is no contribution from  $Z_N$  acting on  $A_{H\gamma}$  and  $A_{h\gamma}$ .

- **Process-dependent scheme using  $H^+ \rightarrow W^+ H$ :** See discussion in the subsequent Sec. 5.2.4.

#### 5.2.4. Process-dependent Schemes Revisited

In Sec. 4.4.4 the decay  $H^+ \rightarrow W^+ H$  has been presented as a first suggestion for a process-dependent renormalization condition for the angle  $\beta - \alpha$ . Given the similarity of the counterterms of the  $H^+W^-h$ -vertex and the  $H^+W^-H$ -vertex, this choice may seem natural when aiming for the NLO amplitude of the decay  $H^+ \rightarrow W^+h$  and has indeed been used in [16]. Because in this paper Santos *et al.* considered only the contributions from top and bottom quarks in the virtual corrections, infra-red divergent loops did not appear at all. This is why in this approximation the process  $H^+ \rightarrow W^+ H$  may well be used to fix  $\delta(\beta - \alpha)$ .

The full electroweak virtual corrections, however, lead to infra-red divergences in  $\delta Z_{H^+H^+}$ ,  $\delta Z_{WW}$  and  $F_{H^+W^-H}^{\text{NLO}}$ , where the latter is the vertex form factor as defined in Eq. (5.8). The renormalization condition for  $\delta(\beta - \alpha)$  in Eq. (4.45) (with  $C^{\text{finite}} = 0$ ) was said to follow from requiring  $\Gamma_H^{\text{NLO}} \stackrel{!}{=} \Gamma_H^{\text{LO}}$ . If naively applying the same condition in case of the full electroweak

corrections,  $\delta(\beta - \alpha)$  will contain additional IR divergences and as a result  $\Gamma_\phi^{\text{obs}}$  would not be IR finite.

Requiring that the NLO decay width is equal to the LO one, actually involves real, soft photon corrections

$$\Gamma_H^{\text{NLO}} = \Gamma_H^{\text{LO}} \left[ 1 + 2 \operatorname{Re} (F_{H^+W^-H}^{\text{NLO}}) + \delta Z_{WW} + \delta Z_{H^+H^+} + \delta Z_{HH} \right. \quad (5.49)$$

$$\left. - \frac{c_{\beta-\alpha}}{s_{\beta-\alpha}} (\delta Z_{G^+H^+} + \delta Z_{hH}) + 2 \frac{\delta g}{g} + 2 \frac{c_{\beta-\alpha}}{s_{\beta-\alpha}} \delta(\beta - \alpha) \right] + \Gamma_{H\gamma}^{\text{soft}}$$

$$\stackrel{!}{=} \Gamma_H^{\text{LO}}. \quad (5.50)$$

This condition would lead to an IR finite  $\delta(\beta - \alpha)$  and hence solve the problem of finiteness for  $\Gamma_h^{\text{obs}}$ . But it defines real corrections into  $\delta(\beta - \alpha)$ , which is seen as unacceptable [39]. Through the photon phase space cut, this counterterm would inevitably depend on some detector sensitivity  $\Delta E$ , which would thereby introduce a dependence on the experimental setting.

In order to circumvent this issue for a process-dependent scheme, Freitas *et al.* [39] therefore suggest to use another process where it is possible to separate the weak virtual corrections from the virtual corrections that come from pure quantum electrodynamics (QED). Only the latter contain the infra-red divergent parts. If this separation is possible and if the QED corrections form a UV finite subset, then one can define the angle counterterm by requiring only the virtual weak corrections to vanish at NLO. In [39] this is discussed for the renormalization of  $\tan(\beta)$  in the context of the MSSM and their suggested choice for such a process is  $A^0 \rightarrow \tau^+ \tau^-$ .

A question, that seems natural, is whether any other process with only neutral external particles could be used. The issue of infra-red divergences in process-dependent renormalization conditions at one-loop level could thereby be avoided right from the start. In order to systematically go through all existing couplings of a CP-conserving THDM, a reasonable minimum set of requirements would be:

1. Vertex with only neutral fields.
2. The coupling constant depends on  $\alpha$  and/or  $\beta$ .
3. No external Goldstone bosons are involved.

The only couplings meeting these criteria are:

- **Yukawa couplings:** none
- **2 scalars - 2 gauge bosons:** none
- **2 scalars - 1 gauge boson:**  $\lambda_{hA^0Z} = \frac{e}{2s_W c_W} c_{\beta-\alpha}$ ,  $\lambda_{HA^0Z} = -\frac{e}{2s_W c_W} s_{\beta-\alpha}$
- **1 scalar - 2 gauge bosons:**  $\lambda_{HZZ} = \frac{ieM_W}{s_W c_W^2} c_{\beta-\alpha}$ ,  $\lambda_{hZZ} = \frac{ieM_W}{s_W c_W^2} s_{\beta-\alpha}$

- **Trilinear scalar couplings:**  $\lambda_{HA^0A^0}$  ,  $\lambda_{hA^0A^0}$  ,  $\lambda_{hHH}$  ,  $\lambda_{hhH}$  ,  $\lambda_{hhh}$  ,  $\lambda_{HHH}$
- **Quartic scalar couplings:**  $\lambda_{A^0A^0A^0A^0}$  ,  $\lambda_{HHA^0A^0}$  ,  $\lambda_{hhA^0A^0}$  ,  $\lambda_{HhA^0A^0}$  ,  
 $\lambda_{HHHH}$  ,  $\lambda_{hhhh}$  ,  $\lambda_{hhHH}$  ,  $\lambda_{hHHH}$  ,  $\lambda_{hHHH}$

The same kind of conditions as discussed above, that require the NLO decay width to be equal to the LO decay width, could in principle be imposed on the decays  $A^0 \rightarrow ZH$ ,  $A^0 \rightarrow Zh$  and  $H \rightarrow ZZ$ . Whether these decay channels are kinematically allowed depends on the mass ratios. A renormalization scheme using one of these processes would therefore only be applicable to certain scenarios. Albeit  $H \rightarrow ZZ$  is the least restrictive in this sense, it is proportional to  $c_{\beta-\alpha}$ . Experimental data favour values for  $s_{\beta-\alpha}$  close to one [52], which means that couplings that involve  $c_{\beta-\alpha}$  are suppressed due to sum rules. This is relevant if the intention of a process-dependent scheme is to eventually measure the corresponding decay width in order to replace the renormalization condition of equating the NLO width with the LO width, by equating the former with the actually measured value.

As far as the trilinear and quartic couplings are concerned, one could in principle think of one scalar decaying into two or three other scalars. However, actually measuring these decays is very challenging. Even if only using a condition of the form  $\Gamma_H^{\text{NLO}} \stackrel{!}{=} \Gamma_H^{\text{LO}}$ , note that due to the kinematics these decays could only be used in a very restricted set of scenarios.

In conclusion there is no process at hand that involves only neutral particles, that has a realistic potential to be measured and that is sufficiently general in the sense that it does not only work for a few special scenarios with particular ratios of scalar masses. From the processes involving charged particles, the decay  $A^0 \rightarrow \tau^+\tau^-$  is not only one where the separation of QED and weak corrections is possible, but also one that is kinematically not very restrictive. But still only  $\delta\beta$  can be fixed through this decay and not  $\delta\alpha$  which is, in contrast to the situation in the MSSM, another independent parameter to be renormalized. Aiming for a process-dependent scheme for both mixing angles, one would therefore still have to use another process in addition to  $A^0 \rightarrow \tau^+\tau^-$ . A possible choice could be the analogous decay of a neutral CP-even Higgs boson,  $H \rightarrow \tau^+\tau^-$ , as the corresponding Yukawa coupling depends on the mixing angle  $\alpha$ . In order to avoid the necessity to renormalize the fermion sector, a process-dependent scheme will not be used hereinafter for the calculation of the NLO decay widths of  $H^+ \rightarrow W^+ h/H$ .

## 6.1. Used Software

The sum of all one-loop vertex corrections  $A_{H/h}^{\text{VC}}$ , as defined in Eq. (5.2), was calculated in **Mathematica** using the packages **FeynArts** 3.9 [38] and **FormCalc** 8.3 [53, 54]. For a CP-conserving THDM the **FeynArts** model file THDM.mod already exists and is included in the mentioned version of **FeynArts**. Note that the couplings therein are parametrized in terms of the set of independent parameters *SP1* (see Eq. (2.36)), but they are based on the alternative parametrization of the scalar potential presented in App. C. As a result the  $\Lambda_5$  of the model file has to be expressed by the parameters of Sec. 2.2 via Eq. (C.7).

All scalar self energies  $\Sigma_{f_i f_j}$  as well as the gauge boson self energies  $\Sigma_{WW}$ ,  $\Sigma_{ZZ}$ ,  $\Sigma_{AZ}$  and  $\Sigma_{ZA}$  have likewise been calculated with the help of these packages. The thereby obtained analytical expressions for the vertex corrections and self energies are formulated in terms of the scalar one-loop integrals as they are defined in [55].

For the calculation of the partial decay widths the Fortran 90 program **CalcGamma** was written, in which the expressions from **Mathematica** have been implemented and used to construct the counterterms of the renormalization schemes introduced in Chapter 4. In order to evaluate numerically the one-point, two-point and three-point functions, the library **LoopTools** 2.9 [55] was linked.

The ultra-violet finiteness of the partial decay widths as given by Eq. (5.9) and Eq. (5.10), was checked numerically. On the one hand the cancellation of the terms proportional to the  $\epsilon^{-1}$ -pole was checked numerically in **Mathematica** by making use of a **FormCalc** function.

In **CalcGamma**, on the other hand, a numerical check for UV finiteness, which uses the renormalization scale  $\mu$ , was performed for all those schemes, which do not involve a  $\overline{\text{MS}}$  condition. The terms which contain the  $\mu$ -dependence are proportional to  $\ln(\mu)$  and always appear together with the  $\epsilon^{-1}$ -poles. In on-shell schemes the cancellation of the UV divergences therefore implies the cancellation of the  $\mu$ -dependent terms. One can make use of this fact to check

the UV finiteness of an amplitude by checking the independence of the NLO amplitude from the renormalization scale  $\mu$ . To this end,  $\mu$  was varied in `CalcGamma` over a wide range of ten orders of magnitude.

Note that this method of checking UV finiteness cannot be applied to the *HybMS* scheme, because the minimal subtraction condition for  $\delta(\beta - \alpha)$  separates the  $\ln(\mu)$ -terms from the  $\epsilon^{-1}$ -poles and hence introduces a remaining dependence of the NLO amplitude on the renormalization scale. However, considering the fact that the only difference between the *HybMS* scheme and the *Kan* scheme is the UV finite part in  $\delta(\beta - \alpha)$ , the UV finiteness of the decay amplitude in the former scheme is manifest as well.

Eventually the formula for the real corrections given in Eq. (5.47) was implemented in `CalcGamma` to obtain infra-red finite results for the physical decay widths. How the infra-red finiteness of  $\Gamma_{H/h}^{\text{obs}}$  as defined in Eq. (5.12), has been checked, is explained in Sec. 5.2.3.

## 6.2. Input Parameters

In the following all parameters are specified, that are needed for the decays  $H^+ \rightarrow W^+ h/H$  at NLO and which therefore enter `CalcGamma` as input parameters.

- **Masses of SM particles**

The masses of the  $W$ - and  $Z$ -boson, the quarks and the leptons were set to [56]<sup>1</sup>,

Mass	Value
$M_W$	80.398 GeV
$M_Z$	91.1876 GeV
$m_u$	190 MeV
$m_d$	190 MeV
$m_s$	190 MeV
$m_c$	1.4 GeV
$m_b$	4.75 GeV
$m_t$	172.5 GeV
$m_e$	510.99891 keV
$m_\mu$	105.658367 GeV
$m_\tau$	1.77684 GeV

- **SM coupling parameters**

For the electroweak fine-structure constant the value

$$\alpha_{\text{EM}} = \frac{1}{137.035999074} \quad (6.1)$$

<sup>1</sup>For the masses of the SM particles the conventions of the LHC Higgs Cross Sections Working Group were followed.



is used as given in [32]. Since unitarity of the CKM matrix  $V$  is required for the cancellation of UV divergences, the standard parametrization [32] through the following three angles

$$\sin(\theta_{12}) = \frac{|V_{us}|}{\sqrt{|V_{ud}|^2 + |V_{us}|^2}}, \quad (6.2)$$

$$\sin(\theta_{23}) = \sin(\theta_{12}) \left| \frac{V_{cb}}{V_{us}} \right|, \quad (6.3)$$

$$\sin(\theta_{13}) = |V_{ud}| \quad (6.4)$$

is used, where the CP-violating phase has been set to zero. The four needed CKM matrix elements

$$|V_{ud}| = 0.97425, \quad (6.5)$$

$$|V_{us}| = 0.2253, \quad (6.6)$$

$$|V_{ub}| = 0.00413, \quad (6.7)$$

$$|V_{cb}| = 0.0411, \quad (6.8)$$

have been taken from [32].

- **SM-like Higgs boson**

Throughout all scenarios, for which numerical results will be presented, it has been assumed that the observed signal of a neutral scalar with a mass of 125 GeV [57], corresponds to the lighter Higgs boson  $h$  of the two neutral CP-even scalars of a THDM.

- **THDM parameters**

Recalling the parametrization *SP1* of a CP-conserving THDM in Eq. (2.36), the free parameters are

$$\{ m_H, m_{H^\pm}, m_{A^0}, t_\beta, s_{\beta-\alpha}, M \}, \quad (6.9)$$

where the mixing angle  $\alpha$  has been replaced by  $s_{\beta-\alpha}$  to prevent confusion with the fine-structure constant and because  $s_{\beta-\alpha}$  appears in many couplings of the THDM.

In order to find parameter points that are neither excluded by theoretical constraints nor by the current experimental data, the THDM parameter space was scanned with the tool **ScannerS** [58, 59]. The theoretical constraints which were imposed, are the unitarity of the tree-level scattering amplitudes from the quartic scalar couplings, the stability of the vacuum and the positivity of the scalar potential. Furthermore, compatibility with the experimental data has been checked: with the EW precision constraints through the S, T and U parameters, with the constraints from flavour physics, the LEP data and the LHC Higgs data.

Note that the parameter  $M$  is fixed by  $m_{12}$  through Eq. (2.25). Since  $m_{12}$  enters **ScannerS** as an independent parameter, the latter will therefore be used below instead of  $M$  to define the scenarios. Also note, that only scenarios respecting the mass relation

$$m_{H^\pm} \geq M_W + m_H, \quad (6.10)$$

will be considered in the following to ensure the decay mode  $H^+ \rightarrow W^+ H$  to be kinematically allowed. For the same reason this mass relation is also required for the

calculation of  $\Gamma_h$  in the *Min* scheme. This is a consequence of the fact that the correctly normalized decay amplitude  $\tilde{A}_h$  (Eq. (4.106)) in that scheme is a mixture of the amplitudes  $A_h$  and  $A_H$ .

In order to study the phenomenology of the decays  $H^+ \rightarrow W^+ h/H$ , the partial decay widths  $\Gamma_{H/h}^{\text{obs}}$  will be plotted over  $m_{H^\pm}$ . To this end, two classes of type I scenarios are defined in Tab. 6.1, where all other masses are fixed with respect to  $m_{H^\pm}$ . In the plots in Sec. 6.3 for these classes  $C_1$  and  $C_2$ , the ranges of parameter points, which are not excluded yet, are indicated as pale green stripes. For illustrative reasons we have also shown parameter regions that are already excluded by experimental and by theoretical constraints.

Name	Type	$m_{H^\pm}$ [GeV]	$m_H$ [GeV]	$m_{A^0}$ [GeV]	$m_{12}$ [GeV]	$\tan(\beta)$	$s_{\beta-\alpha}$
$C_1$	I	[240, 400]	$m_{H^\pm} - 110$	$m_{H^\pm} - 50$	$m_{H^\pm} - 250$	5	0.8
$C_2$	I	[240, 310]	$m_{H^\pm} - 110$	$m_{H^\pm} - 50$	$m_{H^\pm} - 250$	15	0.95

**Table 6.1.:** Definition of two classes of type I scenarios with  $m_{H^\pm}$  as only free parameter.

In Tab. 6.2 three further scenarios are given, that were found to still be allowed in parameter scans with **ScannerS**. Because the parameter points of the classes  $C_1$  and  $C_2$ , which are not excluded, are in the region of relatively low charged Higgs masses, the scenario  $S_1$  is presented as an example of an allowed type I parameter point with  $m_{H^\pm}$  larger than 600 GeV. Similarly the two scenarios  $S_2$  and  $S_3$  are type II scenarios, where the former has a relatively low mass  $m_{H^\pm}$  and the latter a larger mass  $m_{H^\pm}$  ( $m_{H^\pm} > 600$  GeV).

Note that in the plots for the scenarios  $S_1$ ,  $S_2$  and  $S_3$  in Sec. 6.3  $m_{H^\pm}$  is varied while all other parameters are kept fixed. Using **ScannerS** we could not find any allowed parameter point when moving away from the value of  $m_{H^\pm}$  of the allowed points  $S_1$ ,  $S_2$  and  $S_3$ . Hence there are no pale green areas indicated in the corresponding plots Figs. 6.3–6.5. Whether the exclusion is due to experimental or theoretical constraints needs further investigation.

Name	Type	$m_{H^\pm}$ [GeV]	$m_H$ [GeV]	$m_{A^0}$ [GeV]	$m_{12}$ [GeV]	$\tan(\beta)$	$s_{\beta-\alpha}$
$S_1$	I	607.37	145.02	600.96	37.69	13.2	0.84
$S_2$	II	374.31	170.66	348.07	104.41	1.5	0.95
$S_3$	II	658.92	152.24	658.75	105.59	1.26	0.95

**Table 6.2.:** Definition of selected scenarios for type I and II THDMs.

- **Detector sensitivity**

The detector sensitivity  $\Delta E$ , which enters in the real corrections as the photon phase space cut-off (see Sec. 5.2), was set to 10 GeV.

### 6.3. The NLO Results

In the following the numerical results will be presented for the partial decay widths of both decays  $H^+ \rightarrow W^+ h$  and  $H^+ \rightarrow W^+ H$ , that are studied in this thesis. The NLO results are shown for the *Kan* and the *Min* renormalization scheme together with the LO results. In Addition  $\Delta\Gamma$ , defined as

$$\Delta\Gamma \equiv \frac{\Gamma^{\text{NLO}} - \Gamma^{\text{LO}}}{\Gamma^{\text{LO}}}, \quad (6.11)$$

is plotted, to exhibit the relative size of the corrections. The results for the *HybMS* renormalization scheme are discussed in the following Sec. 6.4.

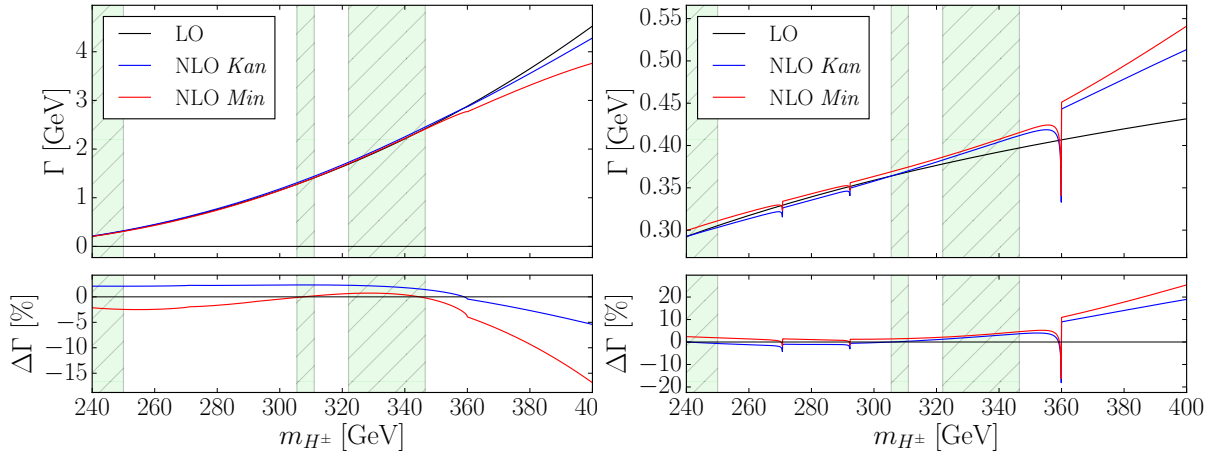


**Figure 6.1.:** Partial decay width  $\Gamma$  (upper part) and  $\Delta\Gamma$  (lower part) of the decays  $H^+ \rightarrow W^+ h$  (left) and  $H^+ \rightarrow W^+ H$  (right) at LO and at NLO in the *Kan* and *Min* scheme for the scenarios of the class  $C_1$ .

Figure 6.1 shows the results for the scenarios of class  $C_1$ , where the pale green stripes represent the parameter points which are not excluded by experimental data or theoretical constraints (see Sec. 6.2). The kinks appear when running into singularities due to the crossing of thresholds. The appearance of such singularities is a general phenomenon that is neither unique to this definition of scenarios nor to one particular renormalization scheme. For example in the right plot of Fig. 6.1 the locations of the three visible kinks are

$$m_{H^\pm} = 270.8 \text{ GeV}, \quad (6.12)$$

$$m_{H^\pm} = 292.38 \text{ GeV}, \quad (6.13)$$

$$m_{H^\pm} = 360 \text{ GeV}. \quad (6.14)$$

Recalling the definition of the class  $C_1$ , these values of  $m_{H^\pm}$  lead to masses of the neutral CP-even Higgs  $H$  that are exactly twice as large as  $M_W$ ,  $M_Z$  and  $m_h$ , respectively. Consequently, the propagators of  $W^-$ ,  $Z^-$  and light Higgs bosons in the one-loop diagrams contributing to the  $HH$  self energy  $\Sigma_{HH}$  become on-shell and thereby cause singularities of the  $B_0$  functions therein. This is to say that the results can only be trusted not too close to the thresholds. In order to obtain physical results at the threshold, one would have to take into account the finite width of the particles which propagate in the loops.

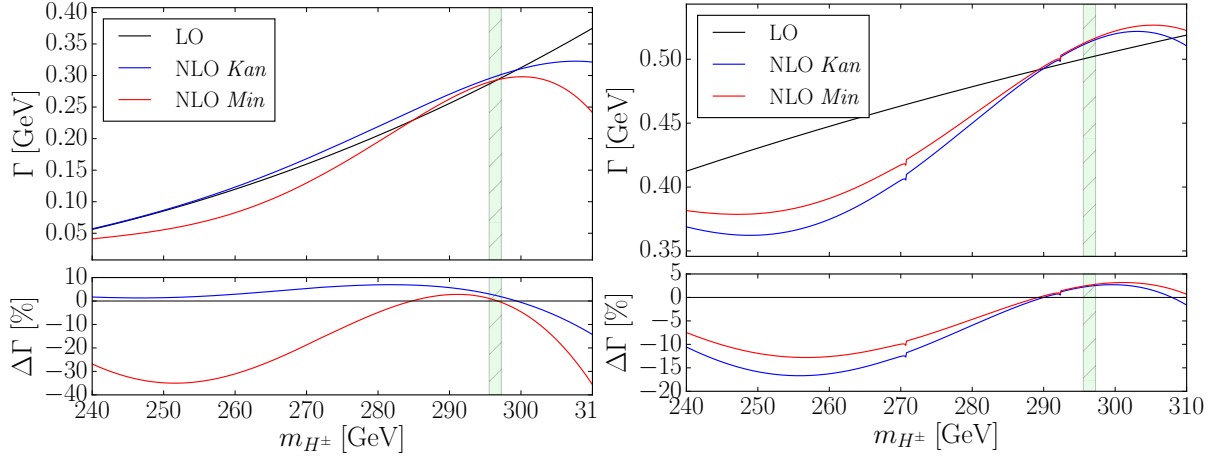
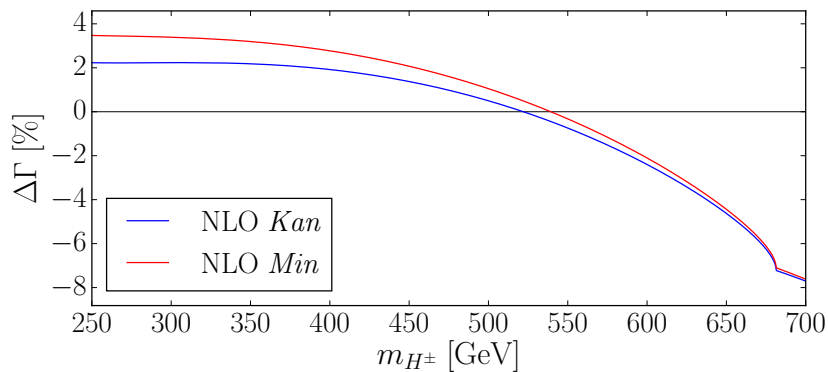


**Figure 6.2.:** Partial decay width  $\Gamma$  (upper part) and  $\Delta\Gamma$  (lower part) of the decays  $H^+ \rightarrow W^+ h$  (left) and  $H^+ \rightarrow W^+ H$  (right) at LO and at NLO in the *Kan* and *Min* scheme for the scenarios of the class  $C_2$ .

In Fig. 6.2 the results for scenarios of the class  $C_2$  are shown, which feature the same kinks as for the class  $C_1$  (as far as they are included in the shown range for  $m_{H^\pm}$ ). This is evident given that the definitions of the two scenario classes differ only in  $t_\beta$  and  $s_{\beta-\alpha}$ .

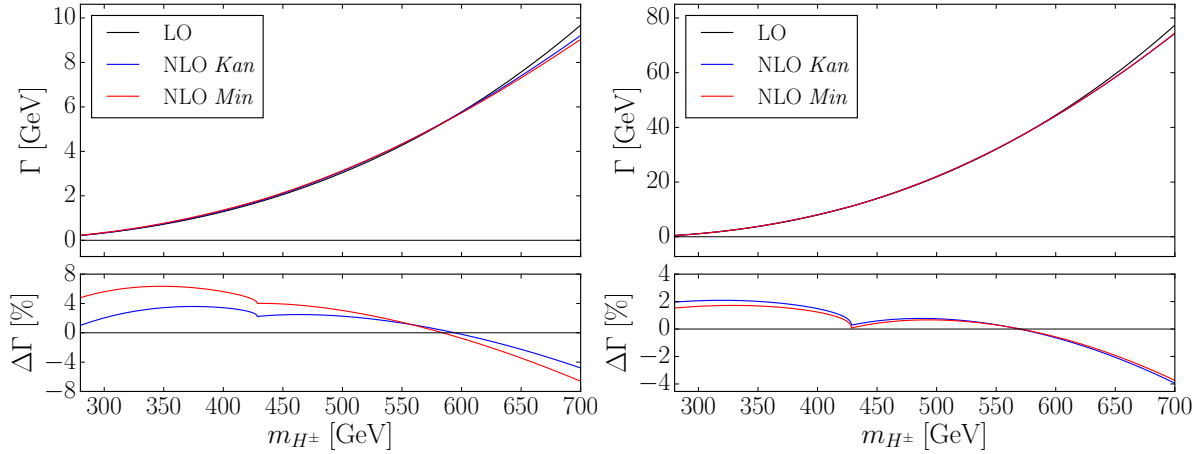
Although the corrections in these type I scenarios can become as large as  $\pm 30\%$  for values of  $m_{H^\pm}$  as displayed in the plots, the corrections are of the order of a few percent in the areas that are not excluded. The decay widths in Fig. 6.1 and Fig. 6.2 are only shown for  $m_{H^\pm}$  up to 400 GeV and 310 GeV, respectively. Beyond these ranges the corrections get very large. In the scenarios of class  $C_1$  they are as large as 80 % for  $m_{H^\pm} = 600$  GeV and for the scenarios of class  $C_2$  the corrections become negative and very large so that for  $m_{H^\pm} \approx 350$  GeV the NLO decay width would already become negative. Note, however, that these parameter regions are excluded.

Figure 6.3 shows  $\Delta\Gamma$  for the decay channel with the heavy Higgs in the final state in the  $S_1$  scenario for varying  $m_{H^\pm}$ , while all other parameters are kept fixed. It is reassuring to



**Figure 6.3.:**  $\Delta\Gamma$  of the decay  $H^+ \rightarrow W^+ H$  in the *Kan* and *Min* scheme for the  $S_1$  scenario with varying  $m_{H^\pm}$  and otherwise fixed parameters.

see that for a scenario with  $m_{H^\pm} > 600$  GeV, but that is not excluded, the corrections are relatively small and do not explode as in the cases of the classes  $C_1$  and  $C_2$  for large  $m_{H^\pm}$ . The knee that is visible in the plot, is again due to analogous threshold effects.



**Figure 6.4.:** Partial decay width  $\Gamma$  (upper part) and  $\Delta\Gamma$  (lower part) of the decays  $H^+ \rightarrow W^+ h$  (left) and  $H^+ \rightarrow W^+ H$  (right) at LO and at NLO in the *Kan* and *Min* scheme for the  $S_2$  scenario with varying  $m_{H^\pm}$  and otherwise fixed parameters.

The plots in Fig. 6.4 and Fig. 6.5 finally show the results for the two selected type II scenarios  $S_2$  and  $S_3$ , where again only  $m_{H^\pm}$  was varied, while all other parameters were kept fixed. With corrections between +10% and -10%, they are moderate over a large range of  $m_{H^\pm}$ .

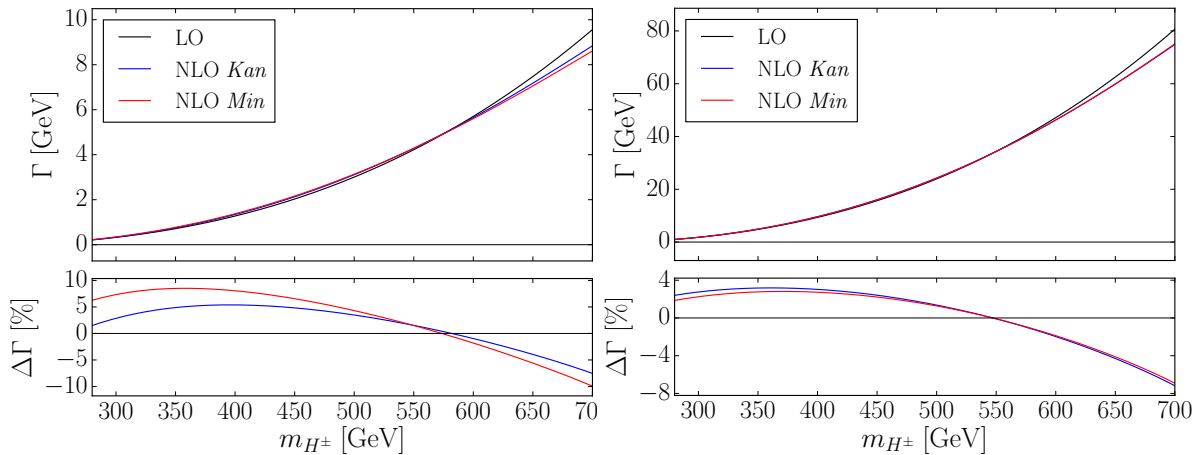


**Figure 6.5.:** Partial decay width  $\Gamma$  (upper part) and  $\Delta\Gamma$  (lower part) of the decays  $H^+ \rightarrow W^+ h$  (left) and  $H^+ \rightarrow W^+ H$  (right) at LO and at NLO in the *Kan* and *Min* scheme for the  $S_3$  scenario with varying  $m_{H^\pm}$  and otherwise fixed parameters.

The decay  $H^+ \rightarrow W^+ H$  is phase space suppressed compared to the decay  $H^+ \rightarrow W^+ h$ . In the classes  $C_1$  and  $C_2$  this suppression gets even enhanced due to  $m_H$  growing with  $m_{H^\pm}$ , while  $m_h$  is fixed at 125 GeV. Nonetheless  $\Gamma_H$  is in most shown scenarios comparable to  $\Gamma_h$  or even larger than the former as it can be seen in Fig. 6.2. This is a consequence of the LO coupling being proportional to  $s_{\beta-\alpha}$  for the case with the heavy Higgs  $H$ , but proportional to

$c_{\beta-\alpha}$  for the case that involves the light Higgs  $h$  (see Eq. (3.3)). Experimental data strongly favour values of  $s_{\beta-\alpha}$  close to one [52, 60]. This is reflected in the fact that the scenarios defined in Sec. 6.2, which were found to still be allowed, have values of  $s_{\beta-\alpha}$  between 0.8 and 1. Hence  $c_{\beta-\alpha}$  is accordingly small and suppresses the decay mode  $H^+ \rightarrow W^+ h$ .

In conclusion, the *Kan* scheme and the *Min* scheme lead to NLO corrections that are of the order of a few percent to ten percent for parameter points which are neither excluded by theoretical nor by experimental constraints. Note, however, that the difference between the corrections in the two schemes is typically of the same size of a few percent. Using the renormalization scheme dependence as a rough estimate for the theoretical uncertainty due to missing higher order corrections, the presented results suggest that the NNLO calculation is needed to obtain a prediction with a smaller theoretical uncertainty.

#### 6.4. The *HybMS* Scheme

When studying the numerical outcome, the *HybMS* scheme defined in Sec. 4.4.4 turns out not to be a good renormalization scheme. This can be seen in Fig. 6.6, where the results for the decay width in the *HybMS* scheme are shown in addition to the ones in the *Min* and the *Kan* scheme. The large corrections of several hundred percent in the *HybMS* scheme are not unique to the scenario of the class  $C_1$  that was chosen for this plot. The situation is similar in other scenarios and Fig. 6.6 is merely one illustrative example.

As mentioned before, the only difference between the *HybMS* scheme and the *Kan* scheme is that the CT  $\delta(\beta - \alpha)$  contains only the pure divergence in the former scheme. While in the *Kan* scheme large finite corrections from the wave function renormalization constants  $\delta Z_{G^+ H^+}$  and  $\delta Z_{Hh}$  are cancelled by the large finite contribution from  $\delta(\beta - \alpha)$ , this cancellation does not occur in the *HybMS* scheme and thus leads to the large corrections in Fig. 6.6.

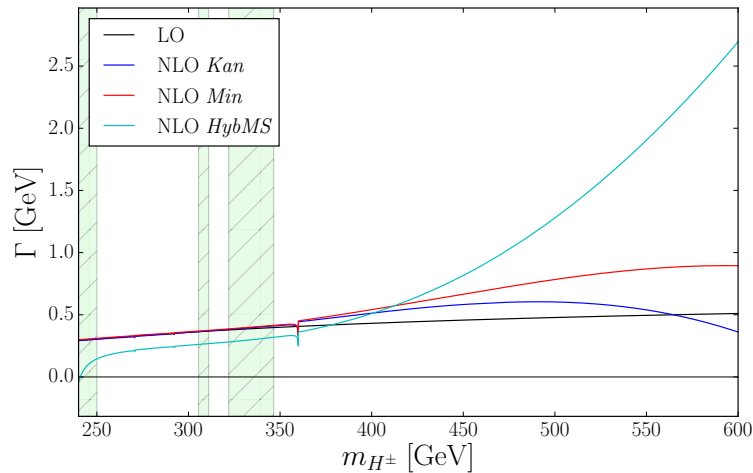


**Figure 6.6.:** Comparison of the NLO partial decay width of the decay  $H^+ \rightarrow W^+ H$  in the *HybMS*, *Kan* and *Min* scheme for the scenarios of class  $C_1$ .

As pointed out in Sec. 6.1, due to the  $\overline{\text{MS}}$  condition for  $\delta(\beta - \alpha)$ , there is a remaining dependence of the decay width on the renormalization scale  $\mu$ . The strength of the dependence on this artificial scale can be seen as a measure for the theoretical uncertainty due to missing

higher order corrections. In Fig. 6.6 the result for the *HybMS* scheme is shown for  $\mu = m_{H^\pm}$ , which motivates the following definition

$$\Delta\Gamma_\mu \equiv \frac{\Gamma(\mu) - \Gamma(\mu = m_{H^\pm})}{\Gamma(\mu = m_{H^\pm})}. \quad (6.15)$$

Varying  $\mu$  between  $m_{H^\pm}/2$  and  $2m_{H^\pm}$  reveals in Fig. 6.7 how strongly the decay width depends on  $\mu$  in this scheme. Whether the large deviations of up to 50% would shrink and the results for the partial decay widths converge with the results in other schemes, once higher order corrections are taken into account, cannot be decided from only looking at NLO. Given how large the differences are, it could also be the case that the *HybMS* scheme is in general not a good scheme.

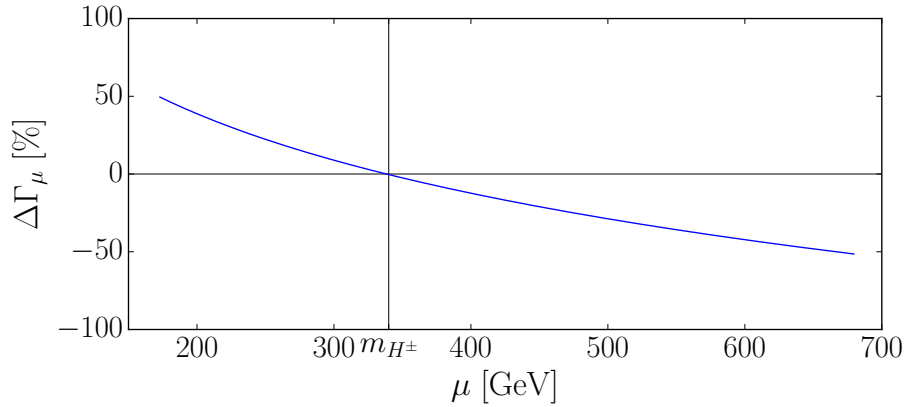


**Figure 6.7.:**  $\Delta\Gamma_\mu$  in the *Kan* scheme for the scenario of class  $C_1$  with  $m_{H^\pm} = 340$  GeV, where  $\mu$  was varied from  $m_{H^\pm}/2$  to  $2m_{H^\pm}$ .

## 6.5. Dependence on the Detector Sensitivity $\Delta E$

The real corrections  $\Gamma_{\phi\gamma}^{\text{soft}}$  were calculated in the soft photon approximation. As has been mentioned in Sec. 5.2.3, this approximation is only justified if the resulting dependence of  $\Gamma_\phi^{\text{obs}}$  on the detector sensitivity  $\Delta E$  is not strong. In order to check that this is indeed the case for the decays  $H^+ \rightarrow W^+ h/H$ , the partial decay width was calculated for different values of  $\Delta E$ , while all other parameters were kept fixed. Given that the results of the previous sections were calculated for  $\Delta E = 10$  GeV,  $\Delta\Gamma_{\Delta E}$  defined as

$$\Delta\Gamma_{\Delta E} \equiv \frac{\Gamma(\Delta E) - \Gamma(\Delta E = 10 \text{ GeV})}{\Gamma(\Delta E = 10 \text{ GeV})}, \quad (6.16)$$

may serve as a measure for the dependence on  $\Delta E$ . In Fig. 6.8  $\Delta\Gamma_{\Delta E}$  is shown for the parameter point of the scenario of the class  $C_1$  with  $m_{H^\pm} = 340$  GeV.

In the possibly relevant range for  $\Delta E$  in experiments the relative difference is of the order of a few permille. In comparison to the size of the typical NLO corrections which are of the order of a few % up to 10%, this is an acceptable remaining dependence on  $\Delta E$ . The curve in Fig. 6.8 exhibits the  $\ln(\Delta E)$  dependence from the  $I_{ij}$  integrals of Eq. (5.23), that feed into the soft bremsstrahlung corrections. For the shown plot the *Kan* scheme was used, but the drawn conclusion holds for all schemes presented in Chapter 4, as they all share the same  $\Gamma_{\phi\gamma}^{\text{soft}}$ .

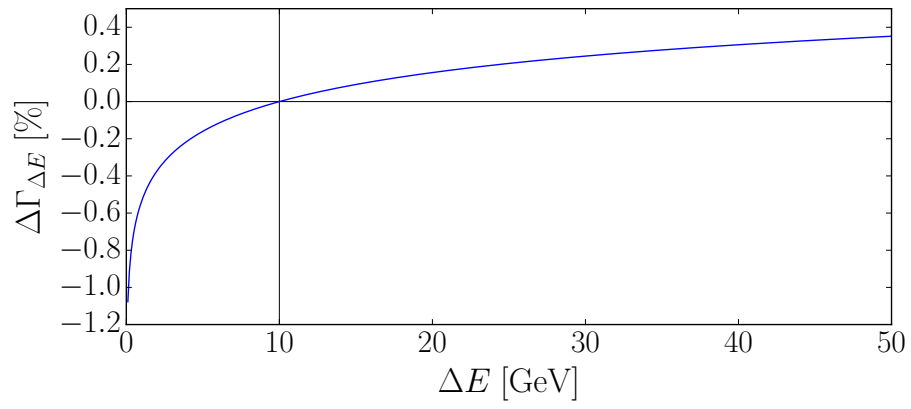


**Figure 6.8.:**  $\Delta\Gamma_{\Delta E}$  in the *Kan* scheme for the scenario of the class  $C_1$  with  $m_{H^\pm} = 340$  GeV, where  $\Delta E$  was varied from 0.1 GeV to 50 GeV.



---

## Summary and Conclusion

---

This thesis has dealt with the calculation of the full NLO partial decay width of the two decay modes  $H^+ \rightarrow W^+ h$  and  $H^+ \rightarrow W^+ H$  of the charged Higgs boson in a CP-conserving THDM. Charged Higgs bosons provide the cleanest signature of THDMs [16] and given the recent start of run II at the LHC, predictions for the production and decay of charged scalars are of great interest. Although the dominant decay channel is  $H^+ \rightarrow t\bar{b}$ , this is a challenging search channel due to the large QCD background. Hence the decay modes considered in this thesis could prove to be relevant for searches.

In Sec. 6.3 the results were presented in a selection of different scenarios for two different renormalization schemes, the *Kan* scheme and the *Min* scheme. In a previous publication it was found that for the partial decay width of the decay mode with the light Higgs in the final state, the corrections from only top and bottom quarks can in some scenarios be as large as 80% [16]. In their analysis only constraints from tree-level unitarity arguments had been imposed, while now, almost twenty years later, the available experimental data severely restrict the allowed parameter space. In scenarios that emerged as compatible with the theoretical and the current experimental constraints (using the tool *ScannerS* [52, 59]), the full EW corrections turn out to be typically of the order of a few percent up to ten percent.

The difference between the two schemes is however, of same order of a few percent for the allowed parameter points. Taking the renormalization scheme dependence as a rough estimate for the theoretical uncertainty these results thus suggest that the NNLO calculation is needed to obtain a reliable prediction.

Although the decay into  $W^+ H$  is phase space suppressed compared to the decay into  $W^+ h$ , in the presented scenarios the former channel either has a comparable decay width or an even larger one than the latter. This is due to the fact that experiments favour  $s_{\beta-\alpha}$  close to one so that consequently the coupling  $\lambda_{H^+ h W^-}$  is suppressed, as it is proportional to  $c_{\beta-\alpha}$ .

The study of the decays  $H^+ \rightarrow W^+ h/H$  at NLO was embedded in a discussion of more general questions on the renormalization of CP-conserving THDMs. The intention was to

understand what the differences between various renormalization schemes are, what their advantages and disadvantages are and in particular what subtleties arise when renormalizing the mixing angles. Ultimately, one would like to know whether there is one scheme which is generally preferable.

The intuition behind on-shell conditions was explained in Sec. 4.2 and it was pointed out in Sec. 4.3 that in a CP-conserving THDM it is possible to renormalize all 4 scalar masses on-shell in order to preserve their physical meaning beyond LO. For all practical purposes, these masses are part of the complete set of independent parameters describing the Higgs sector, as are the tadpole parameters which are renormalized such that the vevs are ensured to be minima of the potential also beyond LO (Eq. (4.26)). It is also natural to renormalize the massive gauge boson masses  $M_W$  and  $M_Z$  on-shell and to define the electric charge  $e$  in the standard way in the Thomson limit. Recalling the set of independent parameters  $SP1$ ,

$$\{ m_h, m_H, m_{H^\pm}, m_{A^0}, M_W, M_Z, e, t_\beta, T_h, T_H, \alpha, M \}, \quad (7.1)$$

what a renormalization scheme still has to specify, is how to renormalize  $t_\beta$ ,  $\alpha$  (or equivalently  $s_{\beta-\alpha}$ ) and  $M$  as well as the scalar fields. In contrast to the other parameters, there is no obvious way of relating the mixing angles and  $M$  to observables.

Different renormalization schemes assign different UV finite parts to the CTs and as a consequence different numerical values for the parameters  $t_\beta$ ,  $s_{\beta-\alpha}$  and  $M$  are inferred from experimental measurements. These different definitions of the parameters can differ with respect to

- gauge independence
- numerical stability
- process independence.

These partly necessary, partly desirable features are discussed by Freitas *et al.* for the prevailing schemes in the context of the MSSM [39]. In the MSSM however, there is only one parameter for which these issues play a role, namely  $t_\beta$ , while in a general THDM there are three of them, two angles and the soft symmetry breaking parameter  $M$ . The results of their paper do thus not necessarily translate to the case of a general THDM.

While the requirement of numerical stability has to be fulfilled by any scheme in practice, gauge independence and process independence are not mandatory features. Given the gauge invariance of the theory, any relation only between observables will be gauge independent. The relation between unphysical parameters of the model and observables, however may well depend on the gauge. But if one wishes to assign a more physical interpretation to the parameters, in particular to the mixing angles which play a prominent role in THDMs, they ought to be gauge independent and process-independent.

In view of the given criteria, the schemes that were presented in Chapter 4 shall be briefly recapitulated here:

### 1. Process-dependent schemes

In Sec. 4.4.4 the basic idea of a process-dependent renormalization condition for mixing angles was explained by trying to use the decay  $H^+ \rightarrow W^+ H$  to fix  $\delta(\beta - \alpha)$ . At NLO

such a condition is in general of the form

$$\Gamma^{\text{NLO}} \stackrel{!}{=} \Gamma^{\text{LO}} . \quad (7.2)$$

As observables, partial decay widths are gauge independent. If all other counterterms in the NLO decay amplitude have already been fixed in a gauge independent way, e.g. through on-shell conditions, then the gauge independence of the angle CT fixed by Eq. (7.2) is manifest. Consequently the value for the corresponding angle which would be inferred from an experimental measurement would likewise be gauge independent.

But this approach also implies that a process-dependent UV finite part is defined into the angle. This gives the scheme its name and the angle a non-universal meaning. One may hope to replace Eq. (7.2) by the condition  $\Gamma^{\text{NLO}} \stackrel{!}{=} \Gamma^{\text{measured}}$ , which of course rests on having already discovered a BSM scalar and on being able to measure this particular decay channel. As pointed out in Sec. 5.2.4, requiring the measurability of the process that is used in the renormalization condition, strongly restricts the eligible processes for such a scheme.

The discussion in Sec. 5.2.4 also showed that the decay  $H^+ \rightarrow W^+ H$  cannot be used to define a renormalization condition. This is due to the fact that the IR divergent virtual QED corrections cannot be separated as a UV finite subset. Therefore Freitas *et al.* suggest to use the decay  $A^0 \rightarrow \tau^+ \tau^-$  instead in order to circumvent this issue for the process-dependent renormalization of  $\tan(\beta)$  in the MSSM. As stated in [39], this scheme is not affected by numerical instabilities.

For the THDM with two mixing angles, one would have to rely on two different processes. With the potential problem of IR divergences in mind, the decay  $H \rightarrow \tau^+ \tau^-$  could be used in addition to the decay of the pseudoscalar. Despite the strong advantage of the manifest gauge independence of angles, this scheme is technically involved, in particular if going beyond NLO.

## 2. *Kan* scheme

As far as one can tell from studying the decays  $H^+ \rightarrow W^+ h/H$  at NLO, the *Kan* scheme does not suffer from numerical instabilities. Also, this scheme was used by Kanemura *et al.* to calculate a large set of one-loop corrected couplings in the CP-conserving THDM [18].

The characteristic feature of this approach is that the angle counterterms show up as part of the field renormalization matrix, which reflects the strong link between the renormalization of the mixing angles and the scalar fields. The angle CTs are fixed by on-shell conditions in a way that is technically simple and could easily be extended to a next-to-next-to leading order calculation. Despite the fact that the renormalization conditions come across in the spirit of physically intuitive on-shell conditions, this scheme introduces a gauge dependence for  $\beta$ . In their recent paper [18] Kanemura *et al.* give a solution to circumvent this issue. It is unclear, however, what their suggestion - beyond being a formal solution - implies in practice; unless the calculation is done with a general gauge fixing parameter.

### 3. *Min* scheme

The *Min* scheme is ‘minimal’ in the sense of the minimum number of field renormalization parameters that are necessary to obtain UV finite  $S$ -matrix elements and Green’s functions. Concerning the renormalization of the angles it is a mixture of what was called the Kanemura approach and the condition  $\delta v_1/v_1 = \delta v_2/v_2$  [43–45] that feeds into the renormalization of  $\tan(\beta)$ . At this stage it is not clear whether this combination will lead to a gauge dependent definition of  $\tan(\beta)$ . It was beyond the scope of this thesis to examine the gauge dependence.

Dealing with the wave function normalization matrix  $Z_N$  of Eq. (4.95) may technically speaking appear to be inconvenient. Once the self energies which are anyway needed for a complete on-shell renormalization scheme are implemented, the required technical effort is negligible. In the end, the same amount of parameters and equally many conditions are necessary in both cases to ensure all scalars to satisfy the on-shell relations - be it in the form of renormalization conditions or in the derivation of the wave function normalization matrix  $Z_N$ .

### 4. *HybMS* scheme

The numerical results for the *HybMS* scheme in Sec. 6.4 showed that the corrections in this scheme become extremely large compared to the on-shell schemes (see Fig. 6.6). In the *Kan* scheme, large finite corrections from the wave function renormalization constants  $\delta Z_{G^+H^+}$  and  $\delta Z_{Hh}$  are cancelled by the large finite contribution from  $\delta(\beta - \alpha)$ . The latter finite term is missing in the *HybMS* scheme, which is the reason for the unphysically large corrections and the strong dependence on the renormalization scale (see Fig. 6.7). The *HybMS* scheme thus turns out not to be a useful renormalization scheme for the decays explored in this thesis.

Freitas *et al.* establish a ‘no-go-theorem’ for the MSSM, that basically says that there is no such perfect renormalization scheme, that suffers neither from numerical instabilities, nor from gauge dependence or process dependence. A general CP-conserving THDM has more independent parameters that do not represent an observable quantity. It hence gives even more freedom to choose renormalization conditions. For the time being it is not clear whether an analogous ‘no-go-theorem’ also holds for the case of the THDM.

It would certainly be interesting to investigate the gauge dependence of the *Min* scheme and other schemes one can think of, but that have not been covered in this thesis. On the one hand this should be done in a general manner with the tool of extended Slavnov-Taylor-identities as in [39]. On the other hand it could prove helpful to follow the suggestion by Kanemura *et al.* to avoid a gauge dependence of  $\tan(\beta)$  (Eq. (4.69)). To this end, one would have to calculate the self energy  $\Sigma_{G^0A^0}$  as well as the tadpole diagrams in a general gauge. Once this was done, the obtained expression for  $\delta\beta$  would be a candidate for a perfect scheme in the above sense.

This thesis has shed some light on the differences between various renormalization schemes, on the issues that arise when mixing angles are renormalized and on the different intuitions that lie behind them.

Vertex Corrections

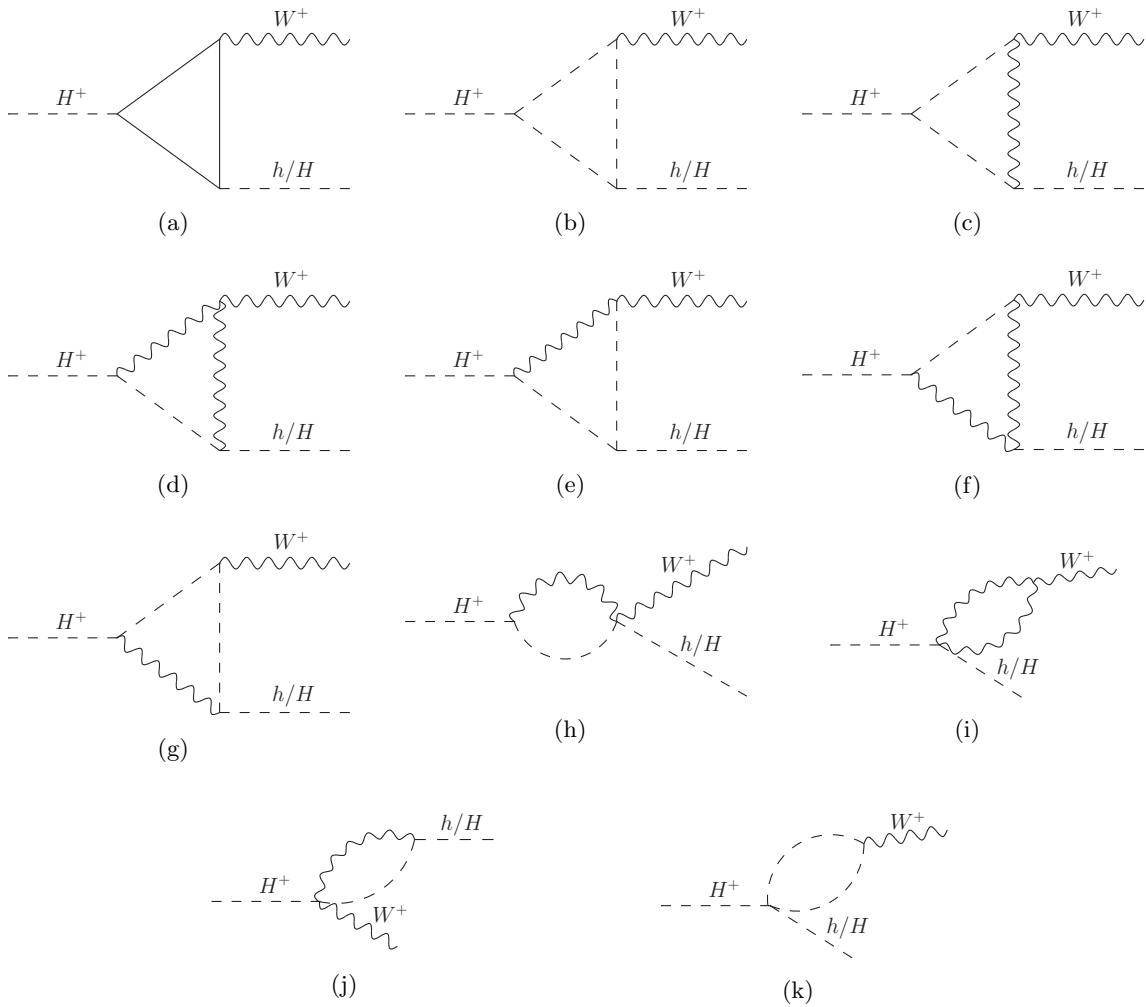


**Figure A.1.:** Generic Lorentz structures contributing to the vertex corrections of the  $H^+W^-h$ -vertex and the  $H^+W^-H$ -vertex, respectively.

## APPENDIX B

---

### Tadpole Parameters

---

The matrices  $\delta T$  with the tadpole renormalization parameters, defined in Eq. (4.25), are given explicitly in the following. For  $\theta = \beta$  the entries of the symmetric matrices

$$\begin{pmatrix} \delta T_{G^+G^+} & \delta T_{G^+H^+} \\ \delta T_{H^+G^+} & \delta T_{H^+H^+} \end{pmatrix} = \begin{pmatrix} \delta T_{G^0G^0} & \delta T_{G^0A^0} \\ \delta T_{A^0G^0} & \delta T_{A^0A^0} \end{pmatrix}, \quad (\text{B.1})$$

are given by

$$\delta T_{G^+G^+} = \frac{c_\beta}{v} \delta T_1 + \frac{s_\beta}{v} \delta T_2 = -\frac{c_{\beta-\alpha}}{v} \delta T_H - \frac{s_{\beta-\alpha}}{v} \delta T_h, \quad (\text{B.2})$$

$$\delta T_{G^+H^+} = \frac{c_\beta}{v} \delta T_2 - \frac{s_\beta}{v} \delta T_1 = \frac{s_{\beta-\alpha}}{v} \delta T_H - \frac{c_{\beta-\alpha}}{v} \delta T_h = \delta T_{H^+G^+}, \quad (\text{B.3})$$

$$\delta T_{H^+H^+} = \frac{s_\beta^2}{c_\beta v} \delta T_1 + \frac{c_\beta^2}{s_\beta v} \delta T_2 = -\frac{c_\alpha s_\beta^3 + s_\alpha c_\beta^3}{v s_\beta c_\beta} \delta T_H + \frac{s_\alpha s_\beta^3 - c_\alpha c_\beta^3}{v s_\beta c_\beta} \delta T_h \quad (\text{B.4})$$

and for  $\theta = \alpha$ , the entries of the matrix

$$\begin{pmatrix} \delta T_{HH} & \delta T_{Hh} \\ \delta T_{hH} & \delta T_{hh} \end{pmatrix}, \quad (\text{B.5})$$

are given by

$$\delta T_{HH} = \frac{c_\alpha^2}{c_\beta v} \delta T_1 + \frac{s_\alpha^2}{s_\beta v} \delta T_2 = -\frac{c_\alpha^3 s_\beta + s_\alpha^3 c_\beta}{v s_\beta c_\beta} \delta T_H + \frac{s_\alpha c_\alpha^2 s_\beta - c_\alpha s_\alpha^2 c_\beta}{v s_\beta c_\beta} \delta T_h, \quad (\text{B.6})$$

$$\delta T_{Hh} = \frac{s_\alpha c_\alpha}{s_\beta v} \delta T_2 - \frac{s_\alpha c_\alpha}{c_\beta v} \delta T_1 = \frac{s_{2\alpha}}{v s_{2\beta}} (s_{\beta-\alpha} \delta T_H - c_{\beta-\alpha} \delta T_h) = \delta T_{Hh}, \quad (\text{B.7})$$

$$\delta T_{hh} = \frac{s_\alpha^2}{c_\beta v} \delta T_1 + \frac{c_\alpha^2}{s_\beta v} \delta T_2 = -\frac{s_{2\alpha}}{v s_{2\beta}} c_{\beta-\alpha} \delta T_H + \frac{s_\alpha^3 s_\beta - c_\alpha^3 c_\beta}{v s_\beta c_\beta} \delta T_h. \quad (\text{B.8})$$

## APPENDIX C

## Alternative Parametrization of the Scalar Potential

The Higgs Hunter's Guide [14] uses a different parametrization of the scalar potential compared to the one given in Eq. (2.6). In particular because the parametrization of the coupling constants in the `FeynArts` model file `THDM.mod` is based on the former, this alternative is presented as well, including the transformation rules between both parametrizations. The CP-conserving potential (i.e. setting  $\Lambda_7$  and the relative phase  $\xi$  between the vevs to zero) reads

$$\begin{aligned}
V(\Phi_1, \Phi_2) = & \Lambda_1 \left( \Phi_1^\dagger \Phi_1 - V_1^2 \right)^2 + \Lambda_2 \left( \Phi_2^\dagger \Phi_2 - V_2^2 \right)^2 \\
& + \Lambda_3 \left[ \left( \Phi_1^\dagger \Phi_1 - V_1^2 \right) + \left( \Phi_2^\dagger \Phi_2 - V_2^2 \right) \right]^2 \\
& + \Lambda_4 \left[ \left( \Phi_1^\dagger \Phi_1 \right) \left( \Phi_2^\dagger \Phi_2 \right) - \left( \Phi_1^\dagger \Phi_2 \right) \left( \Phi_2^\dagger \Phi_1 \right) \right] \\
& + \Lambda_5 \left[ \text{Re} \left( \Phi_1^\dagger \Phi_2 \right) - V_1 V_2 \right]^2 + \Lambda_6 \left[ \text{Im} \left( \Phi_1^\dagger \Phi_2 \right) \right]^2 .
\end{aligned} \tag{C.1}$$

To prevent confusion with the  $\lambda_1 - \lambda_5$  of Eq. (2.6) and the definition of the vevs  $v_1$  and  $v_2$  there, capital letters are used for this alternative. The different vevs are related to each other via

$$V_i = \frac{v_i}{\sqrt{2}}, \quad i = 1, 2, \tag{C.2}$$

while the parameters  $\Lambda_1 - \Lambda_6$  can be identified with the following combinations of the pa-

parameters of Eq. (2.6) [31],

$$\Lambda_1 = \frac{1}{2} \left[ \lambda_1 - \lambda_{345} + 2 \frac{M^2}{v^2} \right], \quad (\text{C.3})$$

$$\Lambda_2 = \frac{1}{2} \left[ \lambda_2 - \lambda_{345} + 2 \frac{M^2}{v^2} \right], \quad (\text{C.4})$$

$$\Lambda_3 = \frac{1}{2} \left[ \lambda_{345} - 2 \frac{M^2}{v^2} \right], \quad (\text{C.5})$$

$$\Lambda_4 = 2 \frac{M^2}{v^2} - \lambda_4 - \lambda_5, \quad (\text{C.6})$$

$$\Lambda_5 = 2 \frac{M^2}{v^2}, \quad (\text{C.7})$$

$$\Lambda_6 = 2 \frac{M^2}{v^2} - 2\lambda_5. \quad (\text{C.8})$$



---

## Acknowledgement

---

First and foremost, I want to express my gratitude to my supervisor Prof. Dr. Margarete Mühlleitner, who gave me the opportunity to engage in this interesting research project, to learn a great amount, and to get a first glimpse of the joys and challenges of research. She both gave me freedom to develop my own ideas and, despite her myriad responsibilities, always took the time to discuss and answer my questions whenever I sought her advice. I would like to thank her for having supported me in many ways with her kind manner throughout the past year and also for having given me the chance to participate in a week-long research stay in Aveiro, Portugal.

I also want to thank Prof. Dr. Ulrich Nierste for being so kind as to act as the second reviewer of this thesis and for drawing my attention to helpful and important literature.

My sincere thanks also goes to Prof. Dr. Rui Santos who co-supervised this research project. Despite the geographical distance to Lisbon, he was always available and happy to discuss my questions and gave very helpful advice when I was stuck. I would also like to say thank you for the great time we had during the research stay in Aveiro.

I am also much obliged to Hanna Ziesche who not only cross-checked my calculations, but who helped me with admirable patience to understand many technical issues and discussed all the problems I was facing from the early stages of this project to the final submission of the thesis. Although I dropped in to her office almost daily, I always found her happy to discuss my questions.

In addition I want to particularly thank Dr. Kathrin Walz for the very fruitful discussions throughout the past year. I have been a frequent visitor to her office too, and especially during the last weeks she helped a great deal in resolving some persistent points of confusion.

I owe a lot of help to Raul Costa and Dr. Marco Sampaio, who generously provided me with samples of allowed parameter points and who took the time to answer my naive questions on the software tool **ScannerS**.

I also want to thank all those who helped proofreading parts of this thesis. The feedback that I got from Hanna Ziesche, Dr. Kathrin Walz, Alexander Wlotzka, Juraj Streicher and Jessica Davies, was very thoughtful and helpful. I thank them for all of their efforts.

Finally I would like to express my gratitude to my parents. They have always supported me, and without their help I could have never studied so freely. Having been given the chance to pursue my passion and engage in my studies wholeheartedly cannot be taken for granted and means a lot to me.

# References

- [1] S. Glashow, “Partial Symmetries of Weak Interactions,” *Nucl.Phys.* **22** (1961) 579–588.
- [2] S. Weinberg, “A model of leptons,” *Phys. Rev. Lett.* **19** (Nov, 1967) 1264–1266.  
<http://link.aps.org/doi/10.1103/PhysRevLett.19.1264>.
- [3] A. Salam, “Weak and Electromagnetic Interactions,” *Conf.Proc.* **C680519** (1968) 367–377.
- [4] N. Cabibbo, “Unitary symmetry and leptonic decays,” *Phys. Rev. Lett.* **10** (Jun, 1963) 531–533. <http://link.aps.org/doi/10.1103/PhysRevLett.10.531>.
- [5] M. Kobayashi and T. Maskawa, “Cp-violation in the renormalizable theory of weak interaction,” *Progress of Theoretical Physics* **49** no. 2, (1973) 652–657,  
<http://ptp.oxfordjournals.org/content/49/2/652.full.pdf+html>.  
<http://ptp.oxfordjournals.org/content/49/2/652.abstract>.
- [6] P. W. Higgs, “Broken symmetries and the masses of gauge bosons,” *Phys. Rev. Lett.* **13** (Oct, 1964) 508–509. <http://link.aps.org/doi/10.1103/PhysRevLett.13.508>.
- [7] P. W. Higgs, “Spontaneous symmetry breakdown without massless bosons,” *Phys. Rev.* **145** (May, 1966) 1156–1163. <http://link.aps.org/doi/10.1103/PhysRev.145.1156>.
- [8] F. Englert and R. Brout, “Broken symmetry and the mass of gauge vector mesons,” *Phys. Rev. Lett.* **13** (Aug, 1964) 321–323.  
<http://link.aps.org/doi/10.1103/PhysRevLett.13.321>.
- [9] G. S. Guralnik, C. R. Hagen, and T. W. B. Kibble, “Global conservation laws and massless particles,” *Phys. Rev. Lett.* **13** (Nov, 1964) 585–587.  
<http://link.aps.org/doi/10.1103/PhysRevLett.13.585>.
- [10] T. W. B. Kibble, “Symmetry breaking in non-abelian gauge theories,” *Phys. Rev.* **155** (Mar, 1967) 1554–1561. <http://link.aps.org/doi/10.1103/PhysRev.155.1554>.
- [11] **ATLAS** Collaboration, G. Aad *et al.*, “Observation of a new particle in the search for the Standard Model Higgs boson with the ATLAS detector at the LHC,” *Phys.Lett.* **B716** (2012) 1–29, [arXiv:1207.7214](https://arxiv.org/abs/1207.7214) [hep-ex].
- [12] **CMS** Collaboration, S. Chatrchyan *et al.*, “Observation of a new boson at a mass of 125 GeV with the CMS experiment at the LHC,” *Phys.Lett.* **B716** (2012) 30–61, [arXiv:1207.7235](https://arxiv.org/abs/1207.7235) [hep-ex].
- [13] T. D. Lee, “A theory of spontaneous  $t$  violation,” *Phys. Rev. D* **8** (Aug, 1973) 1226–1239. <http://link.aps.org/doi/10.1103/PhysRevD.8.1226>.
- [14] J. F. Gunion, H. E. Haber, G. L. Kane, and S. Dawson, “The Higgs Hunter’s Guide,” *Front.Phys.* **80** (2000) 1–448.

- [15] G. Branco, P. Ferreira, L. Lavoura, M. Rebelo, M. Sher, *et al.*, “Theory and phenomenology of two-Higgs-doublet models,” *Phys.Rept.* **516** (2012) 1–102, [arXiv:1106.0034 \[hep-ph\]](#).
- [16] R. Santos, A. Barroso, and L. Brucher, “Top quark loop corrections to the decay  $H^+ \rightarrow h^0 W^+$  in the two Higgs doublet model,” *Phys.Lett.* **B391** (1997) 429–433, [arXiv:hep-ph/9608376 \[hep-ph\]](#).
- [17] S. Kanemura, Y. Okada, E. Senaha, and C.-P. Yuan, “Higgs coupling constants as a probe of new physics,” *Phys.Rev.* **D70** (2004) 115002, [arXiv:hep-ph/0408364 \[hep-ph\]](#).
- [18] S. Kanemura, M. Kikuchi, and K. Yagyu, “Fingerprinting the extended Higgs sector using one-loop corrected Higgs boson couplings and future precision measurements,” *Nucl.Phys.* **B896** (2015) 80–137, [arXiv:1502.07716 \[hep-ph\]](#).
- [19] **Particle Data Group** Collaboration, K. Nakamura *et al.*, “The review of particle physics,” *Journal of Physics G* **37** (2010) 075021. <http://pdg.lbl.gov>.
- [20] D. Volkov and V. Akulov, “Is the neutrino a goldstone particle?,” *Physics Letters B* **46** no. 1, (1973) 109 – 110. <http://www.sciencedirect.com/science/article/pii/0370269373904905>.
- [21] J. Wess and B. Zumino, “Supergauge transformations in four dimensions,” *Nuclear Physics B* **70** no. 1, (1974) 39 – 50. <http://www.sciencedirect.com/science/article/pii/0550321374903551>.
- [22] P. Fayet, “Supersymmetry and weak, electromagnetic and strong interactions,” *Physics Letters B* **64** no. 2, (1976) 159 – 162. <http://www.sciencedirect.com/science/article/pii/0370269376903191>.
- [23] E. Witten, “Dynamical breaking of supersymmetry,” *Nuclear Physics B* **188** no. 3, (1981) 513 – 554. <http://www.sciencedirect.com/science/article/pii/0550321381900067>.
- [24] H. Haber and G. Kane, “The search for supersymmetry: Probing physics beyond the standard model,” *Physics Reports* **117** no. 2–4, (1985) 75 – 263. <http://www.sciencedirect.com/science/article/pii/0370157385900511>.
- [25] M. Trodden, “Electroweak baryogenesis: A Brief review,” *pre-print* (1998) , [arXiv:hep-ph/9805252 \[hep-ph\]](#).
- [26] K. Funakubo, A. Kakuto, and K. Takenaga, “The Effective potential of electroweak theory with two massless Higgs doublets at finite temperature,” *Prog.Theor.Phys.* **91** (1994) 341–352, [arXiv:hep-ph/9310267 \[hep-ph\]](#).
- [27] L. Fromme, S. J. Huber, and M. Seniuch, “Baryogenesis in the two-Higgs doublet model,” *JHEP* **0611** (2006) 038, [arXiv:hep-ph/0605242 \[hep-ph\]](#).
- [28] M. Laine and K. Rummukainen, “Two Higgs doublet dynamics at the electroweak phase transition: A Nonperturbative study,” *Nucl.Phys.* **B597** (2001) 23–69, [arXiv:hep-lat/0009025 \[hep-lat\]](#).
- [29] J. M. Cline and P.-A. Lemieux, “Electroweak phase transition in two Higgs doublet models,” *Phys.Rev.* **D55** (1997) 3873–3881, [arXiv:hep-ph/9609240 \[hep-ph\]](#).
- [30] J. E. Kim, “Light pseudoscalars, particle physics and cosmology,” *Physics Reports* **150** no. 1–2, (1987) 1 – 177. <http://www.sciencedirect.com/science/article/pii/0370157387900172>.

- [31] J. F. Gunion and H. E. Haber, “The CP conserving two Higgs doublet model: The Approach to the decoupling limit,” *Phys.Rev.* **D67** (2003) 075019, [arXiv:hep-ph/0207010](#) [hep-ph].
- [32] **Particle Data Group** Collaboration, K. Olive *et al.*, “Review of Particle Physics,” *Chin.Phys.* **C38** (2014) 090001.
- [33] A. Djouadi, “The Anatomy of electro-weak symmetry breaking. II. The Higgs bosons in the minimal supersymmetric model,” *Phys.Rept.* **459** (2008) 1–241, [arXiv:hep-ph/0503173](#) [hep-ph].
- [34] M. E. Peskin and D. V. Schroeder, *An introduction to quantum field theory*. The advanced book program. Westview Pr., Boulder, Colo. [u.a.], [nachdr.] ed., 2006.
- [35] G. 't Hooft and M. Veltman, “Regularization and renormalization of gauge fields,” *Nuclear Physics B* **44** no. 1, (1972) 189 – 213. <http://www.sciencedirect.com/science/article/pii/0550321372902799>.
- [36] G. 't Hooft, “Dimensional regularization and the renormalization group,” *Nuclear Physics B* **61** no. 0, (1973) 455 – 468. <http://www.sciencedirect.com/science/article/pii/0550321373903763>.
- [37] A. Denner, “Techniques for calculation of electroweak radiative corrections at the one loop level and results for W physics at LEP-200,” *Fortsch.Phys.* **41** (1993) 307–420, [arXiv:0709.1075](#) [hep-ph].
- [38] T. Hahn, “Generating Feynman diagrams and amplitudes with FeynArts 3,” *Comput.Phys.Commun.* **140** (2001) 418–431, [arXiv:hep-ph/0012260](#) [hep-ph].
- [39] A. Freitas and D. Stockinger, “Gauge dependence and renormalization of tan beta in the MSSM,” *Phys.Rev.* **D66** (2002) 095014, [arXiv:hep-ph/0205281](#) [hep-ph].
- [40] M. Frank, *Strahlungskorrekturen im Higgs-Sektor des Minimalen Supersymmetrischen Standardmodells mit CP-Verletzung*. PhD thesis, Berlin, 2003. <http://swbplus.bsz-bw.de/bsz107705591abs.htm>. Zugl.: Karlsruhe, Univ., Diss., 2002.
- [41] M. Frank, T. Hahn, S. Heinemeyer, W. Hollik, H. Rzehak, *et al.*, “The Higgs Boson Masses and Mixings of the Complex MSSM in the Feynman-Diagrammatic Approach,” *JHEP* **0702** (2007) 047, [arXiv:hep-ph/0611326](#) [hep-ph].
- [42] D. Lopez-Val and J. Sola, “Neutral Higgs-pair production at Linear Colliders within the general 2HDM: Quantum effects and triple Higgs boson self-interactions,” *Phys.Rev.* **D81** (2010) 033003, [arXiv:0908.2898](#) [hep-ph].
- [43] P. H. Chankowski, S. Pokorski, and J. Rosiek, “Complete on-shell renormalization scheme for the minimal supersymmetric Higgs sector,” *Nucl.Phys.* **B423** (1994) 437–496, [arXiv:hep-ph/9303309](#) [hep-ph].
- [44] P. Chankowski, S. Pokorski, and J. Rosiek, “One-loop corrections to the supersymmetric higgs boson couplings and {LEP} phenomenology,” *Physics Letters B* **286** no. 3–4, (1992) 307 – 314. <http://www.sciencedirect.com/science/article/pii/037026939291780D>.
- [45] A. Dabelstein, “The One loop renormalization of the MSSM Higgs sector and its application to the neutral scalar Higgs masses,” *Z.Phys.* **C67** (1995) 495–512, [arXiv:hep-ph/9409375](#) [hep-ph].

- [46] K. E. Williams, H. Rzehak, and G. Weiglein, “Higher order corrections to Higgs boson decays in the MSSM with complex parameters,” *Eur.Phys.J.* **C71** (2011) 1669, [arXiv:1103.1335 \[hep-ph\]](#).
- [47] R. Santos and A. Barroso, “On the renormalization of two Higgs doublet models,” *Phys.Rev.* **D56** (1997) 5366–5385, [arXiv:hep-ph/9701257 \[hep-ph\]](#).
- [48] L. Baulieu, “Perturbative gauge theories,” *Physics Reports* **129** no. 1, (1985) 1 – 74. <http://www.sciencedirect.com/science/article/pii/0370157385900912>.
- [49] D. Ross and J. Taylor, “Renormalization of a unified theory of weak and electromagnetic interactions,” *Nuclear Physics B* **51** no. 0, (1973) 125 – 144. <http://www.sciencedirect.com/science/article/pii/0550321373905051>.
- [50] F. Bloch and A. Nordsieck, “Note on the radiation field of the electron,” *Phys. Rev.* **52** (Jul, 1937) 54–59. <http://link.aps.org/doi/10.1103/PhysRev.52.54>.
- [51] G. ’t Hooft and M. Veltman, “Scalar one-loop integrals,” *Nucl. Phys.* **B153** (1979) 365–401.
- [52] P. Ferreira, R. Guedes, M. O. Sampaio, and R. Santos, “Wrong sign and symmetric limits and non-decoupling in 2HDMs,” *JHEP* **1412** (2014) 067, [arXiv:1409.6723 \[hep-ph\]](#).
- [53] T. Hahn and M. Rauch, “News from FormCalc and LoopTools,” *Nucl.Phys.Proc.Suppl.* **157** (2006) 236–240, [arXiv:hep-ph/0601248 \[hep-ph\]](#).
- [54] T. Hahn, “A Mathematica interface for FormCalc-generated code,” *Comput.Phys.Commun.* **178** (2008) 217–221, [arXiv:hep-ph/0611273 \[hep-ph\]](#).
- [55] T. Hahn and M. Perez-Victoria, “Automatized one loop calculations in four-dimensions and D-dimensions,” *Comput.Phys.Commun.* **118** (1999) 153–165, [arXiv:hep-ph/9807565 \[hep-ph\]](#).
- [56] **LHC Higgs Cross Section Working Group** Collaboration, S. Dittmaier *et al.*, “Handbook of LHC Higgs Cross Sections: 1. Inclusive Observables,” [arXiv:1101.0593 \[hep-ph\]](#).
- [57] **ATLAS, CMS** Collaboration, G. Aad *et al.*, “Combined Measurement of the Higgs Boson Mass in  $pp$  Collisions at  $\sqrt{s} = 7$  and 8 TeV with the ATLAS and CMS Experiments,” *Phys.Rev.Lett.* **114** (2015) 191803, [arXiv:1503.07589 \[hep-ex\]](#).
- [58] R. Coimbra, M. O. Sampaio, and R. Santos, “ScannerS: Constraining the phase diagram of a complex scalar singlet at the LHC,” *Eur.Phys.J.* **C73** (2013) 2428, [arXiv:1301.2599](#).
- [59] R. Costa, R. Guedes, M. Sampaio, and R. Santos, “Scanners.” <https://www.hepforge.org/downloads/scanners>.
- [60] J. Baglio, O. Eberhardt, U. Nierste, and M. Wiebusch, “Benchmarks for Higgs Pair Production and Heavy Higgs boson Searches in the Two-Higgs-Doublet Model of Type II,” *Phys.Rev.* **D90** no. 1, (2014) 015008, [arXiv:1403.1264 \[hep-ph\]](#).